Lisendra Marbelia

Suportes à base de quitosano para regeneração óssea

Chitosan based scaffolds for bone regeneration

Lisendra Marbelia

Suportes à base de quitosano para regeneração óssea

Chitosan based scaffolds for bone regeneration

Dissertação apresentada à Universidade de Aveiro para cumprimento dos requisitos necessários à obtenção do grau de Mestre em Ciência e Engenharia de Materiais, realizada sob a orientação científica das Doutoras Maria Margarida Tavares Lopes de Almeida, e Maria Elizabete Jorge Vieira da Costa, Professoras Auxiliares do Departamento de Engenharia Cerâmica e do Vidro da Universidade de Aveiro.

o júri

presidente

Prof. Doutor Joaquim Manuel Vieira

professor catedrático do Departamento de Engenharia Cerâmica e do Vidro da Universidade de Aveiro

Profª Doutora Natália Maria Araújo Alves

professora auxiliar do Departamento de Engenharia de Polímeros da Escola de Engenharia da Universidade do Minho

Profª Doutora Maria Elizabete Jorge Vieira da Costa

professora auxiliar do Departamento de Engenharia Cerâmica e do Vidro da Universidade de Aveiro

Profª Doutora Maria Margarida Tavares Lopes de Almeida

professora auxiliar do Departamento de Engenharia Cerâmica e do Vidro da Universidade de Aveiro

agradecimentos
(acknowledgement)

The present report is submitted as my master thesis to finalize my study in European Masters in Materials Science.

I would like to thank to my main supervisor in Universidade de Aveiro, Portugal, Prof. Margarida Almeida and Prof. Elizabete Costa. Thank you for the guidance during my work, I did study a lot of new things. I am also grateful to thank Jens Christian M. Rauhe as my co-supervisor from Aalborg Universitet, Denmark.

My appreciations also go to Marta, Celia, Ana, Maria Joao, Maria Celeste, and all people in Ceramics Department who have been really helpful. For my colleagues in the lab 9.3.6, Joel, Patrick, Luis, and Cristina, thanks for the welcome and friendliness during my stay in the lab. My pleasure also to thank Dr. Vitor from UMinho who made the µ-CT analysis possible.

For my family in Indonesia, Mama, Papa, Mbak Onid, Nia, Mas Faisal, and Mas Vido, thanks for the support and prayer, this thesis would not have been possible without all of your support. Also, for my friends, Zakka, Cassie, Mas Fatikul Arif, Catia, Adi, Mas Bayu, Mas Dhany, Didi and many more, thanks! Thanks for the friendship, and beautiful moment we spent in Europe!

I would like to appreciate EMMS consortium for holding this program and the European Commission for financing my study through Erasmus Mundus Scholarship. I am also grateful to mention all my EMMS colleagues, Cris, Ananth, Binh, Aaron, Gabisa, Jintao, and Erik; thank you for the friendship and the unforgettable moments during this master.

Finally, Al hamdu lillahi robbil ‘alamin, my greatest praise and thanks are to Allah swt, for all of His blessing in my life.

palavras-chave Quitosano, fosfatos de calico, hidroxiapatite, compósitos "scaffolds", porosidade, bioatividade, comportamento mecânico, libertação controlada de fármacos, regeneração óssea, engenharia de tecidos

resumo A investigação em engenharia de tecidos (ET) tem procurado soluções para as necessidades de reforço e de regeneração dos tecidos recorrendo por vezes a substâncias bioactivas que podem favorecer a proliferação celular. Os avanços recentes em ET têm beneficiado da utilização de matrizes tridimensionais porosas (scaffolds) que permitem a adesão, proliferação e regeneração das células bem como a vascularização, estimulando a formação de novo tecido. A obtenção de scaffolds de quitosano (CH) para a regeneração óssea tem merecido especial interesse devido às suas propriedades biológicas e físicas, apresentando no entanto o inconveniente da falta de resistência mecânica e de bioatividade. A obtenção de scaffolds compósitos por incorporação na matriz polimérica de materiais bioactivos de fosfato de cálcio, permite reforçar o scaffold, melhorando o seu desempenho mecânico e a sua osteocondutividade.

No presente trabalho, produziram-se scaffolds compósitos de quitosano/hidroxiapatite por processos de congelamento e liofilização de suspensões de fosfatos de cálcio (CaP) em soluções de CH. Utilizaram-se CaP sintetizados laboratorialmente, quer na forma de fibras de hidroxiapatite (HA), quer de lamelas de monetite, quer de mistura dos dois. Os CaP foram sintetizados por um método de precipitação em meio aquoso, tendo-se monitorizado a precipitação de fosfato de cálcio durante 3 dias. Avaliou-se a evolução das fases cristalinas e da morfologia das partículas precipitadas por microscopia eletrónica de varrimento (SEM), difracção de raios X (XRD) e por adsorção de N_2 usando a isotérmica de BET. Os resultados evidenciaram que o aumento da temperatura de refluxo acelera a transformação das fibras de octacalcium fosfato em fibras de HÁ, permitindo reduzir o tempo de precipitação total para obtenção de fibras de HA

As soluções de quitosano e as suspensões de HAP em solução de CH, a dois valores de pH (pH=2 e pH= 5), foram congeladas a três temperaturas diferentes antes de serem liofilizadas. Caracterizaram-se os scaffolds por SEM, DRX, microtomografia computorizada (μ-CT) e espectroscopia de infravermelhos com transformada de Fourier (FTIR), tendo-se ainda avaliado o seu comportamento mecânico em compressão. Obtiveram-se scaffolds compósitos macroporosos com porosidade superior a 80%, tamanho de poro na gama 50-250μm e porosidade interconectada com grau de interconexão de 91-98.5%. Verificou-se que o tamanho e morfologia de poro dos scaffolds é condicionado pelo pH das suspensões e pela temperatura de congelamento. O valor de pH mais elevado (pH=5) e a temperatura de congelamento mais elevada (T=0ºC) são as condições que mais favorecem o crescimento de cristais de gelo e por conseguinte a formação de poros de maior dimensão. Verificou-se também que a incorporação de partículas de CaP na matriz polimérica de CH aumenta a resistência mecânica do scaffold, que é também condicionada pelo tamanho de poro e pela morfologia da partícula de CaP. O estudo do comportamento bioactivo dos scaffolds compósitos em soluções simuladoras do plasma humano (SBF), monitorizando a variação das concentrações de Ca e P na solução de SBF, evidenciou o contributo das partículas de CaP para a bioactividade do scaffold. Os scaffolds compósitos em que coexistem brushite e HA (preparados a pH=2) evidenciaram bioactividade superior á dos scaffolds compósitos CH/HA.

Preparam-se também scaffolds incorporando grânulos de hidroxiapatite carregados com um fármaco modelo, a dexametasona (DEX), na solução inicial de CH. Os grânulos obtiveram-se por atomização de suspensões de HA nanométrica em solução de DEX. Construíram-se os perfis de libertação da DEX em solução tampão fosfato (PBS) por determinação da concentração de DEX por espectroscopia de ultravioleta (UV) ao comprimento de onda de 242 nm. Entre as várias curvas de libertação de DEX decorrentes das diferentes metodologias testadas para carregamento do fármaco, evidenciou-se um perfil de libertação de DEX segundo o qual cerca de 80% da DEX é libertado ao longo de ~30 dias, assegurando-se assim uma libertação mais lenta e prolongada do que as referidas na literatura para a DEX

As características dos scaffolds compósitos preparados no presente trabalho apontam os materiais produzidos como promissores para aplicação em engenharia de tecidos, apresentando como potencial adicional a capacidade de se comportarem como sistemas de libertação controlada de fármacos.

keywords Chitosan, Calcium Phosphate, Hydroxyapatite, Composite, Scaffolds, Pore Structure, Bioactivity, Mechanical Properties, Drug Delivery, Bone Regeneration, Tissue Engineering

abstract Tissue engineering research attempts to satisfy the needs of support, reinforcement and in some cases organization of the regenerating tissue with a controlled supply of bioactive substances that might positively influence the behaviour of incorporated or ingrowing cells. As demonstrated by the recent advances on biomaterials, the ideal scaffold for tissue regeneration should offer a 3D interconnected porous structure behaving as a template to promote cells adhesion and proliferation and vascularisation as well thus stimulating the new tissue ingrowth. A special interest has been focused on chitosan (CH - the partially deacetylated derivative of chitin) scaffolds for bone regeneration due to its biological and physical properties, in spite of some drawbacks regarding its lack of mechanical strength and bioactivity. The incorporation of bioactive calcium phosphates materials in the polymer matrix is expected to reinforce chitosan scaffolds improving their mechanical performance and osteoconductivity.

In the present work, chitosan based scaffolds were produced by freeze-drying CH solutions containing calcium phosphate (CaP) particles, either as fibers of hydroxyapatite (HA), platelets of monetite or a mixture of both. CaP particles were prepared by a wet precipitation method. The calcium phosphate precipitation was monitored by taking a number of samples during 3-days. Evolution of the morphology and crystal phase composition of the precipitated particles were followed by scanning electron microscopy (SEM), N_2 adsorption using the BET isotherm (BET), and X-ray diffraction (XRD). It was observed that the increase of refluxing temperature allowed a faster transformation of octacalcium phosphate fibers into HA fibers, hence shortening the precipitation time required for obtaining HA fibers,

Chitosan based scaffolds suspensions at two different pH values were frozen at three different temperatures before freeze-drying (thermally induced phase separation-TIPS). SEM, XRD, microcomputed tomography (µ-CT) and Fourier transformed infrared spectroscopy (FTIR) were used to analyze the physical and chemical properties of the composite scaffolds. Compressive mechanical tests were also undertaken to characterize the materials. Bioactivity studies were performed in simulated body fluid (SBF) solutions by monitoring the Ca and P concentration variations of SBF solutions.

Highly interconnected macroporous scaffolds with a pore size ranging from of 50 to 250µm, interconnectivity around 91-98.5%, and porosity higher than 80% were obtained. The freezing temperature and the pH of chitosan solution/suspension revealed to play a significant influence in the pore structure. The higher pH (pH=5) and the higher freezing temperature (T=0ºC) were found as the most favourable conditions for ice crystal growth which resulted in larger pores. It was also observed that CaP particles incorporation in the CH matrix increased the scaffold mechanical strength which was also conditioned by the pore size and by the reinforcing particle morphology. The bioactivity studies revealed the CaP contribution for the scaffold bioactivity. The composite scaffolds having brushite and HA (obtained at pH=2) exhibited enhanced bioactivity as compared to composite CH/HA scaffolds based.

CH based scaffolds were also prepared by incorporating HA granules loaded with dexamethasone (DEX), a drug model, in CH solution. The granules were obtained by spray drying HA nanosized particles suspended in DEX solution. The drug release profiles of DEX were determined in phosphate-buffered solution (PBS) by DEX concentration evaluation in the releasing medium by Ultraviolet (UV) spectroscopy at the wavelength of 242 nm. Among the different DEX release patterns corresponding to the various DEX loading methodologies which were tested, an adequate release profile could be selected: it showed that the release of 80% of the DEX loaded amount could be ensured during ~30 days, thus enabling a prolonged and slowest DEX release as compared to literature reports. It is thus found that the CH scaffolds engineered with a calcium phosphate based drug delivery system (DDS) provides the desirable association of a bioactive and osteoconductive matrix with an in situ controlled release of a therapeutic agent. These results point out an additional potential of the composite CH/HA scaffolds for behaving as a controlled drug release system (DDS).

LIST OF CONTENTS

LIST OF FIGURES

LIST OF TABLES

ABBREVIATION

CaP	:	Calcium Phosphate
CH	:	Chitosan
DEX	:	Dexamethasone
DDS	:	Drug Delivery System
FTIR	:	Fourier Transform Infrared
HA	:	Hydroxyapatite
OCP	:	Octacalcium Phosphate
PBS	:	Phosphate Buffered Saline
PGA	:	Poly(glycolic acid)
PLA	:	Poly (lactic acid)
PLGA	:	Poly (lactic acid-co-glycolic acid)
PCL	:	Poly (ε-caprolactone)
PPF	:	Poly (propylene fumarate)
SBF	:	Simulated Body Fluid
SEM	:	Scanning Electron Microscope
TE	:	Tissue Engineering
TIPS	:	Thermally Induced Phase Separation
XRD	:	X-Ray Diffraction
μ-CT	:	Micro Computed Tomography

GLOSSARY

Biomineralization	:	The process by which living organisms produce minerals, often to harden or stiffen existing tissues
In vitro	:	Refers to study in experimental biology in which take place in glass/plastic container in the laboratory (outside the living body)
In vivo	:	Refers to study in experimental biology in the living organism (opposite of in vitro)
Lyzozome	:	Enzyme responsible for breaking down the polysaccharide walls of many kinds of bacteria and thus it provides some protection against infection; also degrade chitosan.
Osteoblast	:	Mononucleate cells which are responsible for bone formation
Osteogenesis	:	A process of new bone materials deposition which is done by osteoblasts
Osteoconductivity	:	The ability of a material to support osteoblastic cells adhesion, growth, and differentiation
Vascularization	:	The formation of new blood vessels in tissues
Proliferation	:	The growth and reproduction of similar cells.

Chapter 1
Introduction & Objectives

Tissue engineering (TE) is an important therapeutic strategy aiming at replacing and facilitating the re-growth of injured or diseased tissue[1]. The application of tissue engineering comprises in a wide range area, such as fabricated skin, liver, pancreas, cartilage, bone, ligament, tendon, etc[2]. Its basic concept started believing that cells can be isolated from a patient, expanded in a culture, seeded into a carrier, and finally grafted back into the patient. The goal of tissue engineering which is to fabricate living replacement parts for the body is achieved by combining three main elements: biomaterials (scaffold), cells, and bioactive/signaling molecules[3].

One of tissue engineering applications is bone regeneration. Bone loss due to trauma or disease is one vital health problem. In United States at least 6,3 million fractures happen every year, bone problem due to osteoporosis harm over 10 million Americans, and disease due to low bone mass affect another 34 millions[3]. In all those cases and also other cases, such as bone cancers, bone regeneration is critical in order to restore the function.

Several medical treatments are available for bone injuries, being autograft one of them. In the case of autograft, implantation is done by harvesting bone tissue from one certain site in patient's body and fixing it to the injured site. However, several limitations were found in these treatments, such as loosing function in the place where the bone was harvested, infection, and pain. Besides autograft, allograft and xenograft can also be done for bone implantation where the bone grafts are obtained from another person and another species, respectively. In this case, spreading of danger diseases and negative response from the body might occur[3]. Bone implantation can also be done by using metallic materials, such as iron, cobalt, titanium. Nevertheless, some drawbacks mainly related to the inappropriate mechanical properties appear. Ceramic materials are also able to be utilized for surgical implantations. However, besides their inadequate mechanical performance, several shortcomings from both ceramics and metals are their low or non-biodegradability and limited processing.

The development in TE area might be one of the solutions of the previous problems. By utilizing scaffolds, cells, and or bioactive molecules to support and facilitate the growth of new bone tissue, a bone defect will be restored without the use of any permanent implant[3]. TE approach in general, including for bone regeneration, can be done in several ways as shown in Figure 1-1. Based on the existence of cells prior to implantation, systems can be divided into two: cellular systems and acellular systems[4]. In acellular systems, scaffolds are implanted directly in the human body without cell addition. While in cellular system, two approaches can be done: (1) seeding cell at point of delivery

and (2) seeding and allowing cells to remodel the scaffold into natural tissue in the laboratory prior to implantation[5].

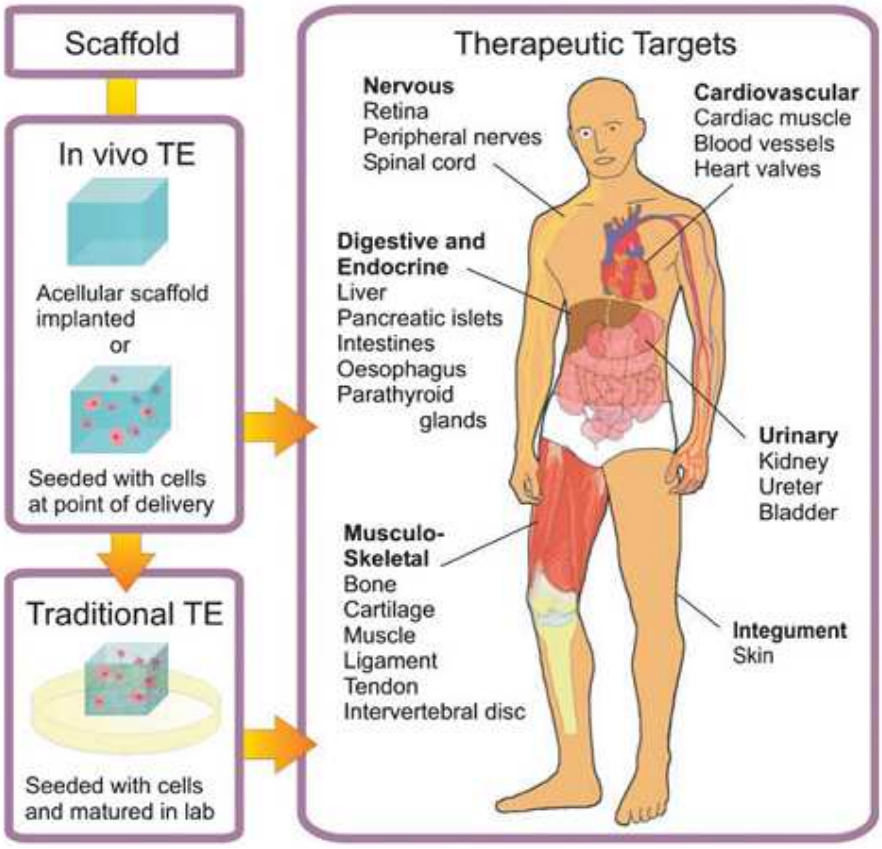

Figure 1-1 Application of scaffolds in tissue engineering (TE) approach consisting of (1) in vivo approaches with or without cells and (2) traditional TE which involves seeding and growing cells in the laboratory [5]

Based on explanation above, it is clear that the scaffold has an important role in TE approach. In order to fulfill its purpose, the scaffold has to meet several requirements, such as: biocompatibility, bioactivity, biodegradability, and appropriate mechanical properties. Several materials, including ceramics, polymer, and ceramics-polymer composite have been used for preparing scaffolds. The advantages of using ceramics, such as CaP (Hydroxyapatite/HA, β-Tricalcium phosphate/β-TCP) and bioglass, are their biocompatibility, osteoconductivity and sufficient mechanical strength. HA is one compound which is most used since its chemical composition is similar with inorganic component of bone in human body. In the other hand, they also have several shortcomings, such as being slowly degradable and brittle[6]. Utilizing polymers have some limitations, mainly poor stiffness and compression strength. As compared to ceramics, some polymers, such as polylactid acid (PLA, PLLA, PDLA), polyglycolic acid (PGA), collagen, alginate, and chitosan, may easily degrade. The adequate combination of ceramics and polymers is

thus being addressed as a promising approach for producing scaffolds displaying the desired characteristic for bone TE.

Another function of the scaffold in bone regeneration besides its supporting structure role for cells grow is as drug delivery system (DDS). During its function as cell growth support, ideal scaffolds are supposed to degrade[6, 26, 7]. Based on this nature, drugs can be loaded into the scaffold and later released to implantation sites during scaffold degradation.

Among the most studied composite scaffold, it is worthy to mention chitosan/CaP (CH/CaP) composite materials due to chitosan biocompatibility and biodegradability and to bioactivity of CaP (as HA and TCP). A number of studies on the area of CH/CaP has been carried out[8, 9, 10, 11, 7, 43] showing that the addition of CaP has improved the mechanical properties of CH/β-TCP scaffold[9], the biocompatibility and bioactivity of CH/nano-HA scaffold[8, 43] . Furthermore it was also shown that CH scaffold may play a retarding role during a drug release, i.e. gentamincin sulphate, which is kept under release for more than 3 weeks[7], thus pointing its potential for DDS applications. However the combination of scaffold and DDS performance in the same biomaterial device has been scarcely exploited. Furthermore CH based scaffolds still present relatively modest pore sizes, very often less than 100μm[8, 43]. Studies aiming to improve CH scaffolds microstructure are thus still welcome.

In the framework of the CH issues stated above, it is necessary to further exploit both the composition and the manufacturing method of CH/HA composite scaffold in order to improve its structural characteristics (including pore size, porosity, interconnectivity) and potentialities as a DDS. The present study is thus targeted to the development of CH/HA composite scaffolds aimed at bone regeneration, with the following objectives:

1. To exploit and understand the role of processing variables including the pH of chitosan solution, and the freezing temperature on chitosan based scaffolds microstructure.
2. To combine the effects of processing variables and of different types of CaP reinforcing particles for engineering the scaffold microstructure and bioactivity while improving the mechanical properties of the scaffold
3. To evaluate the potentiality of CH scaffolds as drug delivery system.

For achieving these objectives, composite scaffolds with different compositions were produced under different experimental freeze drying conditions. The microstructure, mechanical properties, and bioactivity of the obtained scaffolds are here analyzed and discussed. Furthermore, the scaffolds behavior as drug delivery systems using dexamethasone as a drug model is also analyzed.

This report consists of five chapters. Chapter 1 addresses the interest and objectives of the present study. In Chapter 2, literature review about scaffolds, including its requirements, raw materials and manufacturing techniques are set up to build up better

understanding on this area. The problem formulation of this research is presented in Chapter 3. Materials and methods of the experimental procedure are explained in Chapter 4. The results and respective discussions are presented in Chapter 5. Finally the main conclusions and recommendations are summarized in Chapters 6.

Chapter 2
Literature Review

In the following section, basic knowledge and information regarding to the topic from recent publications and books are presented in order to have better understanding. In section 2.1 a number of issues related to porous scaffold requirements for bone regeneration are explained. Section 2.2 describes the material choices for scaffold; information about chitosan and CaP are written here. And in section 2.3, a number of scaffold manufacturing processes are illustrated.

2.1. Porous Scaffold for Bone Regeneration

In tissue engineering, scaffold has an important role. Scaffold is designed as three-dimensional biodegradable structure which possesses a high porosity and pore interconnectivity. It performs as structural support for cells while they gradually degrade and the new tissue being formed[6].

As mentioned in chapter 1 about scaffold requirements, the criteria for choosing materials to perform as scaffold are quite complicated and challenging since it has to face complex biological and sensitive system as the human body. In the case of bone regeneration application, several requirements should be fulfilled as shown in Table 2-1.

Table 2-1 Scaffold Basic Design Parameters for Bone Tissue Engineering[12]

Parameter	Requirements
Porosity	Maximum possible without compromising mechanical properties (typical porosity around 90%)
Pore size	200-400μm
Pore structure	Interconnected
Mechanical properties of cancellous bone	
Tension and compression	Strength : 5-10 MPa Modulus : 50-100 MPa
Mechanical properties of cotical bone	
Tension	Strength : 80-150 MPa Modulus 17-20 GPa
Compression	Strength : 130-220 MPa Modulus : 17-20 GPa Fracture Toughness : 6-8MPa √m
Degradation Properties	
Degradation time	Must be tailored to match the application in patients
Degradation mechanism	Bulk dissolution in medium
Biocompatibility	No chronic inflammation
Sterizability	Strerizable without altering material properties
Bioactivity	Bioactive

Basically, mechanical properties of scaffold should match with the tissue at the implantation sites and provide the correct stress environment for the neotissues[2,6]. Biocompatibility is needed; in which generation of any unwanted tissue response to the implant is avoided so that not inflammatory response occurs[3]. In the case of biodegradability, scaffold is required to degrade in a controlled manner to facilitate load

transfer to develop bone and allow bone growth into the defect. Furthermore, it is compulsory for the degradation products to be non-toxic to the body[3]. High interconnected porosity structure and high surface area are needed to allow cell adhesion, proliferation, facilitating cell contacts, and cell migration in order to encourage bone ingrowths and repair[1,2]

Osteoconductive materials are preferable, in which the properties of a material show an ability to support bone growth by providing a site for cell attachment and vascular ingrowth[3]. Another requirement is bioactivity; bioactive materials allow and enhance the formation of apatitic layer which allow bonding to the bone tissue.

2.1.1. Mechanical Properties

In the case of mechanical properties, porous scaffold materials should match with the properties of target sites. It should be able to give enough strength to the damaged locations and in the same time allow gradual load transfer in order to facilitate the newly growth tissue for bone recovery[3].

Bone has very unique mechanical properties which are originated from its chemical components and hierarchical organization[13, 14, 15]. As shown in Figure 2-1, bone is a complex biological material which consists of collagen fibril and HA crystal. Inorganic material which is mainly HA covers 60% composition of bone, organic material covers 30%, and the remaining 10% is water. This composition makes bone with outstanding mechanical properties in which the compressive strength is originated from the rigid HA, while collagen fibrils are capable of energy dissipation and impart the tensile properties[3].

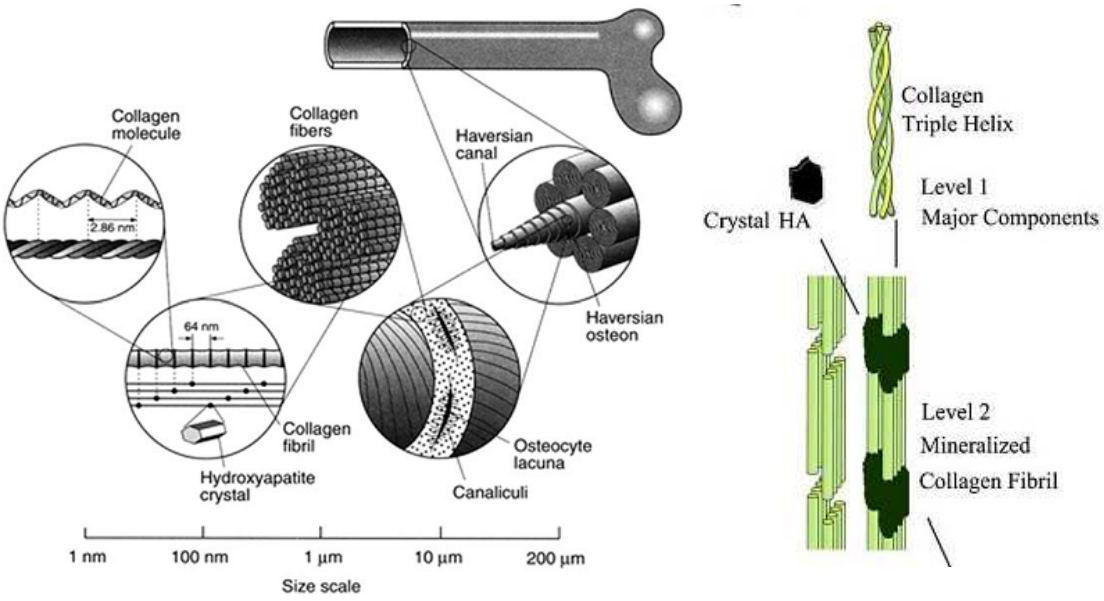

Figure 2-1 Hierarchically structured biological material in which the building components are precisely arranged at scales (left)[13]. Nanocomposite consisting of crystal HA and collagen fibril in bone (right)[15]

Two types of bone exist in human body, i.e. cortical bone and cancellous bone. Cortical bone which covers 80% of adult skeleton is hard, compact, dense bone which posses only 10% porosity[3]. Its strength values are 79-151MPa in tension and 131-224MPa in compression; its modulus is 17-20GPa in both compression and tension. Cancellous bone on the other hand is spongy and may have 50-90% porosity. Its compressive strength is 4-12MPa and its modulus is 0.1-0.5GPa[13].

Figure 2-2 shows a comparison of mechanical properties between several polymer and ceramic-based biomaterials with natural bone. It is shown that dense biodegradable polymer has close mechanical properties with cancellous bone, and dense bioactive ceramics with cortical bone[21]. However, when it comes to porous materials, mechanical properties of both porous biodegradable polymer and porous bioactive ceramics need to be improved. By combining the two materials: ceramics and polymer; porous biodegradable composites are able to improve the mechanical properties closer to cancellous bone.

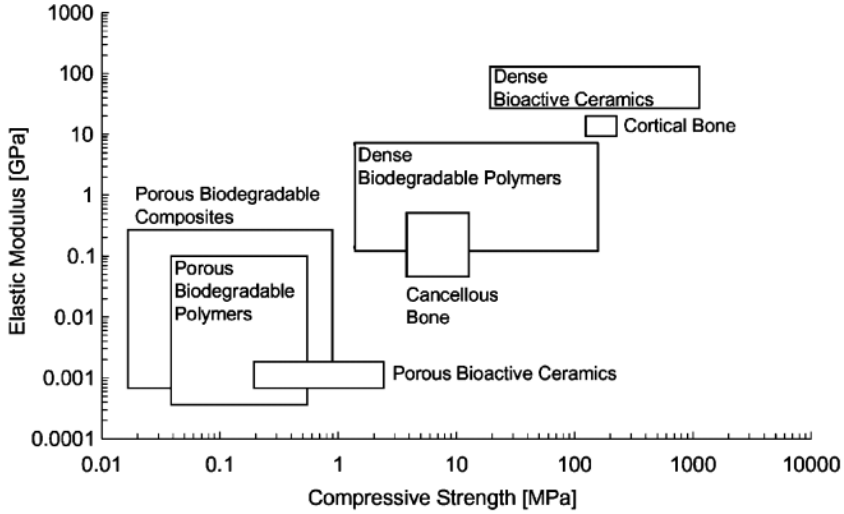

Figure 2-2 Mechanical properties (both compressive strength and elastic modulus) of biodegradable polymer, bioactive ceramics and composite[21]

A huge number of materials including the class of synthetic polymers (PLA, PGA, PCL, PPF), natural polymers (chitosan, collagen), bioactive ceramics, bioactive glass, and polymer-ceramic composite[21] have been investigated to imitate the properties of bone. In the area of porous biodegradable composite, numerous researches have been done; for instance amorphous CaP, HA, Bioglass were used to reinforce PLGA, PLLA, and PLA[21], chitosan[9,10,11], and collagen[16]. Boccaccini and Maquet achieved three times higher compressive modulus of PLGA by addition of 50%wt of bioglass[17], Zhang and Zhang[9] were able to improve compressive modulus of chitosan from 0.967 to 2.191 MPa and the yield strength from 0.109 to 0.208 MPa with reinforcement of β-TCP.

2.1.2. Scaffold Morphology

Control of scaffold morphology is very crucial for its application in tissue engineering since it influences its degradation kinetics, mechanical properties, and also controls the cellular colonization rates and organization within an engineered tissue[18].

High porosity and critical pore size are essential. High interconnected porosity is needed to facilitate diffusion of nutrients and waste (degraded materials); it also supports the vascularization of ingrown tissue. A typical porosity of 90% is obligatory for good vascularization and cell penetration. Large surface area is needed for cell attachment and growth; while large pore volume is required to facilitate sufficient place for tissue repair. A certain pore size is necessary to be fulfilled depending on the type of applications; in the case of bone optimum size should be in the range of 100-350µm, 20-125µm for adult mammalian skin, 5-15 for fiberblast ingrowth, etc[2].

Table 2-2 illustrates the pore size and porosity dependence of bone regeneration development as summarized by Yang et al.[2]. It is known that porosity is one important variable for bone regeneration after one research which shows that there was no new bone formed on the solid particle, while in porous scaffold direct osteogeneis occurred[19]. However, it is not only porosity which influence bone growth as shown in Table 2-2, but also pore size. One material with porosity of 33.5% with very small pore (2-6µm) shows no tissue ingrowth.

In the point of view of pore size, from Table 2-2, research from Klawitter et al.[19] which implanted calcium aluminate cylindrical pellet to dog femorals showed that pore size of ~100µm is typical minimum pore for bone regeneration. Data provided by Whang et al.[20] shows that higher pore size (<350µm) showed significant bone growth, however this data is not complete since unavailability of the pore distribution. On contradiction to Klawitter et al., one research with titanium plates which were implanted to rabbit femorals defects under non-load-bearing showed that all pore sizes (50, 75, 100, and 125 µm) indicated no significant differences in the ingrowth bone[19]. These suggested that ~100 µm may not be the critical pore for non-load-bearing applications. Whang et al.[20] also succeeded to prove another method of bone growth via hematoma stabilization. In this case, scaffold with porosity of 90% and pore size in the range of 16-32 µm are capable of osteoinduction to grow new bone.

From those descriptions, minimum pore size for bone regeneration may not be ~100 µm for some cases: such as non-load bearing conditions and another mechanism of bone growth based on hematoma stabilization. However, it is suggested to have at least 100 µm in order to allow proper cell penetration and vascularization of the ingrown tissue[2,21]. Furthermore, pore size bigger than 300 µm is recommended due to enhance new bone formation while small pores favored hypoxic conditions in which there is a lack of oxygen and ultimately can cause bone diseases[19].

Table 2-2 Studies defining optimal pore size for bone regeneration[2]

Reference	*Scaffold pore size (μm)*	*Porosity*	*Mineralize tissue ingrowth/comments*
Klawitter et al.[40]	Type I: 2–6 μm	33.5%	No tissue ingrowth
	Type II: 15–40 μm	46.2%	No bone ingrowth, fibrous tissue ingrowth
	Type III: 30–100 μm 80% pores < 100 μm	46.9%	50 μm of bone ingrowth, osteoid and fibrous tissue ingrowth
	Type IV: 50–100 μm 63% pores < 100 μm	46.9%	20 μm of bone ingrowth by 11 weeks and 500 μm of ingrowth by 22 weeks, osteoid and fibrous tissue ingrowth
	Type V: 60–100 μm 37% < 100 μm	48.0%	600 μm of bone ingrowth by 11 weeks and 1,500 μm of ingrowth by 22 weeks, osteoid and fibrous tissue ingrowth
Whang et al.[24]	≦100 μm	35.3%	Not statistically different from untreated controls
	≦200 μm	51.0%	Not statistically different from untreated controls
	≦350 μm	73.9%	Statistically significant more bone than all other groups

Figure 2-3 shows several typical morphologies of porous scaffold which are produced with different manufacturing techniques. Figure 2-3-a shows one typical 3-D porous scaffold with interconnected open pore prepared with freeze drying or particulate leaching. Different structural types are also available; such as in nanofibrous matrix (Figure 2-3-b) and microsphere (Figure 2-3-c). Each type is produced with different techniques and also can be used for different application. Nanofiber mesh type is usually produced by fiber bonding method. Microsphere scaffold can be used with injection method. Further information about scaffold manufacturing methods will be presented in section 2.2.

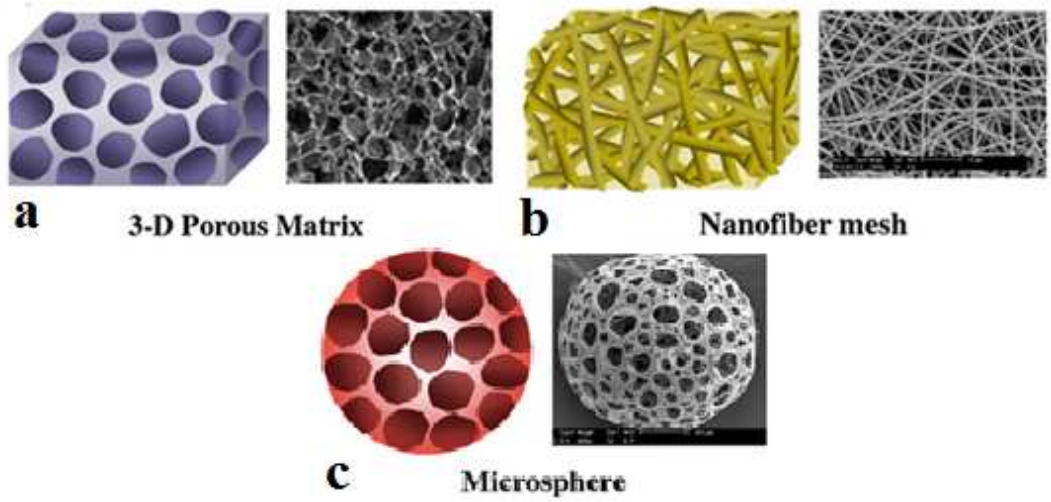

Figure 2-3 Different forms of polymeric scaffolds for tissue engineering: (A) a typical 3-D porous matrix in the form of a solid foam, (B) a nanofibrous matrix, (C) porous microsphere[50]

2.1.3. Scaffold Bioactivity

Implant materials which are placed in the injured sites have a tendency to be encapsulated by fibrous tissue and become isolated from the surrounded bone[22]. This tendency depends much on type of materials; for instance, in chitosan based materials, this occurrence is minimal to happen[23]. However, in the point of view of bone repair, since this adherence of implant materials and surrounding bone are crucial[22], the occurrence of this materials encapsulation should be avoided furthermore bonding with the surrounding tissue should be enhanced. This phenomenon is related with the property of materials so called bioactivity.

Bioactivity is the ability of materials to stimulate the growth of apatite layer on its surface when placed in human body. This apatite layer normally consists of nano-crystals of carbonate-ion-containing apatite that has a defective structure and low crystallinity. This biological active carbonate HA layer is chemically and structurally equivalent to the mineral phase in bone. Due to this similarity, bone producing cells, i.e., osteoblasts, can preferentially proliferate on the apatite, and differentiate to form an extracellular matrix composed of biological apatite and collagen[22]. Finally, as shown in Figure 2-4-a, the surrounding bone comes into direct contact with the surface apatite layer which connects to the artificial materials.

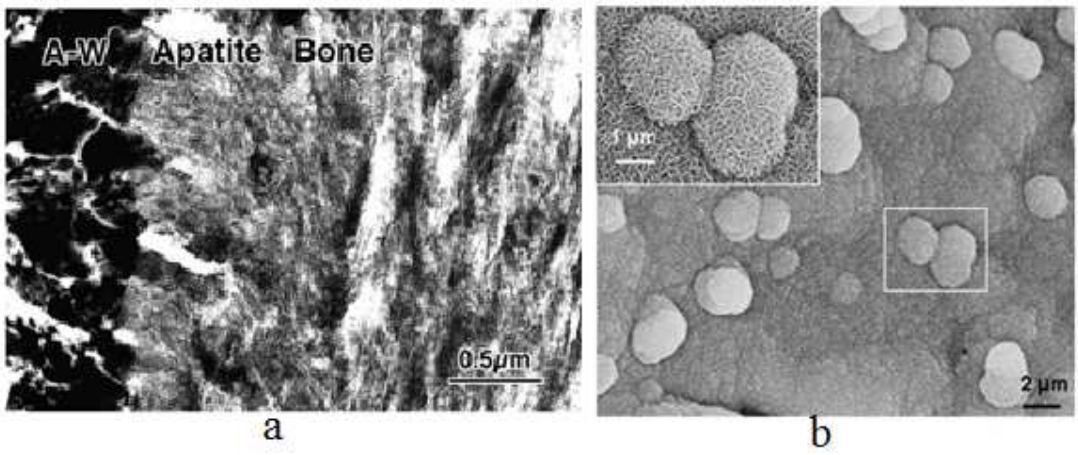

Figure 2-4 (a) TEM photograph illustrating the apatite layer in the interface between glass-ceramic A-W and a rat tibia - 8 weeks after implantation[22]; (b) SEM image showing HA formation in the surface of 45S5 Bioglass®[21]

Some materials are known to be bioactive, such as: bioactive glass (contains SiO_2, Na_2O, CaO, and P_2O_5) like, for instance, 45S5 Bioglass® which contains 45% SiO_2, 24,5% NaO, 24,4% CaO, and 6% P_2O_5; HA; and glass-ceramics (containing HA besides components, such as CaO and P_2O_5)[21]. Materials which don't posses any bioactivity, addition or layer of bioactive materials are needed to improve their properties.

In vitro formation of apatite layer can be promoted by immersing tested materials in SBF (simulated body fluid). SBF is a fluid prepared with ion concentration equal to those of the human blood plasma; as shown in Table 2-3.

Table 2-3 Nominal ion concentrations of SBF in comparison with those in human blood plasma[24]

Ion	Ion Concentration	
	Blood Plasma	**SBF**
Na^+	142.0	142.0
K^+	5.0	5.0
Mg^{2+}	1.5	1.5
Ca^{2+}	2.5	2.5
Cl^-	103.0	147.8
HCO_3^-	27.0	4.2
HPO_4^{2-}	1.0	1.0
SO_4^{2-}	0.5	0.5
pH	7.2-7.4	7.40

2.1.4. Scaffold Biodegradability

In most cases, implanted scaffolds are supposed to degrade prior to the insertion to the body. Instance or partially degradation is expected to occur while the tissues or organs remodel and grow[1, 25]. In the view point of TE applications, understanding of degradation mechanism is crucial. How these materials degrade, how long time is needed to degrade, and what is the degradation product need to be studied prior to its application in human body. Tunable degradation time and non-toxic waste of degradation are urgent in TE applications. Toxic waste of degradation process might trigger the occurrence of inflammatory response

Ceramic and metal materials are known to have limited and non biodegradability. On the contrary, most of polymers are biodegradable[2]. Basically, there are two main mechanisms of polymer materials degradation in vivo: enzymatic and non-enzymatic degradation process. Synthetic polymer such as PLA, PGA, PLLA degrades through non-enzymatic degradation which involves de-esterification process[21]. One issue which addresses to synthetic polymer degradation is the possibility of strong inflammation to occur if the acidic degradation product is released abruptly. On the contrary of synthetic polymers; natural polymers degrade mainly by enzymatic process; for example chitosan which degrade through hydrolysis of acetylated residues by lysozyme[1].

Biodegradation time of scaffolds is supposed to be able to be tuned easily depending on its certain application. By combining ceramics with polymers, for instance, one can tailor the degradation time of the produced scaffold. Boccaccini et al.[17] succeeded to retard the degradation time of PLGA by addition of bioglass.

A wide range of degradation time depending on type of materials is available. PLGA basically degrades too quickly in which they lost 50% of their tensile strength during two weeks; while PGA degrades too slowly where 3-6 years are needed for

complete resorption[1]. Others example are poly(propylene fumarate) or PPF in which lose about 13.6-27.9% of their weight during 12 hours in PBS immersion; poly(glycolide-co-caprolactone) or PGCL lose 50% mass during 6 weeks[25].

2.1.5. Scaffold as Drug Delivery System

Basically, human body has the ability of initiating tissue regeneration after injury, such as in bone marrow and skin. However, this ability varies much depending on size and cause of injury, and also on the age of each individual. In this case, having drug which can support and stimulate the regeneration process will be advantageous. Scaffold which can combine synergies of the porous support structure and of the drug delivery for promoting bone tissue regeneration may be envisaged the solution for this challenge.

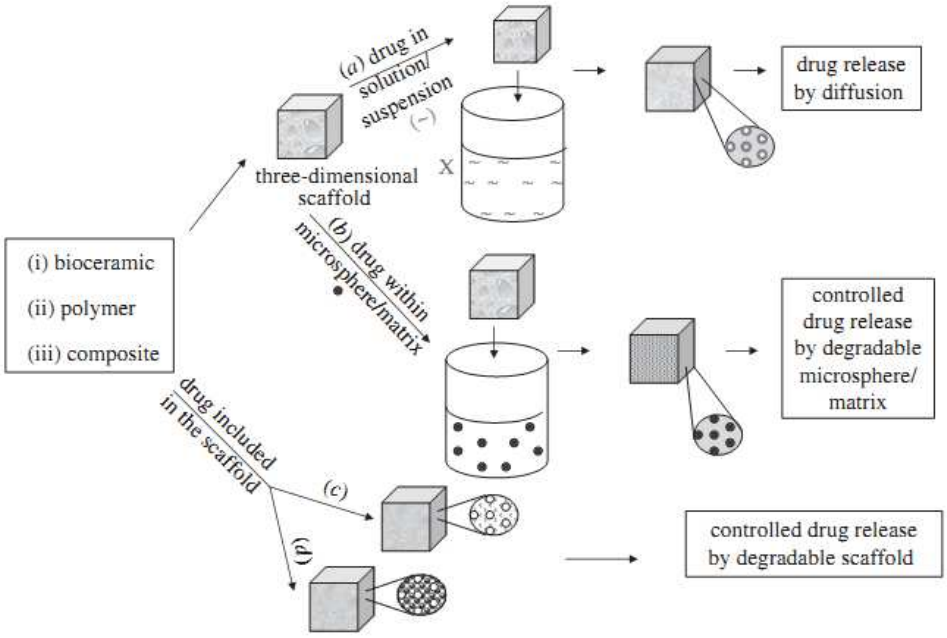

Figure 2-5 Schematic illustration of the most common strategies to fabricate DDS in 3-D scaffold: drugs adsorption either in their unprotected (a) or protected (b) forms and drug entrapment either in their unprotected (c) or protected (d) forms [6]

Delivery system has been applied in several therapies, such as: delivery of insulin, anticancer, anti-inflammatory agents, growth factors, etc[26]. Regarding to bone regeneration, several bioactive molecules and/or drugs can be loaded into the carriers (i.e. scaffold): (1) biomolecules or also known as growth factors [14, 27, 28] such as BMP/bone morphogenetic protein, EGF/epidermal growth factor, PDGF/platelet-derived growth factor, TGF-β1/transforming growth factor-beta1, FGF/fibroblast growth factors, VEGF/vascular endothelial growth factor, (2) antibiotics such as gentamicin, tetracycline, ciprofloxacin, polymiyxin B and (3) anti-inflammatory drug such as dexamethasone, ibuprofen[6].

Several types of carriers have been used in drug delivery, such as nanoparticles, microspheres, membranes, rods, hydrogels and also 3D scaffolds[28, 29]. In the case of scaffolds, the drugs can be loaded into the scaffold by using several techniques, as shown in Figure 2-5. The drugs can be adsorbed or entrapped and also protected (with microspheres) or unprotected. Furthermore, the preparation method also influences whether the drug release is dominated by diffusion or degradation of the matrix.

Ideally the drugs are delivered locally into the injured sites in controlled release manner which allows an adequate concentration level to be built up in a certain desired time. This is the benefit of having controlled drug delivery system, offering a tailored drug release pattern. Without controlled release, the drug might be released quickly thus enabling the possibility of the entire drug amount to be supplied before the infection stop.

The materials which have been used as drug delivery are varied, from polymers to inorganic materials[28]. The polymers which can be applied as drug delivery systems can be divided into two main groups: (a) natural polymers, including alginate, chitosan, and collagen; and (b) synthetic polymers, including polyesters, polyaminoamides, polyacrylates, and their copolymers and blends. All these biodegradable materials degrade during its application while releasing the loaded-drug.

2.2. Scaffold Materials Choices

Basically, there are three main types of materials which can be used to prepare scaffolds, i.e. polymers, ceramics, and composites.

Both natural and synthetic polymers have been used in tissue engineering applications. Natural polymers; such as collagen, gelatin, chitin, chitosan, alginate, cellulose, starch[14, 33] have been widely applied. However poor mechanical performance of some of them limits their usage. Synthetic polymers, belonging mainly to the polylactic/polyglycolic acid group, have been in use for more than 20 years in surgical sutures[2].

A wide range of ceramics has been employed in biomedical applications. In the field of bone regeneration, HA-based CaP compounds and bioactive glass have been the most widely used due to their bioactivity and osteoconductivity properties.

Table 2-4 Summary of Scaffold Materials Choices[12]

Biomaterials	Positive	Negative
Ceramics		
CaP (e.g. HA, triCaP, and biphasic CaP)	1. Excellent biocompatibility 2. Supporting cell activity 3. Good osteoconductivity	1. Too fragile in amorphous structure 2. Nearly bioinert in crystalline structure
Bioactive glass and glass-ceramics (e.g. bioglass, apatite-wollastonite, ceravital)	1. Excellent biocompatibility 2. Supporting cell activity 3. Good osteoconductivity 4. Vascularization 5. Tailorable degradation rate	1. Mechanically brittle and weak in glass state 2. Degrade slowly at crystalline structure
Synthetic Polymer		
Biodegradable polymer (poly(lactic acid)/PLA, poly(glycolic acid)/PGA, poly(propylene fumarate)/PPF)	1. Good biocompatibility 2. Bioresorbable 3. Good processability 4. Good ductility	1. Inflammation caused by acid degradation product 2. Accelerated degradation rates cause collapse of scaffold
Surface bioerodible polymer (poly(ortho esters)/POE, poly(anhydrides), poly(phosphazane)/PPHOS)	1. Good biocompatibility	1. They cannot be completely replaced by new bone tissue
Natural Polymer		
Polysaccharides (alginate, chitosan)	1. Good biocompatibility 2. Good Biodegradability	1. Mechanically weak
Protein (collagen, fibrin)		
Composites	1. Excellent biocompatibility 2. Supporting cell activity 3. Good osteoconductivity 4. Tailorable degradation rate *5.* Improved mechanical properties	Fabrication techniques can be complex

2.2.1. Chitosan

Naturally derived polymers are of special interest mainly due to their degradability, biocompatibility, low cost, and availability[30]. Besides, as natural component of living structures, their biological and chemical similarities to natural tissues are also the reasons why they are used abundantly in TE[1].

Basically, there are two main classes of natural origin polymers which have been widely used: protein-based polymers and polysaccharide or carbohydrate-based polymers[33,30]. Protein-based polymers, such as collagen, gelatin, and fibrin, have the advantage of mimicking many features of extracellular matrix and thus have the potential to promote better cell migration, growth, and organization during tissue regeneration[30]. Polysaccharide class such as chitosan, alginate, hyaluronan, and starch, have very good compatibility with blood (haemocompatibility properties) which might be due to their chemical similarities with heparin (component of blood)[14, 30].

Chitosan is a linear polysaccharide, derived from chitin by (partial) deacetylation of chitin in the solid state under alkaline condition (NaOH concentrated) or by enzymatic

hydrolysis in the presence of chitin deacetylase[31]. It is composed of glucosamine and N-acetyl glucosamine units linked by β (1-4) glucosidic bonds[1]. The structure of both chitosan and chitin can be seen in Figure 2-6. Chitin is the second most abundant polymer after cellulose. It can be obtained from exoskeleton of arthropods, such as shrimp, and also from the cell walls of fungi and yeast[31]. The properties of chitin and chitosan such as biocompatibilty and nontoxicity make them important materials in biomedical applications.

Chitosan can be used in the form of gel sponge, membrane, bead, and porous scaffold. Its easy processability by dissolving it in acid solution (pH < 6), makes chitosan become one of the most used materials in biomedical applications. The practical use of chitosan has been developed recently by modification to improve its solubility or to introduce desired properties. The main chemical modifications applied to chitosan work based on graft copolymerization and chemical grafting[32, 1]. Some examples of modified chitosan applications are: (1) specific recognition of cell can be introduced to chitosan by sugar modification; such as galactosylated chitosan for hepatocyte attachment, (2) sialic acid bounded chitosan to inhibit influenza[1], (3) ethylene diamine tetraacetic acid (EDTA) grafted onto chitosan increases the antibacterial activity of chitosan[32], etc. Furthermore, functional biomaterials made from chitosan have been used in wide range of applications, such as tissue engineering (both cartilage and bone), wound dressing, drug delivery, and cancer diagnosis[31].

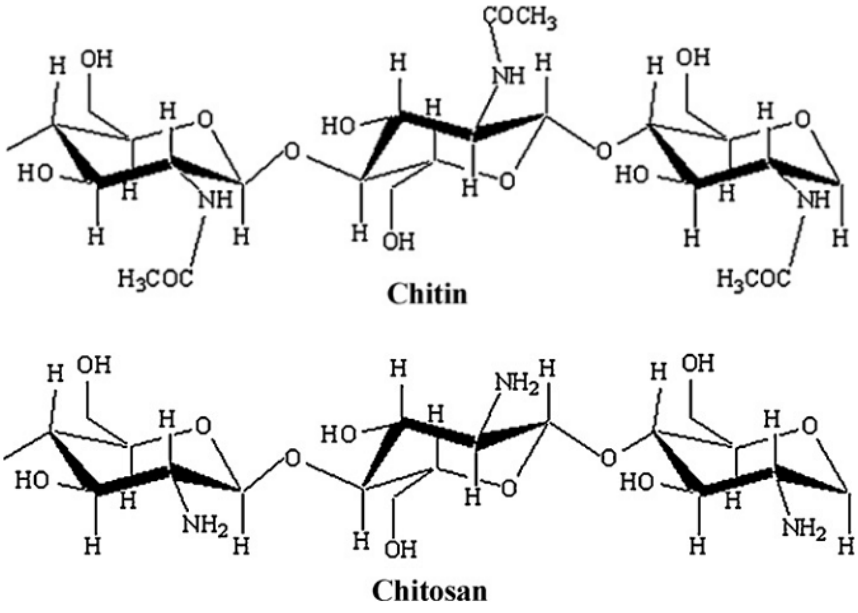

Figure 2-6 Structure of Chitin and Chitosan[31]

The illustration of chitosan applications in tissue engineering field is shown in Figure 2-7. Chitosan can be processed with cells and combined also with other biomaterials (such

as bioceramics: CaP; and other polymers like gelatin). Chitosan scaffolds for tissue engineering application are mainly produced by lyophilization, as can be seen in Figure 2-7. Despite all advantages of using chitosan as mentioned above, several drawbacks of using chitosan are found, such as their poor mechanical properties and absence of bioactivity. In order to overcome these problems and obtain better properties, reinforcement with inorganic bioactive particles might be one of the solutions.

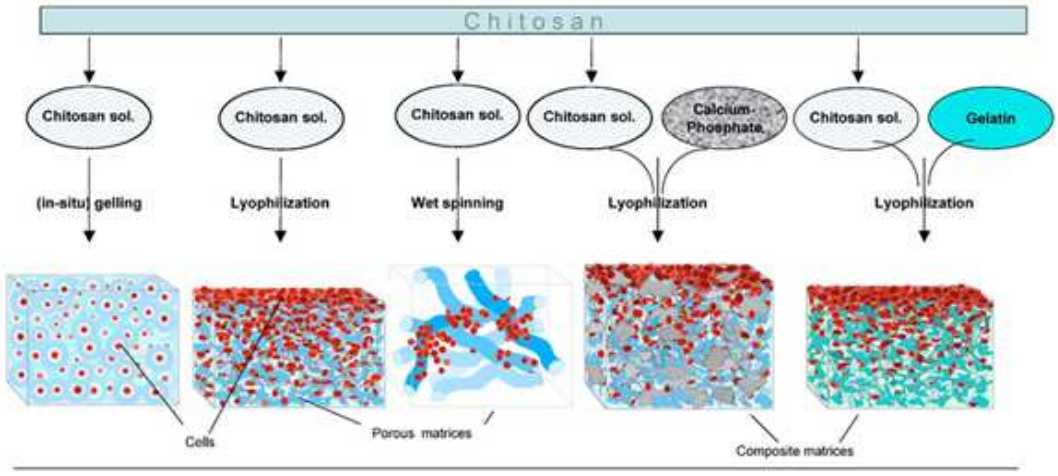

Figure 2-7 Illustrations of selected examples of chitosan scaffold processing in tissue engineering (from left to right): (1) in situ gelling, (2) lyophilization, (3) wet spinning, (4) and (5) lyophilization of mixture of chitosan solution and calcium phosphate and other polymer (gelatin)[23]

2.2.2. Calcium Phosphates

An extensive variety of ceramics has been utilized in the area of medical applications due to their positive interactions with human body, such as: CaPs, silica, alumina, zirconia, and titanium dioxide. The characteristics of these ceramics are usually high mechanical strength, good-body response, and low or non-existing biodegradability[33]. One type of ceramics which have been used widely is calcium phosphate (CaP), mainly class of calcium orthophosphate[34] which naturally exist as the main compounds of bone and teeth.

Among wide range of CaP compounds (as shown in Table 2-5), HA is one type of ceramics which is applied most in bone tissue field since around 60% of bone is made from HA[21, 35]. HA have an outstanding biocompatibility due to their close chemical and crystal resemblance to bone mineral. Besides HA, β-TCP and BCP (mixture between TCP and HA) are also used extensively.

In the point of view of biodegradability, β-TCP degrades faster than HA. However, when it is pHA (precipitates HA which contains smaller crystallites size) compared to sintered HA, the biodegradation is strongly enhanced due to higher solubility[36]. Regarding the mechanical properties, it depends on several factors: porosity, composition,

microstructure, and flaws/reliability[16]. Increase in pore size and porosity lead to lower mechanical strength. In the point of view of composition, one study shows that in BCP, increasing the amount of β-TCP resulted in lower mechanical strength[16]. Regarding biological response, these CaP compounds might also behave differently. Kruyt et al. investigated the bone ingrowth of HA, BCP, and β-TCP by addition of BMSC (bone marrow stromal cells). The results show that bone ingrowth was better in BCP and β-TCP compared to HA[33].

Table 2-5 Abbreviations of CaP-compounds with corresponding chemical formula and Ca/P-ratio[33]

Abbreviation	Name	Formula	Ca/P-Ratio
ACP	Amorphous Calcium Phosphate	-	1.25<x<1.55
BCP	Biphasic Calcium Phosphate	$Ca_3(PO_4)_2+Ca_{10}(PO_4)_6(OH)_2$	1.50<x<1.67
CA	Carbonated apatite, dahlite	$Ca_5(PO_4,CO_3)_3$	1.67
CDHA	Calcium deficient Hydroxyapatite	$Ca_{10-x}(HPO_4)_x(PO_4)_{6-x}(OH)_{2-x}$	1.50<x<1.67
DCPA	Dicalcium Phosphate anhydrous, Monetite	$CaHPO_4$	1.00
DCPD	Dicalcium Phosphate dihydrate, Brushite	$CaHPO_4.H_2O$	1.00
HA	Hydroxyapatite	$Ca_{10}(PO_4)_6(OH)_2$	1.67
MCPM	Monocalcium Phosphate monohydrate	$Ca(H_2PO_4)_6.H_2O$	0.50
OCP	Octacalcium Phosphate	$Ca_8H_2(PO_4)_6.5H_2O$	1.33
pHA	Precipitated Hydroxyapatite	$Ca_{10-x}(HPO_4)_x(PO_4)_{6-x}(OH)_{2-x}$	1.50<x<1.67
α-TCP	α-Tricalcium Phosphate, Whitlockite	α-$Ca_3(PO_4)_2$	1.50
β-TCP	β-Tricalcium Phosphate, Whitlockite	β-$Ca_3(PO_4)_2$	1.50
TTCP	Tetracalcium Phosphate, Hilgenstockite	$CaO.Ca_3(PO_4)_2$	2.00

CaP compounds can be used in the form of granules, cement (granules with phosphate salt and water), and 3D scaffold. The type of 3D scaffold employed can be non-porous or porous as can be seen in Figure 2-8. However, a number of drawbacks are found when using ceramics scaffold, such as: slow degradability and too brittle mechanical properties.

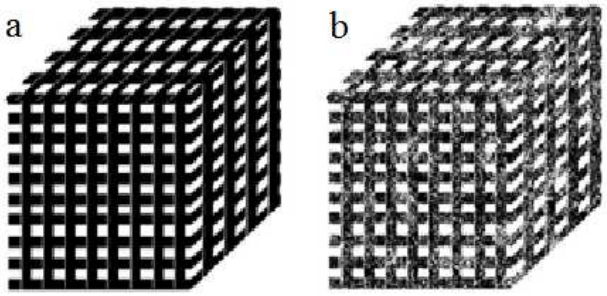

Figure 2-8 Typical ceramic 3D-structure prepared by 3D printing : a. contain only macroporous; b. contain both macroporous & micropores[33]

HA Fibers Precipitations

Besides 3D scaffold, as mentioned before, CaP compound can be used in the form of granules and cement. Furthermore, these days, CaP fibers or whiskers are used to improve mechanical properties of ceramic matrix. For these purposes, HA crystal

preparation has been investigated extensively. Basically, there are two main methods to synthesize HA powders: (1) dry chemical method which include solid-state reaction and (2) wet chemical method which include hydrothermal reaction, precipitation, and hydrolysis methods[37]. By varying the synthesis route, HA particles may display different morphologies (shape and size) as can be seen in Figure 2-9. Plate-shaped apatites can be synthesized by the hydrothermal process using an organic medium. Spherical and fibre-shaped apatites were prepared by ultrasonic spray-pyrolysis, by homogenous precipitation method, by solid state synthesis at high temperature and by sol-gel process[56, 38.]

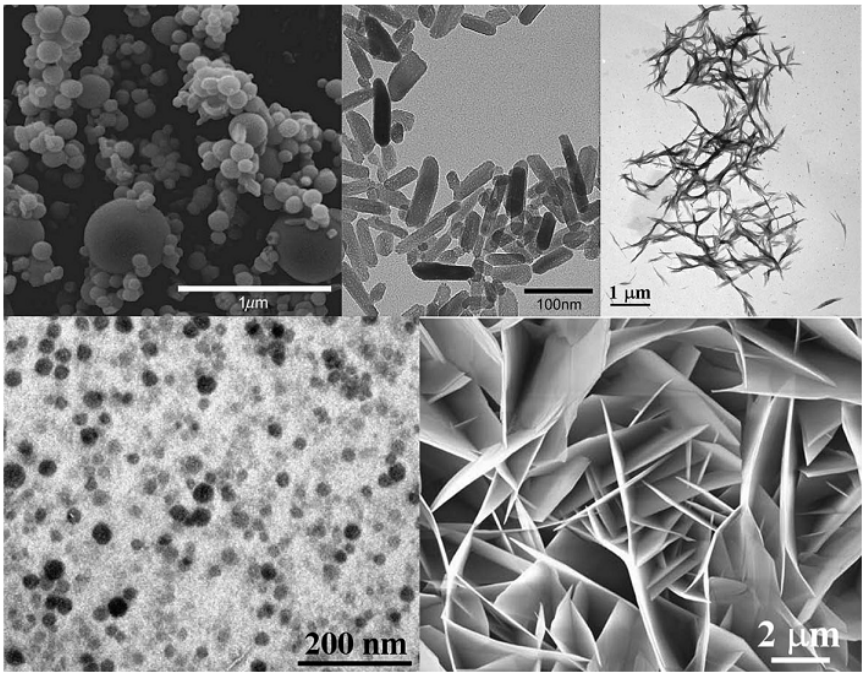

Figure 2-9 Various types of HA morphologies[13]

One popular way to prepare HA crystals is homogenous precipitation. It is claimed to be an easy way to obtain uniform HA particles[39] and tailor the morphologies[38]. It was found that additives can define the final precipitates. The additives can be organic solvents (acetone, methanol, ethanol, buthanol, ethylene glycol, and glycerin) and cations (Na^+, K^+, Mg^{2+}, Sr^{2+}, Ba^{2+}, Al^{3+}, and Y^{3+}). The final crystal can be spherical or fiber-like depending on the additives[38].

Zhang et al.[39] and Aizawa et al.[56] succeeded to produce HA fibers with uniform morphology and good crystalinity. A mixture of 0,167 mol/L calcium ions and 0,1 mol/L phosphate ions were refluxed in a certain temperature. $Ca(NO_3)_2$ was used as the source of calcium; $(NH_4)_2HPO_4$ as the source of phosphate; and urea as additive. Zhang et.al studied different synthetic temperature and time (120h at 85^{o}C, 72h at 90^{o}C, and 48h at 95^{o}C), while Aizawa et.al [56] used 24h at 80^{o}C and followed by 72h at 90^{o}C. It is temperature, synthetic time, pH of the solution, concentration of Ca^{2+} and PO_4^{3-} which become the main factor to influence the HA morphology.

Hydroxyapatite precipitation process may not be a straightforward process since different types of CaP solid phases may precipitate depending on the precipitating medium composition and pH. The formation of HA follows a multistep route which includes solid-solid transformations[13, 40]. The CaP phases involved are: dicalcium phosphate anhydrate (DCPA) or monetite, octacalcium phosphate (OCP) and hydroxapatite (HA). The precipitation of any phase requires supersaturation conditions, being the solubility of each phase a pH dependent parameter. At pH 2.22-5.92, the precipitation order is usually: HA>>OCP>>Monetite[39].

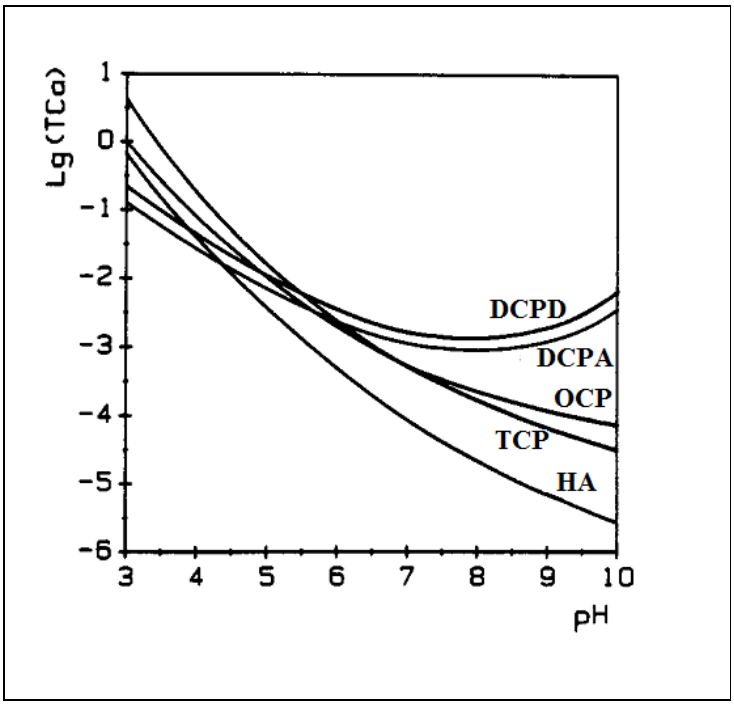

Figure 2-10 Solubility isotherms of calcium phosphate phases in the ternary system of $Ca(OH)_2$-H_3P0_4-$KN0_3$-H_2O at 37 C[41]. The most important CaP compounds may form and subsequently dissolve depending on the solubility depending on this curve

2.2.3. Chitosan/CaP Composite

Combining polymers with ceramics to produce composite scaffold have became one very interesting research approach. Polymer scaffolds have poor mechanical properties and furthermore in the case of chitosan, lack of bioactivity. Conversely, ceramics scaffolds are too brittle and less biodegradable than polymers. Thus composite scaffolds combining these two kinds of materials are expected to present better properties. One problem may arise from composite scaffold manufacturing is as this process might be complex.

A number of researches have been carried out on the topic of chitosan/CaP scaffold. Different phases of CaP were used to prepare scaffold; β-TCP[7,9,10]; nano-HA[42, 43],

and some references used a mixture of CaP invert glasses (consists of CaO, P_2O_5, TiO_2 and Na_2O)[7,10]. Not only variation of the inorganic part, some researches were carried out using chitosan/HA and combination of other polymers, such as gelatin[44,45] and alginate[46].

Thermally induced phase separation (TIPS) which involves freezing and freeze drying is the manufacturing technique mainly used to prepare chitosan/CaP scaffold. Composite scaffolds of chitosan and β-TCP, HA, and invert glass were prepared by addition of CaP powder to a chitosan solution (normally in acetic acid). The solution was put in a container/mold which afterward determines the shape of the scaffold. Instead of using mold, Ang et al.[47] used a robotic desktop rapid prototyping to fabricate the scaffold. The next step prior to both methods is similar which are freezing and subsequently freeze-drying.

Composite scaffold of chitosan/nano-HA were prepared by two methods: (1) addition of $Ca(NO_3)_2$ and $(NH_4)_2HPO_4$ to a chitosan solution; and nano-HA (140-260nm) was formed during the process[8]; this process is called *in situ* and (2) addition of nano HA powder[42]. Chitosan/β-TCP was prepared by adding directly the powder to chitosan solution prior to freezing.

It was reported that several properties were improved by combining chitosan and CaP. Regarding the mechanical properties, Zhang et al.[10] succeeded to increase the mechanical properties of chitosan scaffolds by addition of β-TCP. The adjustment of the type and the amount of the reinforcement enable the production of scaffolds with different microstruture morphology, mechanical properties, and degradation rates too.

Not only mechanical properties, biocompatibility and bioactivity of chitosan/CaP composite scaffold were also improved. Bioactivity test by immersing composite scaffolds on SBF showed (1) mass increase of the chitosan/nHA scaffold which means apatite layer were formed[8] and (2) concentration decrease of the Ca and P concentrations in SBF solution after immersion of chitosan/β-TCP composite scaffold[10]. Biocompatibility study by seeding pre-osteoblasts MC3T3-E1[42,8] and human osteoblast-like MG63[48], shows higher population of cell on composite scaffold of chitosan/nHA. This means that composite scaffolds have superior cytocompatibility.

2.3. Scaffold Manufacturing Techniques

Various manufacturing techniques have been reported to produce polymer composite scaffolds, such as TIPS, solvent casting/particle leaching, solid free-form fabrication, microsphere sintering, scaffold coating, fiber bonding, high pressure processing, hydrocarbon templating, electrospinning, microsphere sintering, and melt molding, etc[2, 14, 21]. Among those manufacturing techniques, solvent casting with or without particle leaching and TIPS combined with freeze-drying are two very popular methods for preparing polymer composite scaffold.

2.3.1. Overview on scaffold manufacturing method

Solvent casting/particulate leaching and TIPS are two methods that require the raw materials to be soluble in order to be processed. Solvent casting procedure involves the casting of a polymer/salt/organic mixture solution followed by solvent evaporation and removal of the salt by dissolution[50]. In solvent casting (as shown in Figure 2-11), the polymer solution is poured into a bed of porogen (the porogen can be salt particles, paraffin microspheres or emulsion drops of defined size). To evaporate the solvent, freeze drying can be applied. The porogen removal can be achieved by rinsing with distilled water or with an organic solvent[2]. In this way, the pore size can be tailored by the size of the porogen and the porosity can be tailored by ratio of the polymer and the amount of porogen[49]. However, two main limitations on using solvent casting are harmful solvents and limited thickness of porous scaffold (film) can be produced.

Figure 2-11 Illustration on scaffold manufacturing using particle leaching method[50]

TIPS is one very popular technique to fabricate 3D porous scaffold with high volume of interconnected micropores. In TIPS, the polymer is dissolved in a certain solvent. Liquid-liquid or solid-liquid phase separation is induced by lowering the temperature. The solvent is then sublimated and leaves a porous polymer scaffold[2, 21]. The limitations of this process are the following: quite long time is needed to sublimate the solvent completely, and shrinkage issues are also a concern.

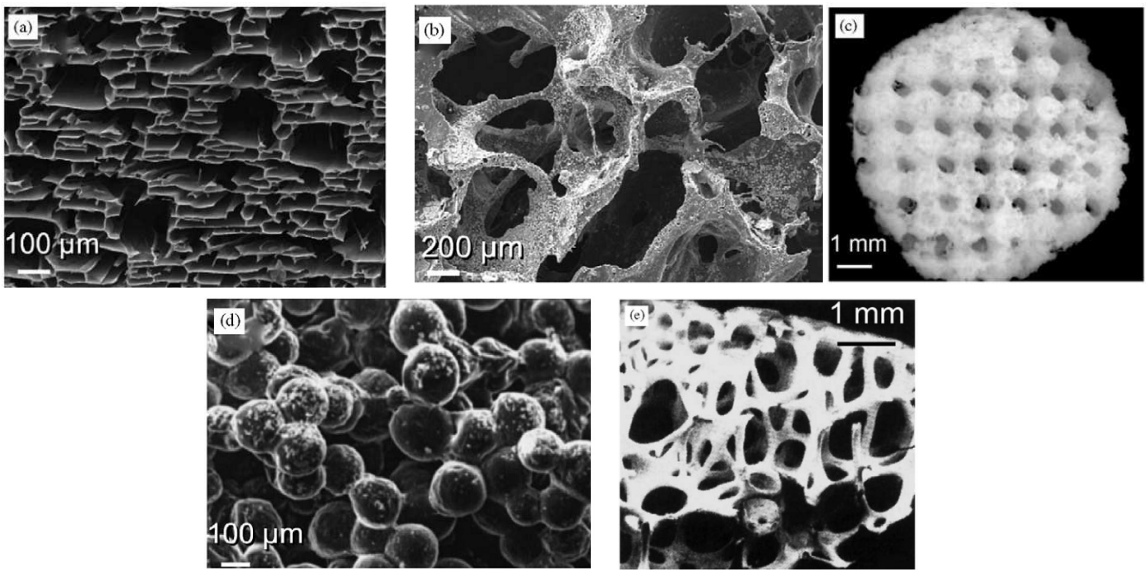

Figure 2-12 Typical morphologies of porous scaffold made by different methods: (a) thermally induced phase separation, (b) solvent casting and particle leaching, (c) solid-free-from techniques, (d) microsphere sintering, and (e) cancellous bone[21]

Table 2-6 Scaffold Manufacturing Techniques List[50]

Fabrication Technology	Required properties	Available pore size (μm)	Porosity (%)	Architecture
Solvent casting /particle leaching	Soluble	30-300	20-50	Spherical pores
TIPS	Soluble	<200	<97	High volume of interconnected pores
Melt molding	Thermoplastic	50-500	<80	Spherical pore
Gas foaming	Amorphous	<100	10-30	High volume of noninterconnected pore
Fused deposition modeling	Thermoplastic	>150	<80	100% interconnected macropores
3-D printing	Soluble	45-150	<60	100% interconnected macropores

For thermoplastic polymer that cannot be dissolved, melt molding, and solid free form fabrication (SFF) techniques can be used. SFF also known as rapid prototyping are computerized fabrication techniques using data generated by CAD systems, computer-based medical imaging modalities, digitizers and other data makers. Several types of SFF are Solid Laser Sintering (SLS), Three-Dimensional Printing (3-DP), and Fused Deposition Modeling (FDM)[51]. The advantage of using SFF is the ability of tailoring porous structures and the good interface with medical imaging.

There are still some other techniques available, such as fiber bonding, membrane lamination, melt molding, hydrocarbon templating, etc. Figure 2-12 shows a typical porous polymer scaffold produced by different methods. Table 2-6 summarizes

information on polymer scaffolds fabrication techniques. It is clear that by using different materials, different methods, and also by controlling the variable in each manufacturing technique, the morphology of the scaffold can be tailored depending on the requirements.

2.3.2. Thermally Induced Phase Separation (TIPS)

Among the wide range of methods for preparing scaffolds, chitosan-based scaffolds have been mostly prepared by TIPS[7,43]. This probably reflects the easy preparation of chitosan solutions by dissolving chitosan in dilute acid.

TIPS works based on the principle that a single homogenous polymer solution prepared at higher temperature is converted via the removal of thermal energy to two-phase separated domains composed of a polymer-rich phase and a polymer-lean phase[52]. The removal of thermal energy is done by lowering the multicomponent system so that it becomes thermodynamically unstable and tends to separate into more than one phase in order to lower the system free energy[49]. After fully frozen, lyophilization/freeze drying is applied to sublimate the solvent-rich phase and leave a porous polymer scaffold. The pore morphology is controlled by any phase transition that occurs during the cooling process[54] i.e. solid-liquid phase separation or liquid-liquid separation.

Basically there are two types of TIPS: solid-liquid phase separation and liquid-liquid phase separation. In solid-liquid phase separation, lowering the temperature induce solvent crystallization from polymer solution; also define as solid formation in liquid phase[49]. Example of solid-liquid phase separation is the separation of chitosan-acetic acid solution; ice of acetic acid solution are formed and separated from chitosan-rich phase. Decreasing temperature can induce liquid-liquid phase separation in the case of a polymer solution with an upper critical solution temperature[49]. An example of this case is a mixture of dioxane and water which have been used to fabricate PLA & PLGA scaffold[52]. However, combination of both separation types can also be used. Lim et al.[53] prepared porous chitosan scaffold from chitosan-acetic acid solution with alcohol as the non-solvent.

Figure 2-13 illustrates a binary phase diagram of polymer solution undergo three different cooling route. Depending on where the end point of quenching is located, whether (1) metastable region between binodal and spinodal curve or (2) unstable region below the spinodal curve, two distinctive morphologies can be achieved: (1) poorly interconnected bead-like structure by nucleation and growth mechanism or (2) well-interconnected open pore structure[52]. Several parameters in TIPS influence the final morphologies (pore size distribution and interconnectivity) of porous scaffold: polymer concentration, quenching rate, and composition of solvent/non solvent[52, 54].

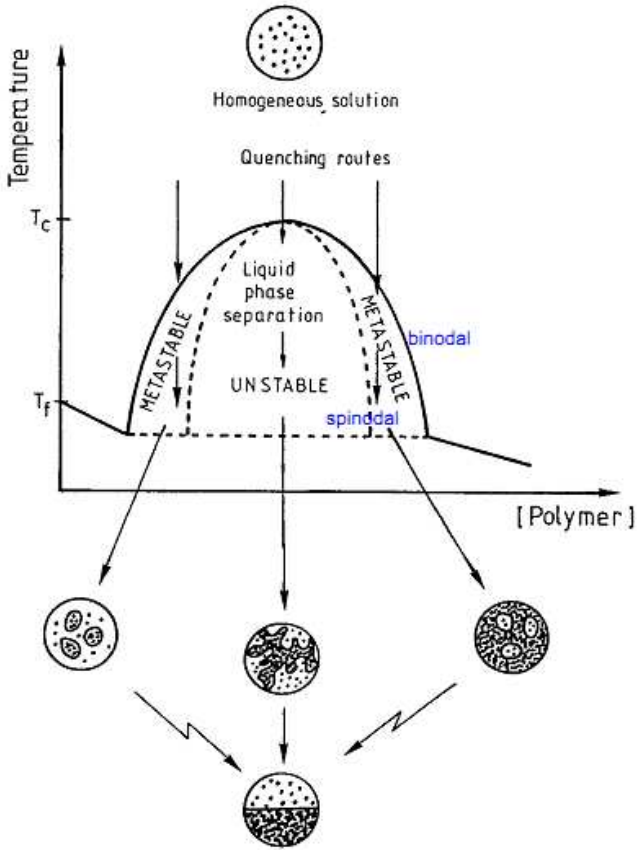

Figure 2-13 Schematic phase diagram illustrating several possibility of morphology depending on cooling route[54]

After the occurrence of phase separation during the cooling process, the frozen solution is freeze dried (or also known as lyophilized), i.e. the solvent is removed at very low pressure and temperature. Such conditions allow a phase change in which the frozen solvent (i.e. water) is converted in gas, i.e. a sublimation process.

Chapter 3
Problem Formulation

In the present work, a systematic study of chitosan based composite scaffolds is carried out. Pure chitosan and composite chitosan scaffolds using different reinforcing particles (HA fibers, monetite platelets and mixture of fibers and platelets) and HA granules loaded with drug) were prepared under different experimental conditions (pH of chitosan solution and freezing temperature).

The HA fibers used to reinforce the scaffolds were prepared by a precipitation method. In this research, two routes combining different time and temperature (4h-80^{o}C followed by 24h-90^{o}C and 24h-80^{o}C followed by 24h-90^{o}C) were applied. The chemical and crystal phase composition and the morphology of the precipitated particles were studied.

Regarding chitosan based scaffolds, some experimental parameters were varied in order to obtain better microstructure, mechanical properties, and bioactivity of the resulting scaffolds. During the preparation of CH solution/suspension, the pH of the solution and the type of reinforcement particles were varied. Two pH values were used: pH 2 and pH 5. The reinforcement particles with different shape and composition were obtained by precipitation: HA-fibers, incipient monetite thin platelets and a mixture between those two types of particles. Furthermore, during TIPS, different freezing temperatures (0, -15, and -196^{o}C (liquid N_2)) were also used. The effects of these variables on scaffold microstructure, mechanical properties, and bioactivity were analyzed and investigated.

For exploiting the potentiality of chitosan scaffolds as a drug delivery system (DDS), dexamethasone (DEX) was selected as a model drug. HA was also selected as a primary drug carrier. HA granules loaded with DEX were independently produced by spray drying HA nanoparticles suspended in a DEX solution. The spray dried HA granules loaded with DEX where then suspended in chitosan solution and subsequently freeze dried. Three different routes for preparing the drug loaded scaffold were adopted and their drug release profiles were studied.

Chapter 4
Experimental Procedure

This research is divided in three main parts: synthesis of CaP particles by precipitation method, preparation of CaPC (calcium phosphate-chitosan) composite scaffold and drug-loaded chitosan composite scaffolds. The CaP precipitates obtained from part one was used to reinforce chitosan scaffolds. While for drug-loaded scaffold, HA granules prepared by spray-drying were used. The overall scheme of this research is described in Figure 4-1.

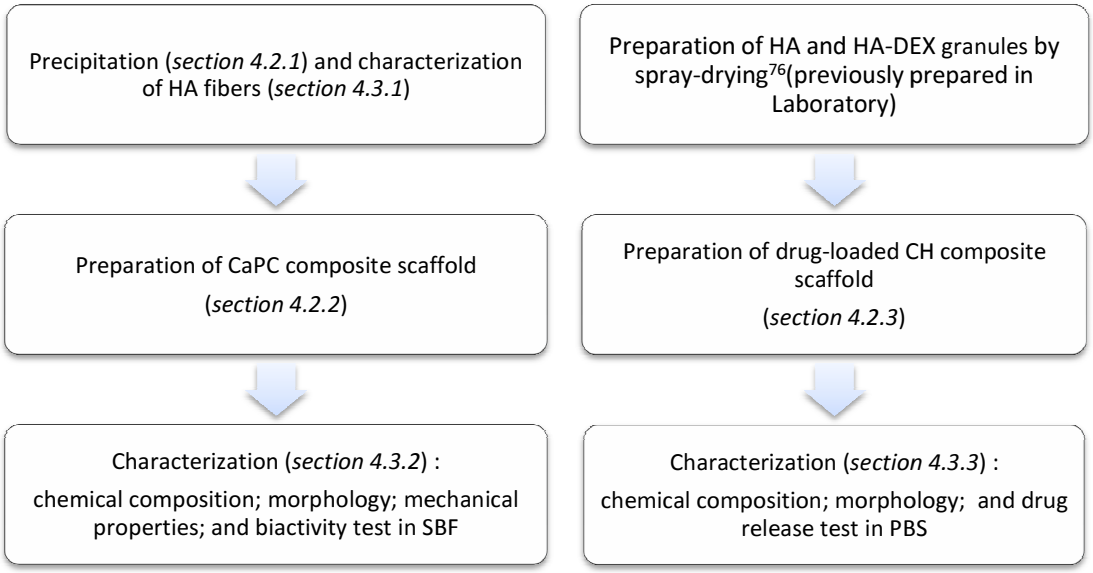

Figure 4-1 Scheme of experimental done: HA fibers precipitation and its chitosan composite (left) and HA granules preparation and its chitosan composite (right)

4.1. Materials

The materials which were used in CaP synthesis experiment are: (1) ammonium hydrogenphosphate, >98%, ACS reagent from Aldrich Chemistry, Germany; (2) calcium nitrate-4-hydrate, analytical reagent from Riedel-de Haen, Sigma-Aldrich. Germany; (3) urea ($(NH_2)_2CO$) from Sigma-Aldrich, Germany; and (4) HNO_3 65%, for analysis from Carlo Erba, Portugal.

For CaPC composite scaffold preparation, the materials used are (1) chitosan, from crab shells, deacetylation degree approximately 80%, practical grade from Aldrich Chemistry (viscosity > 200.000 cps). Germany; (2) acetic acid 96%, pro analysis from Merck, Germany; (3) ethanol 96% from AGA, Portugal; (4) ammonia solution 25% from Riedel-de Haen, Germany. The reagents used in the preparation of SBF test solution are listed in Table 4-3.

In vitro release studies of drug-loaded CH composite scaffold experiments, the following reagents were used: (1) HA Suspension (5% HAp Nanoparticles) from Fluidinova, nanoXIM, Portugal; (2) dexamethasone 96% from ACROS organics, USA; (3) $Na_2HPO_4.2H_2O$ from Carlo Erba, Milano; and (4) $NaH_2PO_4.H_2O$ from Merck, Germany.

4.2. Preparation Methods

4.2.1. Precipitation of HA Fibers

HA fibers were prepared by a precipitation method in aqueous solution, following a procedure described by Aizawa et al.[56]. A solution of 0,167M $Ca(NO_3)_2$, 0,100M $(NH_4)_2HPO_4$, 0,50 M $(NH_2)_2CO$ (urea) and 0,1M HNO_3 was refluxed for a certain time at 80°C and 90°C.

Table 4-1 Raw Materials for HA Fiber Synthesize

Composition		Raw Material for 250 mL solution	
$Ca(NO_3)_2$	0,167 M	$Ca(NO_3)_2.2H_2O$	9,85 g
$(NH_4)_2HPO_4$	0,100 M	$(NH_4)_2HPO_4$	3,30 g
$(NH_2)_2CO$	0,50 M	$(NH_2)_2CO$	7,50 g
HNO_3	0,10 M	HNO_3 65%	1,73 mL

The first experiment (so called *batch 1*) was carried out by refluxing (Figure 4-2-a) the solution for 24h at 80°C, followed by aging at 90°C for 72h. The second experiment (so called *batch 2*) was done by refluxing the solution for 4h at 80°C followed by aging at 90°C for 72h.

Small amounts of the suspension were withdrawn in the middle of the refluxing process in order to follow the phase evolution. This procedure involved mixing and shaking the container to make sure that the suspension is uniformly sampled, and then pouring a little amount to a beaker, filtering in vacuum filter (Figure 4-2-b), washing the solid cake with distilled water, and drying it in the oven at 60°C. During the refluxing process, the pH of the solution was monitored and revealing an increasing from ~1 to ~7,5 since NH_3 was released by the hydrolysis of urea[56].

For *batch 1*, samplings were carried out at 0,5h, 1h, 2h, 4h, 8h, 20h, and 24h at 80°C; followed by 24h, 48h, and 72h at 90°C. For *batch 2*, samplings were performed at 2h and 4h at 80°C; followed by 24h, 48h, and 72h at 90°C. All the obtained dried powders were analysed by X-Ray Diffraction (XRD), N_2 adsorption using the BET isotherm (BET), and Scanning Electron Microscopy (SEM) to characterize the powder crystal phase composition and morphology.

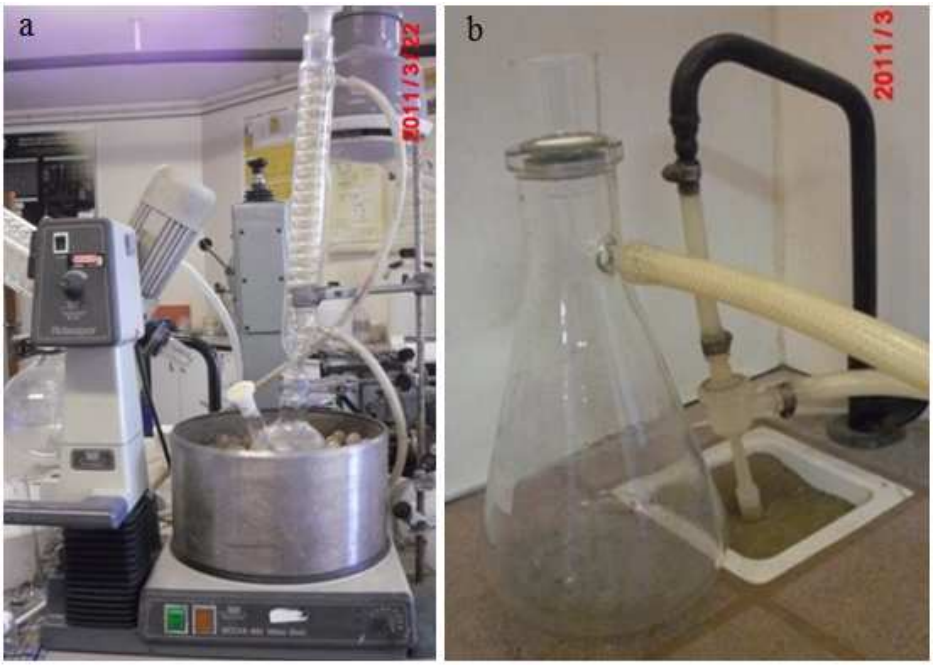

Figure 4-2 (a) Reflux apparatus : round glass container equipped with cooling column immersed in waterbath; (b) vacuum filter with water-driven pump

4.2.2. CH/CH Composite Scaffold Preparation

The main steps of the chitosan scaffold preparation are shown in Figure 4-3. Starting from chitosan solution, the next step was freezing to let the solvent solidify, subsequently followed by freeze-drying to sublimate the solvent and obtain the porous scaffold.

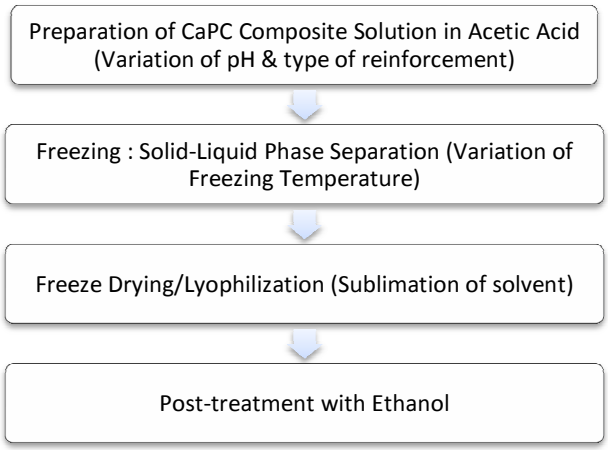

Figure 4-3 Scheme of CaPC composite scaffold preparation

Preparation of Chitosan solution/suspension

2 wt% chitosan solutions were prepared with two different pH values, i.e. pH ~2 and pH ~5. The chitosan solution at pH ~2 was prepared by dissolving 2g of chitosan in 98g acetic acid 2M (pH =2.5-2.6; further these scaffolds are referred with scaffolds pH 2). The mixture was magnetic stirred at 50^{o}C for 3-4 hours until complete dissolution. Chitosan solution at pH ~5 was prepared by weighing 2g of chitosan powder, adding (1) ~70mL of distilled water, (2) acetic acid 25% drop by drop while stirring at 50^{o}C until complete dissolution (pH ~3,5), and (3) ammonia (ammonia 25% : H_2O = 2:1) drop by drop until pH ~5 was reached. Finally, distilled water was added until the total mass 100 g of the solution.

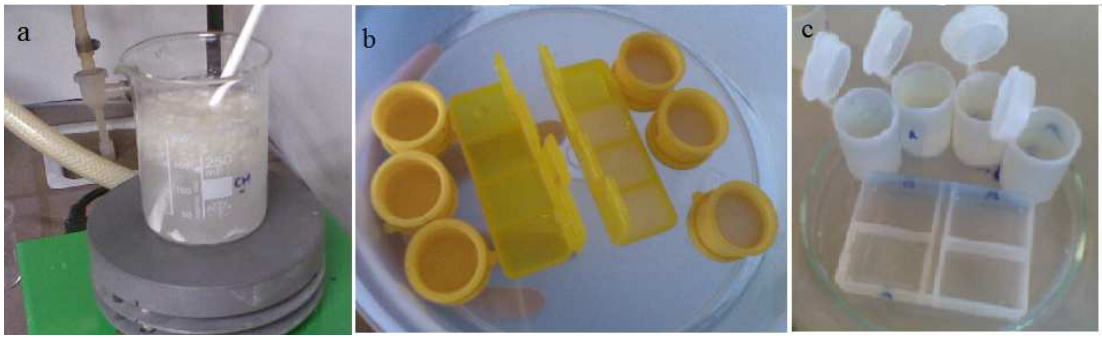

Figure 4-4 (a) Chitosan Solution Preparation with Magnetic Stirer; (b) and (c) Differently shaped containers used for preparing the chitosan-based scaffolds

The composite scaffolds were prepared with a (chitosan:calcium phosphate) ratio of (2:1) by weight. Following the same procedure as described above, before adding the distilled water to 100g of the total mass, 1 gram of calcium phosphate (hydroxyapatite fibers which was obtained via precipitation method (4h 80^{o}C+24h 90^{o}C), monetite powder (30min of reflux), mixture of HA fibers & monetite powder and spray dried-HA granules with or without DEX) were then added to the solution. The resulting suspension was then stirred for 1 to several hours in order to homogenize. Ten minutes of sonication were also allowed in order to ensure a complete mixing. Finally, the chitosan solution or the chitosan/calcium phosphate suspension were poured into a container (a mold which determines the final 3D shape of the scaffold) being then ready to be frozen.

Three different freezing temperature were used in this experiment, i.e. ~0^{o}C , -15^{o}C and -196^{o}C (liquid N_2). The freezing process at ~0^{o}C and -15^{o}C were carried out during 24h. Quenching in liquid N_2 was carried out very rapidly, being the container directly immersed in liquid N_2 for ~4min. After freezing and quenching procedures, the solidified chitosan solution/suspension was quickly transferred to the freeze-dryer.

Freeze-Drying/Lyophilization

Frozen chitosan solution/suspensions were placed in a freeze-dryer as illustrated in Figure 4-5-a. Freeze drying (also known as lyophilization) is a process aiming to remove the solvent through a sublimation process. Labconco Freeze Dry System (operating at ~52^{o}C and 12x10^{-3} mbar) was used in this experiment. In order to reach complete sublimation of the solvent, 3 days of freeze-drying were applied to all the samples. Particular attention was paid to ensure that a constant pressure is required; increase of pressure will not allow phase transformation from ice to water vapor directly but from ice to liquid water. If this occurs in the beginning of lyophilization, the samples might be damaged, since chitosan (in the presence of acetic) might dissolve.

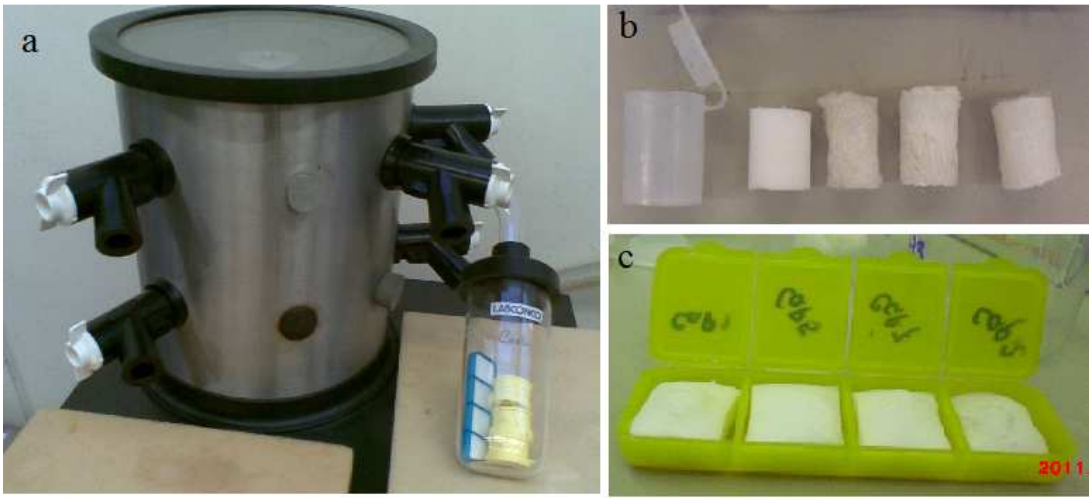

Figure 4-5 (a) Frezee-drying apparatus; (b) and (c) Various shape of CH/CH composite scaffold after freeze-dried

Postprocessing with Ethanol

Freeze-dried samples were rehydrated and stabilized with ethanol treatment following the procedure by Madihally et al.[18] with modifications in order to remove the acetic which still existing in the scaffold. This treatment is needed in order to avoid moisture uptake by the scaffold.

The first treatment was done by immersing the scaffold in absolute alcohol (99%) for 1 hour, followed by 30minutes in 70% ethanol and another 30minutes in 50% ethanol. After immersion in ethanol, the samples were subsequently quenched in liquid N_2 and placed again in freeze-drying for 24h.

4.2.3. Drug-Loaded Composite Scaffold

Drug-loaded composite scaffold was prepared with the same procedure as CH composite scaffold (as written in section 4.2.2) in which drug-loaded HA granules were used instead of fiber to reinforce chitosan. Pure HA granules and drug-loaded HA granules were produced by spray-drying of HA and HA-drug suspension[76]. In this study, dexamethasone (DEX, Figure 4-6) as one anti-inflammatory drug was used as drug model and spray-dried with HA suspension in the proportion of 10%wt (DEX/HA).

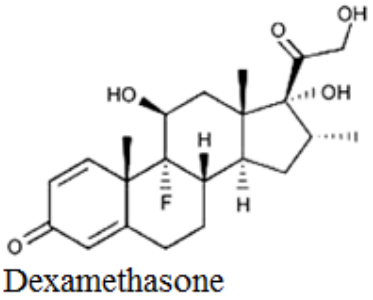

Figure 4-6 Chemical Structure of Dexamethasone[80]

Different procedures were used in the preparation of CH composite solution containing drug-loaded HA granules: (1) pure HA granules and DEX were added to CH solution (pH ~5), (2) drug-loaded HA granules were added to CH solution (pH ~5) without any additional DEX, and (3) additional DEX was added to CH composite solution prepared with the second procedure (Table 4-2)

Table 4-2 CH Composite Scaffold Solution/Suspension Composition for DDS

	Procedure 1	Procedure 2	Procedure 3
2%wt CH solution	10 g	10 g	10 g
HA granules	100 mg pure HA granules	100 mg spray dried HA-DEX granules	100 mg spray dried HA-DEX granules
Additional DEX	-	-	10 mg

CH composite solutions were magnetic-stirred and ultra-sonicated in order to prepare an homogenous solution. The solution was put in a mold (Figure 4-5-c) and subsequently put in the freezer (0^oC) for 24h. Frozen solution was then freeze-dried for 70h to sublimate all the solvent.

4.3. Characterization

4.3.1. Precipitation of HA Fibers

Characterization of the as synthesized calcium phosphate powder was carried out by several methods, including: X-Ray diffraction (XRD), N_2 adsorption with the BET

isotherm, and Scanning Electron Microscopy (SEM). XRD was performed in order to identify the powder crystal phase composition. This test was carried out in a equipment Rigaku Geigerflex DMAX III/C using monochromatic CuKα (1.54056 Å) radiation at 40kV. The 2θ scan range was 3-80^o with the scanning speed 3^o/min.

Relationship between shape of peaks in XRD spectra and crystallite size is explained by The Scherrer equation[57]. The peak broadening can be observed when crystallite size is smaller than 100Å. Smaller crystallite size and more random oriented crystal will have broader diffraction peaks. Scherrer equation is written in equation 4.1.

$$d\ (\dot{A}) = \frac{c.\propto}{B \cdot cos\theta} \tag{4.1}$$

$$B = \frac{(2\theta_{high} - 2\theta_{low})}{180} \cdot \pi \tag{4.2}$$

where α is x-ray wavelength (1.54Å in this case); c is a factor depending on crystal shape (usually in the range of 0.9-1; 0.9 is taken); B is the difference in angles at half of maximum intensity or also called full width at half max (FWHM; which is calculated based on equation 4.2); and θ is the Bragg angle in radian[57]. Monetite crystallites size were measured based on peak (002), OCP based on peak (010), and HA based on peak (300).

In order to calculate the relative amount of each phase in one sample, the area below each peak was calculated. For crystallite size calculation, the same peak area of monetite were measured based on peak (002) at 2θ=~26.5^o, OCP based on peak (010) at 2θ=~4.6^o, and HA based on peak (300) 2θ=~32.5^o.

The surface area of the powder was accessed by N_2 adsorption at 200^{o}C with the BET isotherm in equipment from Micromeritics Gemini.

The powder morphology was evaluated by scanning electron microscopy Hitachi SE-70 SEM. The powder samples were dispersed on the sample holder with the help of carbon-tape and then coated with a conductive layer of gold-palladium and finally observed in SEM at 15kV using different magnifications.

4.3.2. CH/CH Composite Scaffold

X-Ray Diffraction Analysis

X-Ray diffraction analysis (Rigaku Geigerflex DMAX III/C) allowed to identify the chemical composition of samples using monochromatic CuKα (1.54056 Å) radiation at 40kV. The 2θ scan range was 3-80^o with a scanning speed 3^o/min.

Density Studies

Densities of the scaffolds were calculated by dividing the mass of the scaffold by their volume. The mass was measured in an analytical balance with precision of 0.1mg and

the size was measured by a micrometer. Each value of density was an average from 3-5 specimens for each type of scaffold.

Microstructure of Scaffold

Scaffold morphology was evaluated by scanning electron microscopy (SEM Hitachi SU-70). Samples were immersed in liquid nitrogen, cut into smaller pieces, and glued to the sample holder with the use of carbon-glue (as illustrated in Figure 4-7); coated with conductive layer of gold-palladium; and observed in SEM at 15kV using different magnifications.

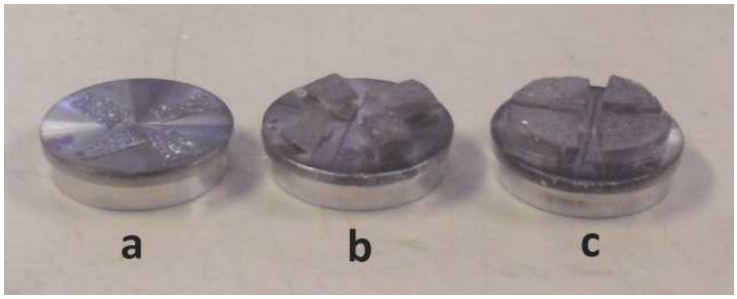

Figure 4-7 Prepared samples for SEM observation: (a) CaP powders; (b) and (c) CH/CH composite scaffold

Average pore size of obtained scaffolds were calculated using ImageJ (Figure 4-8) from 15-20 of pores.

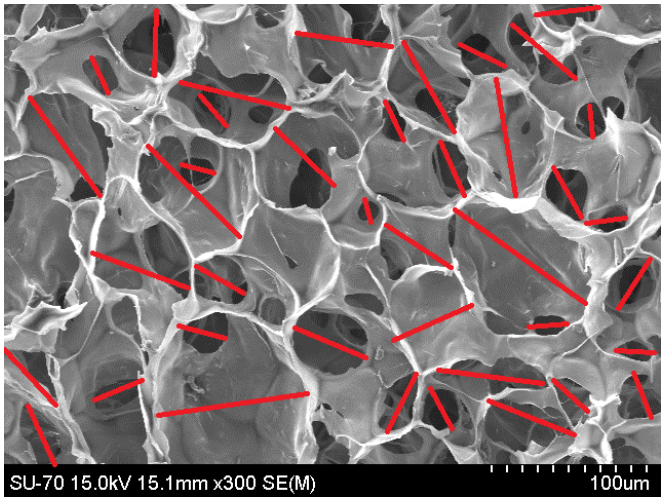

Figure 4-8 Pore Size Calculation using ImageJ

Three-dimensional reconstruction of scaffold structure was done by µ-CT (SKYSCAN 1072) in Characterization Lab II at 3B's Research Group, Department of

Polymer Engineering, UMinho, Guimaraes, Portugal. The selected samples, CH-fibers/pH 5/(-15^{o}C), CH-fibers/pH 5/0^{o}C, CH-fibers/pH 5/(-196^{o}C), and CH-fibers/pH 2/(-15^{o}C) were chosen to be representative to study the influence of pH and freezing temperature. Each sample was cut into small cylinder in the size of ~3mm in diameter and ~7-10mm in height.

Compressive Test

The scaffolds compressive mechanical behavior for the as prepared scaffold (without ethanol treatment) was tested using a Bose Smart Test equipment as shown in Figure 4-9. The specimens were cylindrical about 17-19mm high and 15-17mm in diameter. The crosshead speed was set at 1mm/min, and the load was applied until the specimens deformed to approximately 60-70% of its original thickness. At least three specimens were tested for each type of samples.

Figure 4-9 Compression Test Apparatus

The strain-stress curves were built based on the data obtained from the machine. The compressive modulus was calculated as the slope of the initial linear region; while the compressive strength was taken from the intersection between the linear line and the plateau region.

In vitro biomineralization studies

In vitro biomineralization in SBF (simulated body fluid) was done to the selected samples to observe the bioactivity of the scaffold. The selected samples: pure CH/pH 5/(-15^{o}C), CH-fibers/pH 2/(-15^{o}C), and CH-fibers/pH 5/(-15^{o}C) were chosen to compare different biomineralization ability between pure & composite scaffold and also the composite scaffold which were prepared at different pH.

SBF with the composition shown in Table 2-3 were prepared following the procedure by Kokubo and Takadama[24]. The reagents which were used to prepare 500mL of SBF were listed in Table 4-3.

To prepare 500 mL of SBF, first of all, 350 mL of deionized water was put in a glass beaker and heated to 36,5±1,5^{o}C under stirring. Reagents 1 to 8 were dissolved one by one following their order. Reagent 9 ($CNH_2(CH_2OH)_3$) was added drop by drop while monitoring until it reached pH 7,45. At this value the addition of reagent 9 was stopped and HCl 1M was added in order to lower the pH to 7,42. Again reagent 9 was added until pH raised to 7,45. This process was repeated until all reagent 9 was dissolved. Finally, HCl 1M was added to adjust the pH to 7,40. The solution was poured to volumetric flask and subsequently deionized water was added until a final volume of 500mL. SBF was stored in fridge (5-10^{o}C) and shall be used within 30 days after preparation.

Table 4-3 Reagents for Preparing SBF

Order	Reagent	Quantity	Supplier	Purity (%)
1	NaCl	3,998 g	Merck	99,5
2	$NaHCO_3$	0,175 g	Riedel-de Han	99,7
3	KCl	0,112 g	Merck	99,5
4	$K_2HPO_4.3H_2O$	0,114 g	Merck	99
5	$MgCl_2.6H_2O$	0,1525 g	Merck	99-102
6	HCl 1M	19,5 mL	Prepared in the lab	
7	$CaCl_2.6H_2O$	0,274 g	Fluka	99
8	Na_2SO_4	0,0359 g	Panreac	99
9	$CNH_2(CH_2OH)_3$	3,0285 g	Riedel-de Han	99,5
10	HCl 1M	0-5 mL	Prepared in the lab	

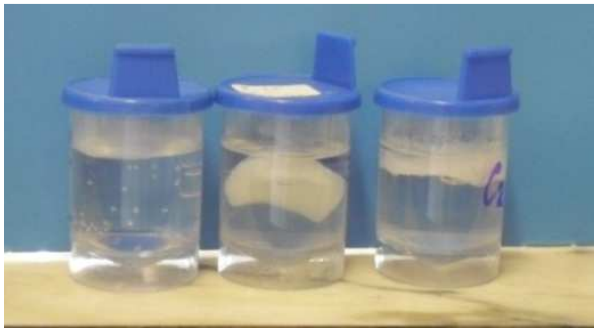

Figure 4-10 Samples for bioactivity test in SBF: blank SBF (left), chitosan/chitosan composite scaffold (middle and right)

Bioactivity test was carried out by immersing a certain size/mass of scaffold in SBF (Figure 4-10). The scaffolds used were ethanol-treated scaffolds. As-prepared scaffold from freeze-drying cannot be used since the acetic acid left in the surface trigger dissolution of chitosan scaffold.

SBF was put in plastic bottles and placed in oven to maintain the temperature at 36-37°C. The volume of SBF that was used for testing was calculated based on equation 4.3.

$$V_S = S_a/10 \quad (4.3)$$

where V_s is the volume of SBF (mL) and S_a is the apparent surface area of specimen (mm^2)[22]. For porous materials, the volume of SBF should be greater than the calculated one.

After immersion for different periods of time (7, 14, and 21days), the scaffolds were separated from the liquid part, washed with deionized water, frozen with liquid nitrogen, and freeze-dried for at least 24 hours. The morphology of the samples after being immersed in SBF was investigated by SEM. Energy-dispersive X-Ray (EDX) spectroscopy analysis was performed on Hitachi SE-70 SEM equipped with Bruker AXS Microanalysis. X-Ray diffraction analysis (Rigaku Geigerflex DMAX III/C) and Fourier transform infrared spectroscopy – attenuated total reflectance (FTIR-ATR), using FT-Infrared Bruker Optics Tensor 27 were performed to allow identification of the chemical phase or functional groups.

The liquid parts were collected with a syringe equipped with 0.22µm filter and analyzed by inductively coupled plasma spectroscopy (ICP) to measure the Ca & P concentrations.

The variations of Ca and P concentrations are expressed as ΔCa and ΔP in mg/L which are calculated based on equation 4.4. and 4.5.

$$\Delta Ca = [Ca]_0 - [Ca]_t \quad (4.4)$$

$$\Delta P = [P]_0 - [P]_t \quad (4.5)$$

Where $[Ca]_0$ and $[P]_0$ are initial concentrations before sample immersion and $[Ca]_t$ and $[P]_t$ are concentrations after immersion of a certain time. If ΔCa and ΔP are positif, it means that there are decreases of ions concentrations.

4.3.3. Drug-Loaded Composite Scaffold

In vitro dexamethasone release in PBS

Release studies of DEX were conducted in PBS (phosphate-buffered solution) at pH 7.4 and 37°C. PBS was prepared by mixing 405mL of 0.2 M $Na_2HPO_4.2H_2O$ and 95mL of 0.2 M $NaH_2PO_4.H_2O$.

To perform the drug release test, specimens with size around 10x6x4 mm^3 and mass around 0.012-0.017g were immersed in 10mL PBS in plastic bottles and kept at 37°C. Figure 4-11 illustrated the drug release test in which a number of containers were prepared. After predefined time intervals, the scaffold was separated from the solution. The solution aliquots were withdrawn using a syringe equipped 0.22µm filter and placed in a plastic container.

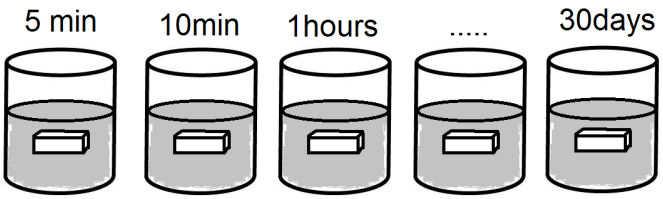

Figure 4-11 Illustration of drug release test in which one piece of scaffold is immersed in PBS for each time of sampling

The evaluation of the DEX concentration in the released medium was carried out by UV-Visible spectroscopy (UV-3100 Shimadzu) at a wavelength of 242 nm. A standard calibration curve was obtained when DEX standard concentration solutions in PBS medium were used.

Microstructure of Scaffolds

Scaffold morphology after and before PBS immersion was investigated by Hitachi SU-70 SEM. Samples were observed by SEM at 15kV using different magnifications.

Chapter 5
Results & Discussions

In the present chapter, the results respecting (i) the precipitation and characterization of calcium phosphate (CaP) particles, (ii) the preparation and characterization of chitosan (CH)-based scaffolds and (iii) the drug (dexamethasone, DEX) release behaviour of DEX loaded scaffolds will be analysed and discussed in the following sections, i.e. sections 5.1, 5.2, and 5.3, respectively.

5.1. Precipitation of HA Fibers

The experimental results respecting the crystal phase composition and morphology aspects of the precipitated calcium phosphate (CaP) particles obtained by the refluxing method will be firstly presented. A comprehensive discussion aiming to compare these results with the previous ones reported for the same method by Aizawa et al.[56] will be then attempted.

5.1.1. Crystal phase composition of precipitated CaP particles

As mentioned in the experimental procedure, two different methodologies were followed aiming at obtaining HA fibers: (1) refluxing the precipitating medium at 80°C for 24h and then at 90°C for 72h and (2) refluxing the solution for 4h at 80°C and then at 90°C for 72h.

Figure 5-1 and Figure 5-2 show the evolution of the XRD spectra for the CaP precipitates withdrawn from the precipitating medium after different periods of time. It is observed that incipient monetite peaks start being detected after 30min of refluxing which then become more intense and sharper after 60min (Figure 5-1). OCP diffraction peaks started to be noticed after 20 hours. Both the peaks of monetite and OCP became sharper with the increase of refluxing time. After 24h at 80ºC monetite and OCP are still the main crystalline phases being detected. This crystalline phase evolution of the precipitates is accompanied by a significant pH variation within the precipitating medium, from ~1 to ~5 as depicted in Figure 5-3. When the particles obtained after refluxing at 80ºC for 24h are now exposed to refluxing at 90ºC during 72h, HA is the dominant crystalline phase with some OCP still detected in the XRD. As shown in Figure 5-3, HA crystallization is followed by a pH increase to 7.5.

Figure 5-2 illustrates the diffraction peak evolution for the particles precipitated by the second methodology, i.e. the CaP precipitates obtained after 4h at 80ºC and then refluxed at 90°C during 72h. After refluxing at 90°C for 24h HA peaks become noticed as well as a strong OCP peak. As refluxing at 90ºC goes HA peaks become more intense while OCP is unnoticed. After 72h at 90ºC the precipitated particles evidence HA as the dominant crystalline phase with traces of monetite. It thus concluded that the increase of

the refluxing temperature from 80°C to 90°C has speed up the formation of HA crystalline phase.

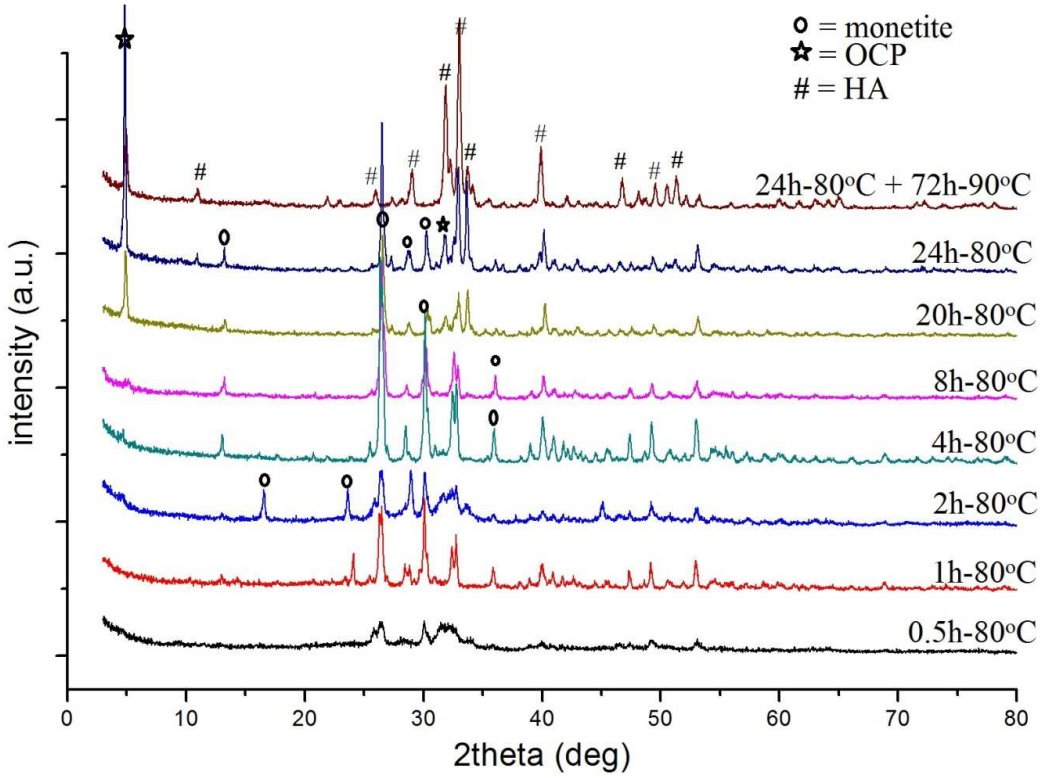

Figure 5-1 XRD spectra of CaP precipitates showing an increase of peaks' sharpness of monetite and OCP during 24hours-reflux at 80°C

Table 5-1 shows the crystallite size development of the three main compounds detected in XRD (monetite, OCP, and HA) during precipitation. It is observed that both monetite and OCP present crystallite size variation curves with maxima while HA crystallite size values increase continuously during refluxing at 90ºC. Moreover it is evident that regardless the used methodology HA crystallites after refluxing at 90ºC are well developed with sizes in the range 170 – 180 Å

Table 5-1 List of crystallites size which increase and decrease during reflux

Samples	Monetite	OCP	HA
2h 80°C	61.77 Å	-	-
4h 80°C	151.39 Å	-	-
8h 80°C	136.81 Å	-	-
20h 80°C	126.43	127.51 Å	-
24h 80°C	-	226.37 Å	121.25 Å
24h-80°C + 72h-90°C		133.18 Å	186.43 Å
4h-80°C + 24h-90°C	-	137.44 Å	133.24 Å
4h-80°C + 48h-90°C	-	82.15 Å	143.55 Å
4h-80°C + 72h-90°C	54.97 Å	-	170.08 Å

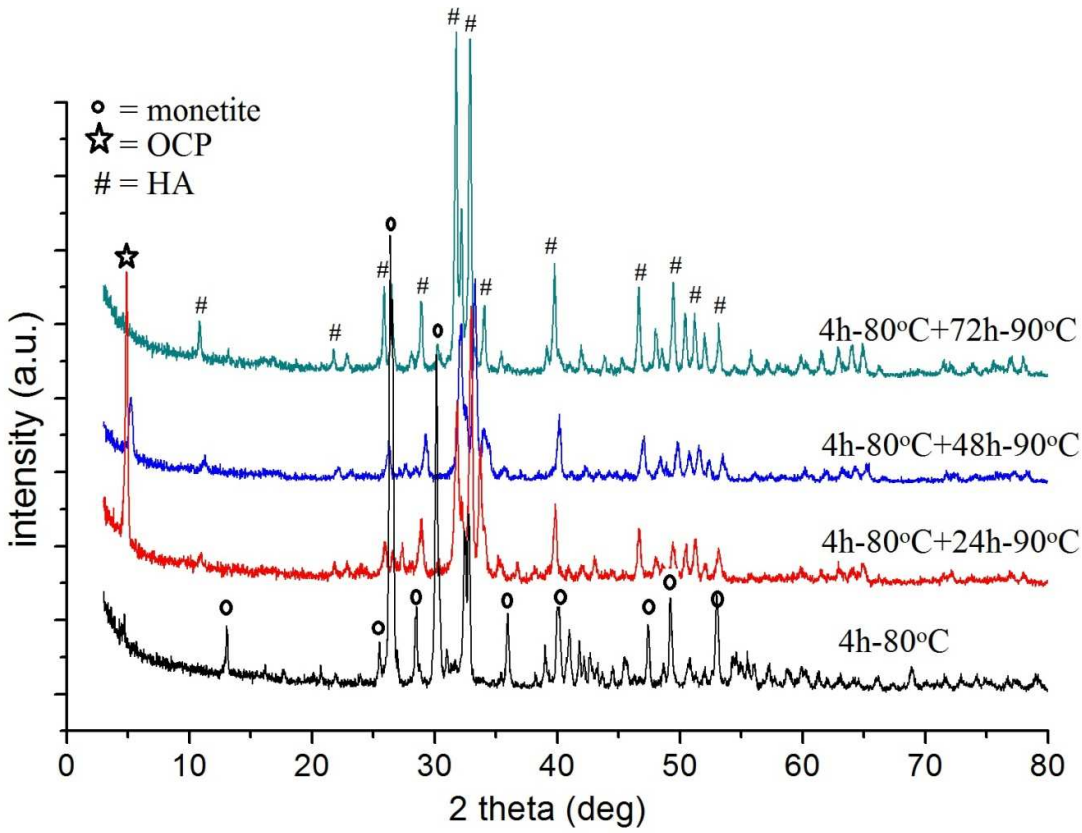

Figure 5-2 XRD spectra showing a decrease of OCP peaks and a increase of HA peaks during reflux at 90°C

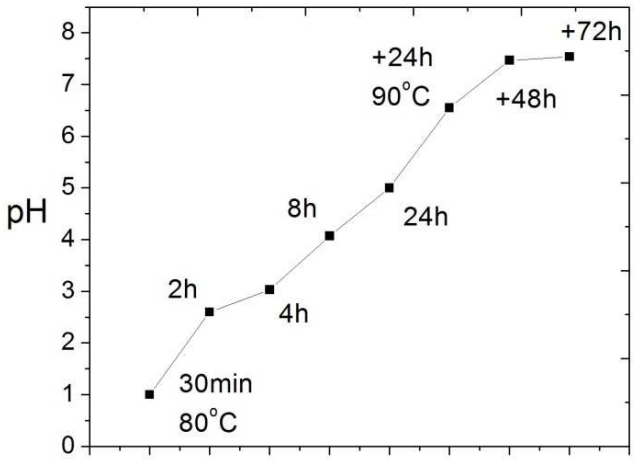

Figure 5-3 pH dependence of the reflux time and temperature during the HA precipitation process (24h 80°C + 72h 90°C)

5.1.2. Crystal Morphology

Figure 5-5 shows SEM images of CaP precipitates obtained after refluxing at 80 and 90°C for different periods of time. Different morphologies are revealed as the refluxing time increases: a mixture of spherical particles and thin platelets assembled in a

florrete-like structure is evidenced after a short period, i.e. 30min, which then converts to thicker platelet-like particles and later on to a prismatic morphology as refluxing continues; after longer periods fibers start to be noticed and become the dominant shape after 24 hours. It is worthy to be mentioned that no relevant morphology change is noticed when the fibers obtained after refluxing at 80ºC are subsequently refluxed at 90ºC. Futhermore, it is observed that fibers are also obtained when the prismatic particles formed after refluxing at 80ºC are then submitted to a 90ºC refluxing.

The evolution of the specific surface area of CaP precipitates during precipitation is illustrated in Figure 5-4. The surface area decreased drastically from $30m^2/g$ to $0.6m^2/g$ during the first 4 hours of refluxing being this low value maintained during the remaining refluxing time. The subsequent refluxing at higher temperature (90ºC) allowed a slight increase of the specific surface area to $2m^2/g$.

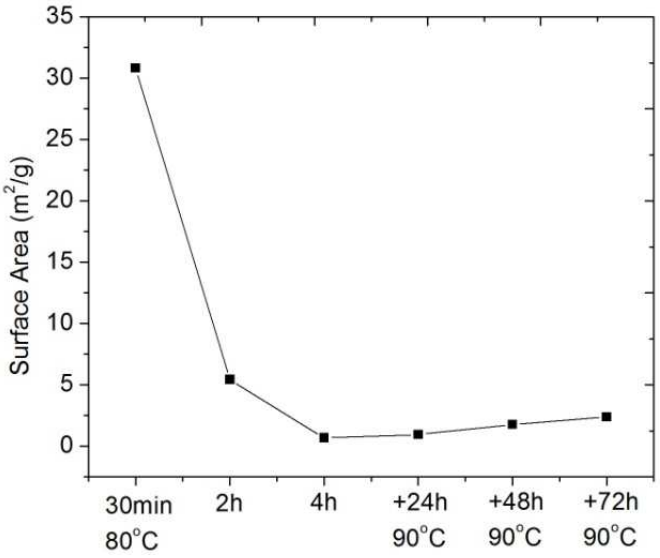

Figure 5-4 variations of precipitates specific surface area during HA precipitation process (4h 80°C + 72h 90°C)

5.1.3. Growth of HA fibers

HA particles precipitation from moderately acidic solution is also known as a soft chemical route in which no subsequent high-temperature annealing process is required for obtaining the desired crystal phase. HA fibers precipitation is a complex process since it might not only involve nucleation and growth of a single crystalline phase but rather secondary nucleation or phase transformation[13]. A number of experimental conditions which influence HA precipitation are known to be reagents concentrations, molar ratio of precursor ions, pH, temperature, presence of additives among others[13, 38, 39]. In the present work, $Ca(NO_3)_2$ and $(NH_4)_2HPO_4$ were used as source reagents of calcium and phosphate, respectively; HNO_3 and urea were used as additives for pH control.

a. 30min-80°C

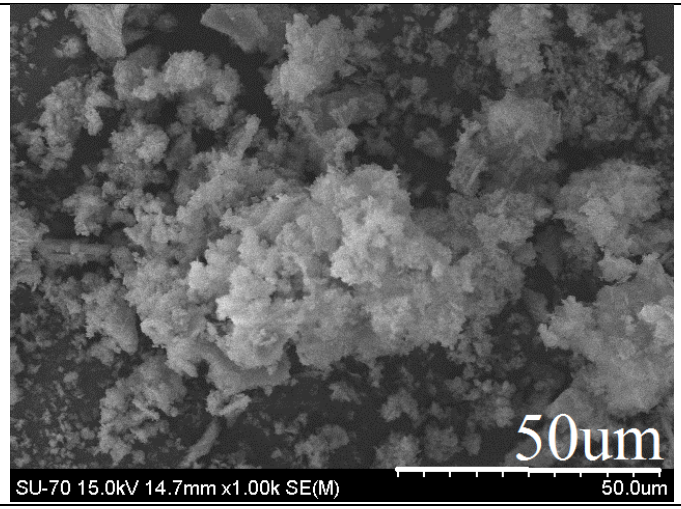

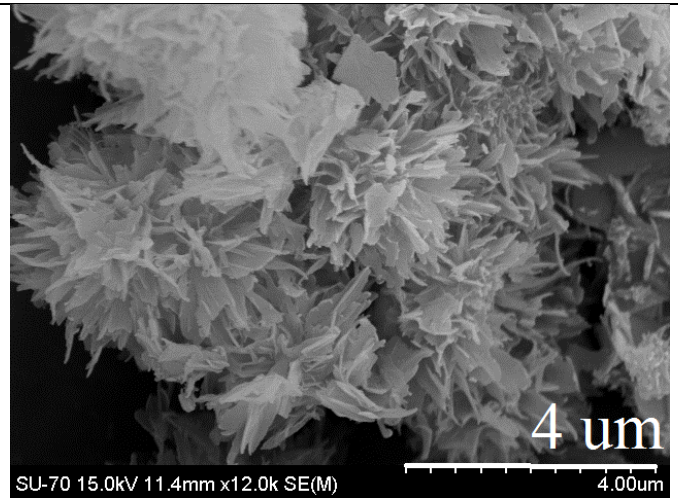

b. 2h-80°C

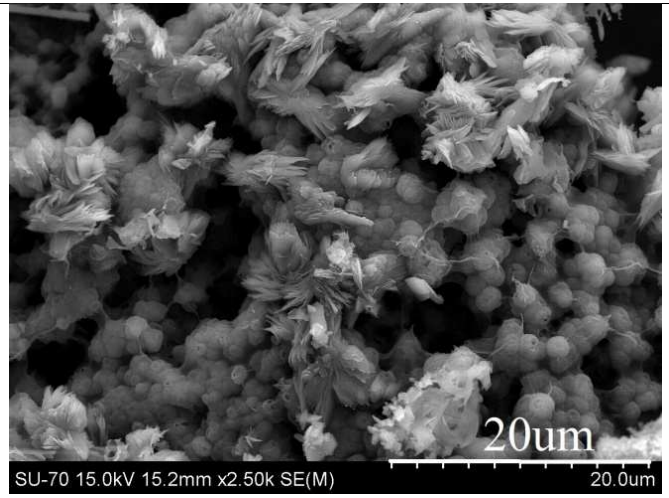

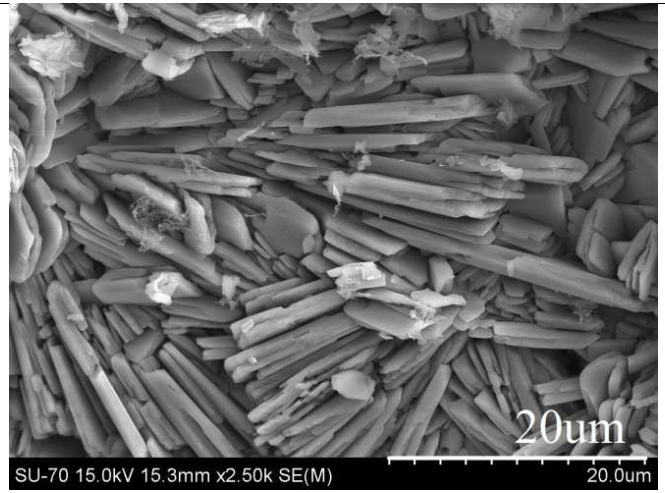

c. 4h-80°C

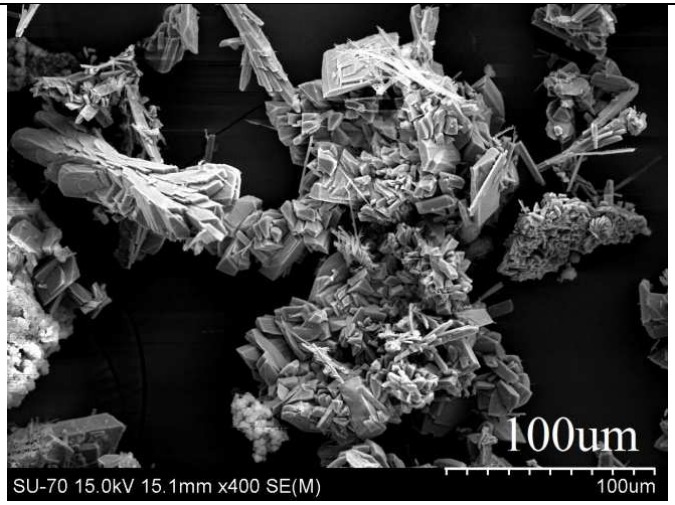

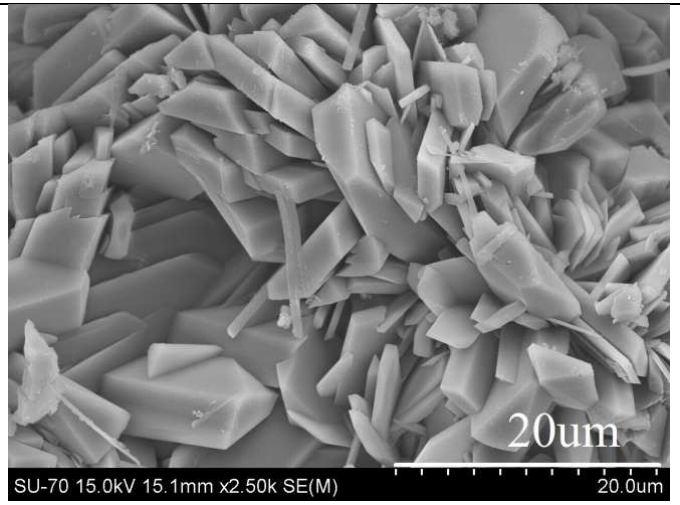

d. 8h-80°C

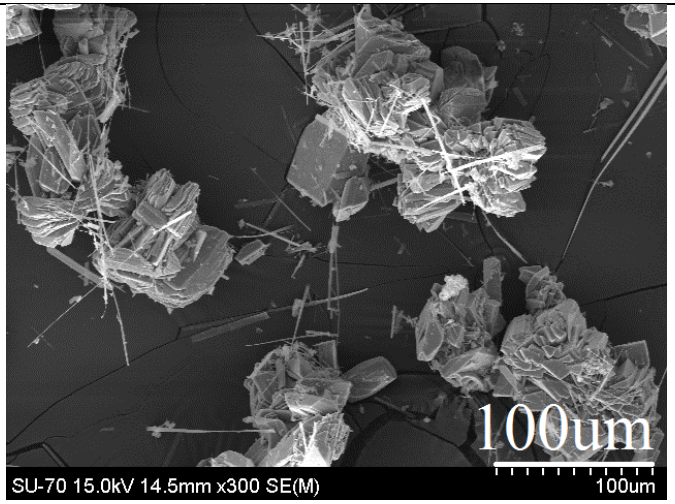

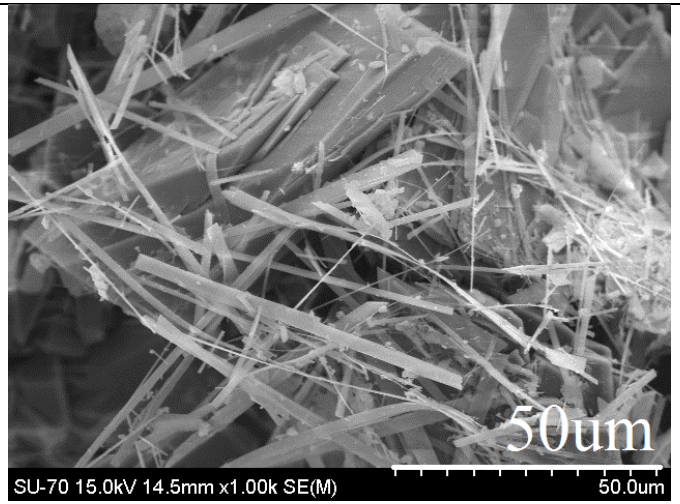

e. 20h-80°C

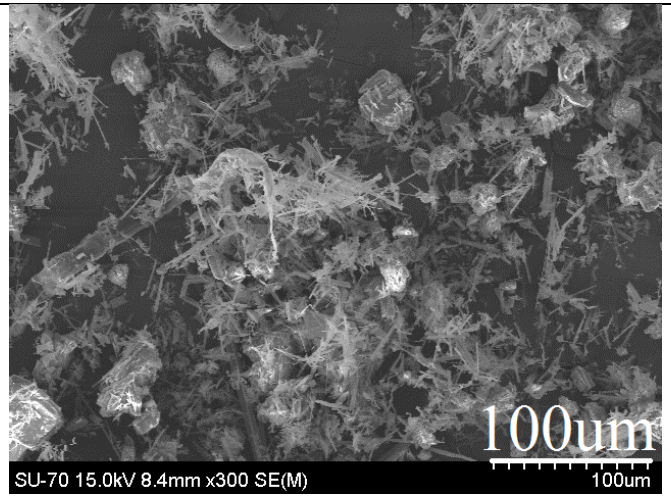

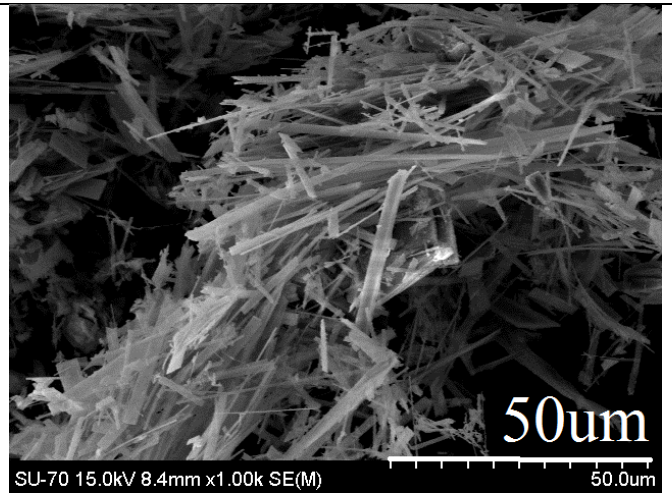

f. 24h-80°C

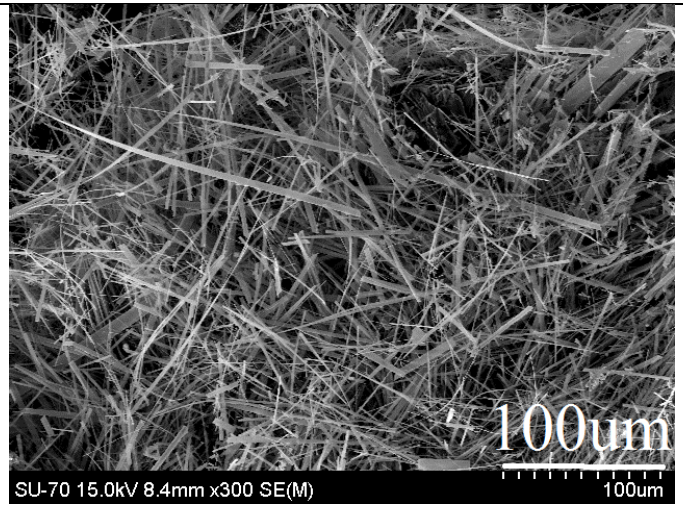

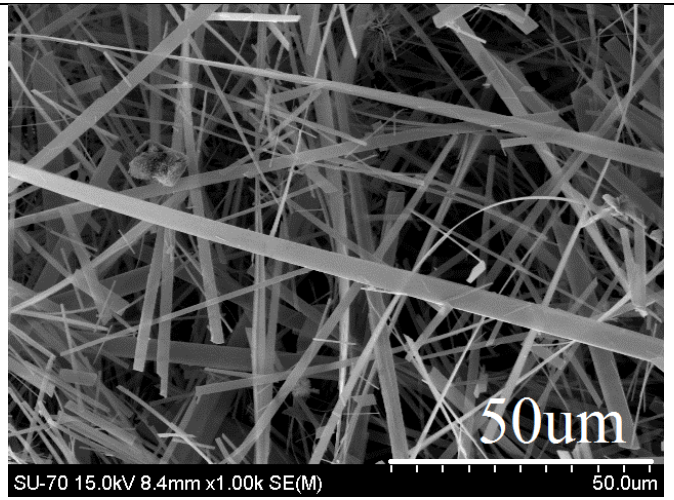

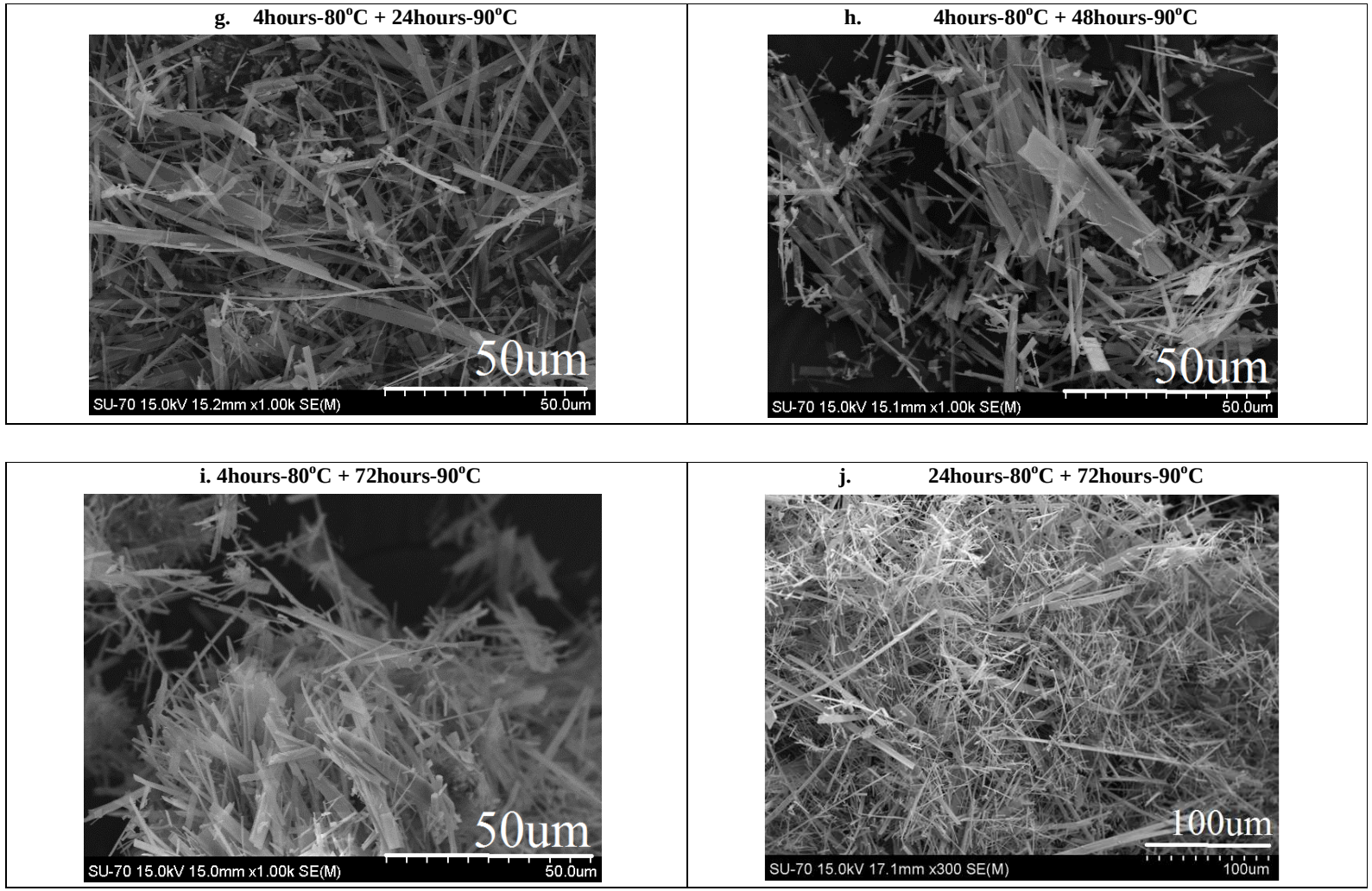

Figure 5-5 SEM Images of CaP precipitates with different time and temperature of reflux. Figure a, c, d, e and f on the left side and on the right side show CaP precipitates in different magnifications. Figure b show the heterogeneity of samples formed after 2hours-80°C reflux. While Figure g, h, i and j show CaP fibers for further reflux with almost similar morphology

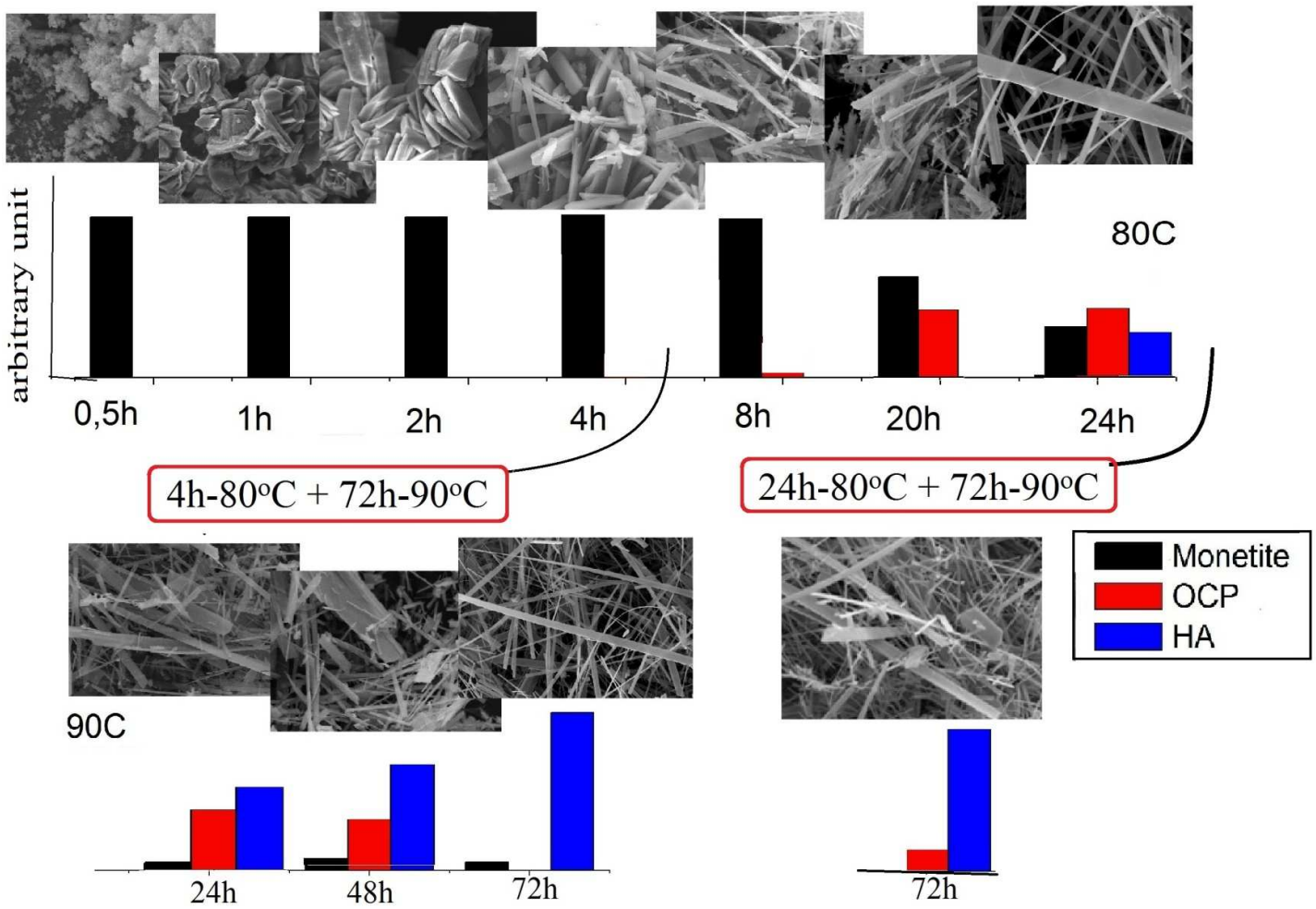

Figure 5-6 phase composition estimation and crystal morphology evolution during refluxing using two different pathways (a) 4h-80°C+72h-90°C and (b) 24h-80°C+72h-90°C

Figure 5-6 puts together the properties variation of the precipitates during the refluxing process, i.e. their crystal phase composition particle morphology. For comparative purposes, the relative amount of each phase estimated trough XRD peak area calculations is also presented. The overall results show basically that CaP precipitation can be divided into three main stages: (1) formation of platelets shaped monetite, (2) formation of fibers-like OCP, and (3) transformation of fibers-like OCP crystal into HA.

In the first stage, as shown in XRD spectra on Figure 5-1, incipient monetite appeared after 30min refluxing. This is in line with the findings from H. Zhang et al.[39] which demonstrated that during this process, urea decomposes and contributes to pH increase until a critical (2,4-3,1) pH range where monetite starts precipitating, the sooner the higher is the temperature: after 12 min at 95^{o}C, 28 min at 90^{o}C, and 46 min at 85^{o}C. In the present case crystalline monetite was obtained at 80ºC after 1 hour at pH~ 2. Other references which also studied HA precipitations are Aizawa et al.[38, 56]. However, none of them followed the crystal morphology evolution during the precipitation process.

Monetite is the first CaP phase to be precipitated. According to CaP solubility isotherms (Figure 2-10), at pH<4.5 monetite is the most insoluble CaP phase and thus is the first to be precipitated[41]. After 60min the XRD peaks became sharper indicating a higher crystallinity which is reflected by the increase of monetite crystallite size (Table 5-1). The existence of crystalline monetite is revealed by SEM images as thick platelet shaped particles which are very clearly detected after 2hours of refluxing. The specific surface area is seen to decrease drastically during the first two hours of refluxing being then followed by a slower decrease until 4hours (Figure 5-3). This surface area decreasing reflects the growth of the large platelet shaped particles from the small sized spherical particles and thin platelets detected at the early stage of the refluxing (Figure 5-5).

Figure 5-5 (b) also documents the heterogeneity of the precipitates. Sphere-like monetite on Figure 5-5 (b-left) and thick platelet-like shaped monetite Figure 5-5 (b-right) coexists in solution after 2h of refluxing. This inhomogeneous condition might indicate that some overlap between nucleation and growth probably took place. Further, this fact may also explain why the final HA fibers possess a relatively wide range of size (50-300µm).

The second stage of the precipitation process involves the formation of OCP. The existence of OCP starts to be detected in the XRD spectra (Figure 5-1) after 4h-80^{o}C refluxing. The strong peaks of OCP observed in XRD spectra after 20h-80^{o}C refluxing corresponds in SEM images to fibers-like OCP (Figure 5-5 (e-f)). At this stage, the monetite thick platelets and prisms previously referred transformed into fibers, being evident that the grow of particles with fiber-like morphology was already initiated after 4h-80ºC refluxing (Figure 5-5 (c)). According to solubility isotherms of calcium phosphate phases in the ternary system $Ca(OH)_2$-H_3PO_4-KNO_3-H_2O at 37ºC (Figure 2-13), HA has lower solubility than OCP in the 3 <pH<10 range. Consequently HA should be preferably

formed instead of OCP at a precipitation temperature of 37ºC. As the current experiments are being performed at a higher temperature it is anticipated that the temperature dependence of OCP solubility might account for some solubility variations as compared to HA. Moreover it is also known that kinetic factors may have a considerable effect in determining the nature of the CaP phases that precipitate, further helped by anions and cations from solution which stabilizing role can not be ruled out[41]. These arguments may explain why OCP preferentially precipitates in a pH range where the solubities of OCP and HA are supposed to be very close.

During the third stage of the precipitation the crystal phase transformation from OCP into HA fibers-like particles takes place. As can be seen in the phase composition summary presented in Figure 5-6, that phase transformation started to occur after 20h-80ºC refluxing. OCP transformation into HA is described by the following equation 5-1[39]:

$$\underbrace{5Ca_8H_2(PO_4)_6.5H_2O}_{(OCP)} \rightarrow \underbrace{4Ca_{10}(PO_4)_6(OH)_2}_{(HA)} + 6H_3PO_4 + 17H_2O \qquad (5.1)$$

For (4h-80ºC+72h-90ºC), the transformation of OCP into HA was completed during refluxing at 90ºC though not all monetite had been converted into OCP being thus noticed in XRD spectra (Figure 5-1). Once again arguments based on the stabilizer role of the precipitation medium ions may be put forward to explain the slow conversion of monetite into other thermodynamically more stable CaP phases. For (24h-80ºC+72h-90ºC), the transformation of OCP seems to be not completed yet, since a small peak of OCP still exist. The morphology variations during the last refluxing step at 90ºC were meaningless. It is thus concluded that OCP is a precursor phase of HA, behaving like a template for HA crystallization as HA fibers keep the shape of OCP fibers.

Figure 5-5 shows SEM images of the fibers obtained after 4h-80ºC refluxing and then refluxed at 90ºC during different times. In spite of the differences underlying the two routes, i.e. (24h-80ºC+72h-90ºC) and (4h-80ºC+72h-90ºC), the characteristics of the final particles either in terms of morphology or of crystal phase composition are very alike: in both cases HA fibers with similar size and crystallite size are the main product of the refluxing at 90ºC regardless the duration of the 80ºC refluxing (Figure 5-5). It is thus concluded that the incipient OCP, with fiber-like morphology, early detected at 80ºC after a 4h refluxing was easily converted into HA fibers at 90ºC, even after 24h. Therefore, overall shorter precipitation times are required if refluxing temperature/time relation is conveniently manipulated. The present results demonstrate that 76hours, i.e. (4h/80ºC+72h/90ºC = 76h) are required for obtaining HA fibers which would otherwise require longer times (96hours), i.e. (24h/80ºC+72h/90ºC= 96h) to precipitate.

Temperature may be also manipulated towards lower values for obtaining HA fibers. The work from Zhang[39] has shown that precipitation of HA at temperatures lower than 90ºC is possible but after much longer times: 120 hours under 85ºC refluxing.

Despite of its advantages of being easy to carry out, preparing HA fibers by this precipitation method has one main drawback. Since several phase transitions are involved in this process, their coexistence in the final product is very likely to occur. For example, as shown in the XRD spectra of the Figure 5-2, the final HA fibers contain a small amount of monetite. This is also illustrated in Figure 5-7 that reveals the non-uniformity of the final precipitate where some non-fiber particle corresponding to a monetite transient phase which didn't transform completely into HA fibers are still observed. Besides thermodynamic and kinetic issues contributing to this non-homogeneity, it is worthy mentioning that experimental conditions may also account for this fact as precipitation was carried out without any stirring. It is foreseen that improving experimental technique in future work in order to include uniform stirring may help to obtain pure HA fibers without other CaP phases.

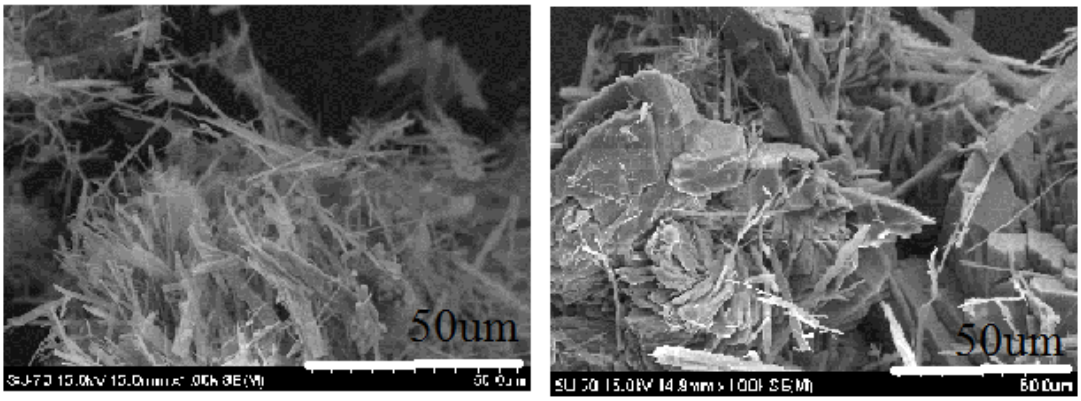

Figure 5-7 SEM images of final precipitates after 4h-80°C + 72h-90°C - HA fibers(left); other transition phase (right) which might be monetite as shown in XRD spectra

5.2. Chitosan based Scaffolds

To fulfill the requirements of a scaffold for bone regeneration, a number of parameters should be met as stated in Table 2-1. In the present research, four main properties are addressed: (1) the chemical and crystal phase composition; (2) the microstructure, including porosity, pore size, and interconnectivity; (3) the mechanical properties, evaluated by compressive tests, and (4) the bioactivity. Different chitosan-based scaffolds, unloaded and loaded with different type of CaP particles, prepared under different experimental conditions of chitosan solution pH and freezing temperature will be analyzed and comparatively discussed in the present chapter. Table 5-2 presents the scaffolds under study and their respective preparation conditions.

Table 5-2 Chitosan and Chitosan composite scaffolds obtained by freeze drying under different conditions of : chitosan solution pH, freezing temperature and type of CaP particles loading.

	pH 2	**pH 2 loaded**	**pH 5**	**pH 5 loaded**		
		HA Fibers		HA Fibers	Monetite Powder	Mixture (HA fibers + monetite powder)
Liq N_2	√		√	√		
(-15°C)	√	√	√	√		√
~0C	√		√	√	√	

Note: the symbol √ identifies the conditions combination effectively used for scaffolds preparation.

5.2.1. Influence of pH and Freezing Temperature on CH Scaffold Properties

CH scaffolds were prepared from chitosan solutions with different pH, i.e. pH=2 and pH=5, and subsequently frozen at different temperatures, i.e. liquid nitrogen (-196ºC), -15ºC and 0ºC. All the samples collected from freeze drier looked like white spongy bodies but exhibiting different shrinkage. As illustrated in figure Figure 5-8, chitosan scaffolds prepared at pH 5 showed larger shrinkage as compared to pH=2 and consequently higher geometrical density (Table 5-3).

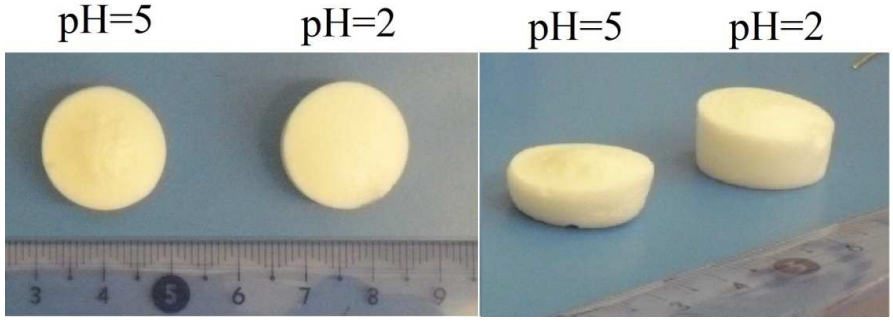

Figure 5-8 Top views (left image) and front views (right image) of chitosan scaffolds prepared under different pH conditions and frozen at (-15°C)

Table 5-3 List of CH composite scaffolds and and respective density values prepared with different pH and freezing temperature

	pH 2	pH 2 loaded	pH 5	pH 5 loaded		
		HA Fibers		HA Fibers	Monetite Powder	Mixture (HA fibers + monetite powder)
-196°C	-	-	0.0524	0.0714	-	-
-15°C	0.03686	0.05074	0.0541	0.0628	-	0.0689
0C	-	-	-	-	0.06167	-

These macroscopic differences were followed by microstructure variations, too. The microstructures of the obtained chitosan scaffolds are imaged in Figure 5-10. Interconnected porous structures are generally observed but with differently sized pores, thus denoting a significant effect of pH and freezing temperature on the scaffold microstructure.

For the freezing temperatures of 0°C or (-15°C), pH effects on pore size reveal a slight tendency for larger pores to be obtained at higher pH (pH=5), as shown in Figure 5-10 (a b, d and e). The calculated average pore sizes presented in Figure 5-9 confirm that scaffolds prepared from chitosan solution at pH 2 resulted in slightly smaller pore size.

The study of freezing temperature influence in chitosan and alginate has been done previously by Madihally and Matthew[18] and ZMora et al.[58]. The results shows similar trend regarding to freezing temperature. However, an attempt to study the effect of pH, haven't been done so far.

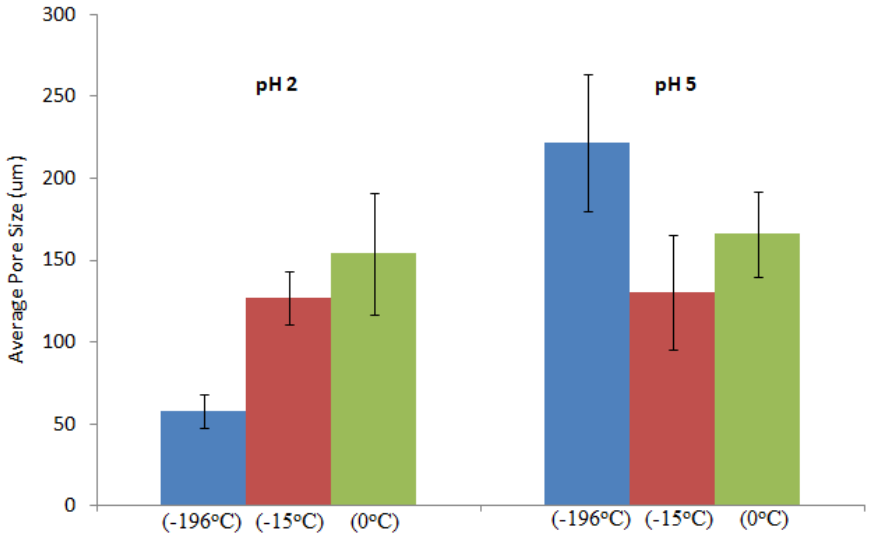

Figure 5-9 Effects of freezing temperature and pH of chitosan solution on mean pore size diameter of chitosan scaffolds

Regarding the freezing temperature effects, a clear tendency for smaller pores as the freezing temperature decreases is observed on the scaffolds prepared at pH 2.

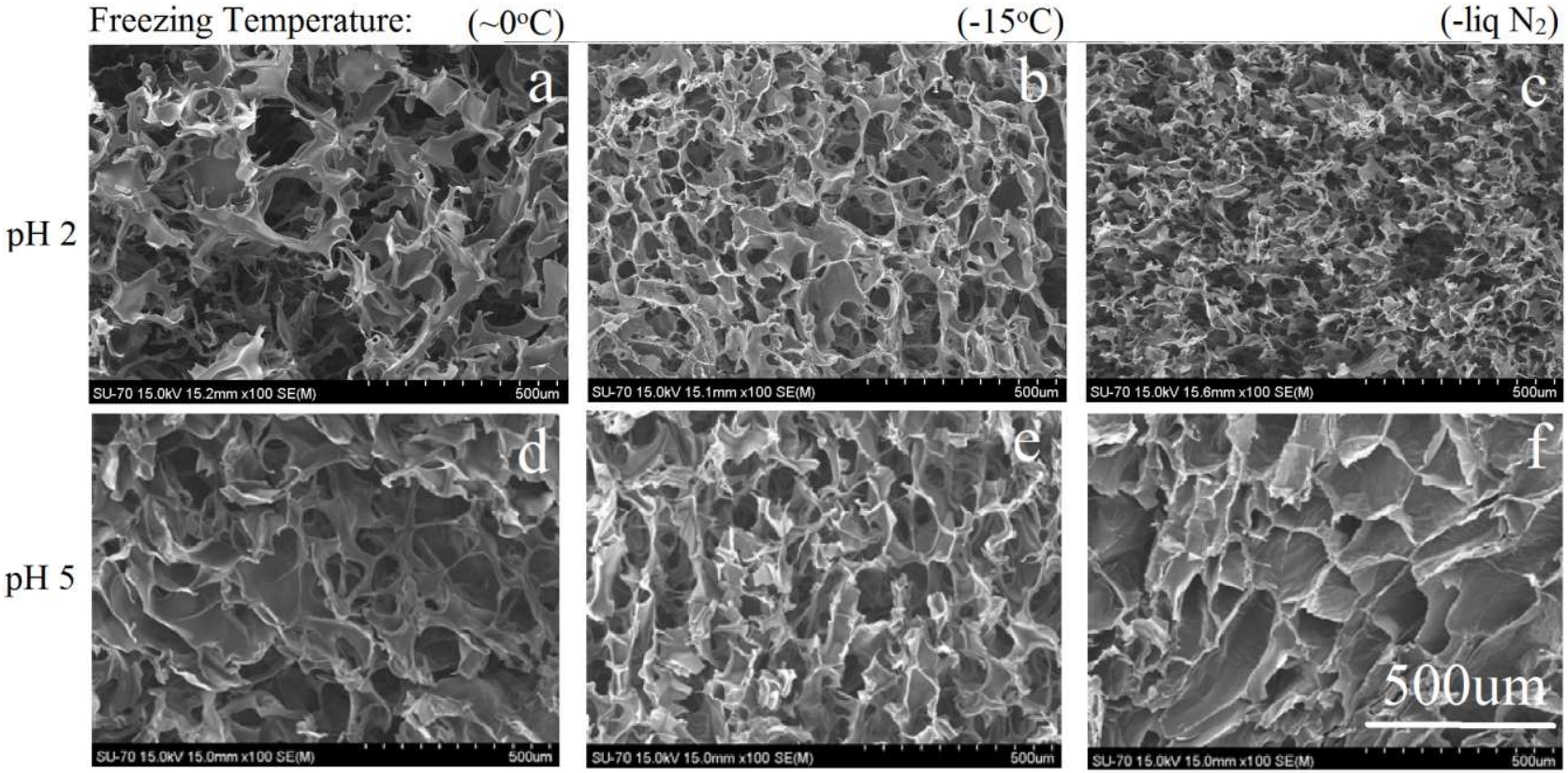

Figure 5-10 SEM images of pure CH scaffold at pH 5 (top images) and pH 2 (bottom images) with freezing temperature: ~0°C(left); -15°C(middle); and -196°C (right)

However, scaffolds prepared at pH 5 do not follow that trend and a quite different pore structure was obtained for the freezing temperature of -196°C (liquid N_2): the pores are larger and seem to be apparently less interconnected than in the other scaffolds. Furthermore freezing scaffold at -196°C also resulted in thicker wall pore as can be seen in Figure 5-11.

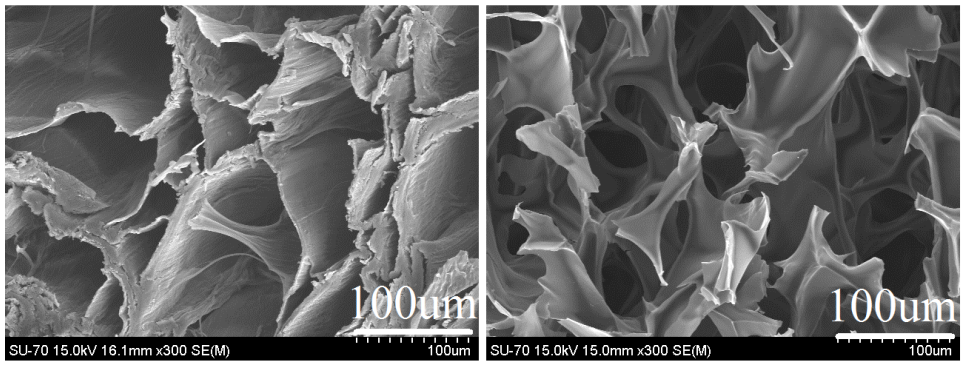

Figure 5-11 Higher magnification of SEM images show wall thickness of: pure CH/pH5/(-196°C) (left) and pure CH/pH5/(-15°C) (right)

It is known that the morphology of the scaffolds manufactured by thermal induced phase separation process depends on several experimental variables such as freezing temperature, freezing rate, solution concentration, solvent type and polymer molecular weight among others[18]. When a chitosan solution is frozen, the magnitude of the temperature gradient (ΔT) imposed during freezing quantifies the equilibrium deviation of the solution so that the higher ΔT the higher is the driving force for ice nucleation and growth. This reasoning anticipates that lowering freezing temperature enhances nucleation rate and thus favors smaller sized pores to be formed. The results obtained at pH=2 (Figure 5-10 a, b and c) seem to fit well to this idea since they point out a trend of pore size decrease with freezing temperature decrease. However increasing the chitosan solution pH from 2 to 5 originates a deviation from that trend. As observed from Figure 5-10 (d and e) pore freezing at 0 or -15ºC resulted in pore sizes slightly larger than their counterparts at pH=2, though less affected by freezing temperature variation. Furthermore, when freezing at -196 the largest pores were obtained. As these results reflect the joint effects of temperature and pH variation it seems that chitosan solution pH plays an important role in the scaffold microstructure design.

It is known that pH variations modulate the amount of cationic groups bounded to chitosan molecule as described by equation 5-2:

$$\text{Chit-NH}_2 + \text{H}_3\text{O}^+ \rightarrow \text{Chit-NH}_3^+ + \text{H}_2\text{O} \qquad (5.2)$$

Chitosan bounded $-NH_3^+$ groups impart to chitosan a polycationic condition that helps maintaining the chains free of attractive interactions among them. This cationic condition explains the pH dependence of chitosan solubity[59]. At higher pH (pH=5), bearing a smaller cationic [NH_3^+] load, chitosan chains may agglomerate easier in solution and form polymeric structures. This will also contribute to increase the viscosity of chitosan solution[60] as was experimetally observed indeed: after adding NH_4OH to chitosan solution to increase its pH from 2 to 5, the resulting solution showed to be effectively more viscous. Thus, for interpreting the pH effect on pore size Figure 5-10 (a, b, d and e) it is thus suggested that the more protonated chitosan chains (pH=2) ensure a true chitosan solution condition in which homogeneous nucleation of ice crystal occurs whereas the less protonated chains condition (pH=5) are prone to the formation of polymeric structures which might offer preferential sites for ice crystal nucleation. In this condition (higher pH) and under a very fast freezing imposed to the solution (-196ºC) it is here suggested that cationic sites probably play as favorable sites for ice nuclei formation and thus, as compared to the first condition (lower pH), a lower amount of ice nuclei is formed and thus allowed to grow further.

The large pores obtained after freezing in liquid N_2 indicate that freezing under liquid nitrogen temperature did favor ice crystal growth rather than ice crystal nucleation. It is thus postulated that the scarcity of cationic groups limits the benefit of large ΔT in nucleation rate which starts occurring at preferential cationic sites; once nucleated, the ice nuclei find appropriate conditions (large ΔT) to undergo a higher growing rate as compared to the other freezing conditions.

5.2.2. Chitosan/CaP Composite Scaffolds

In the present section the effects of the processing conditions (pH and freezing temperature) and of the used CaP particles as reinforcement elements on CH/CaP composite scaffolds characteristic are analyzed and discussed. Two different reinforcement particles were used in this current research: HA fibers (4h-80^{o}C+72h-90^{o}C reflux), florrete-like monetite powder (30min-80^{o}C reflux) and a mixture between these two particle type was also used in order to understand their differences.

5.2.2.1. Scaffold Microstructure

Chitosan scaffolds loaded with different types of CaP particles were produced from CaP particles suspensions in chitosan solutions upon freezing at -196ºC, -15ºC or 0ºC. As noticed before the variation of CH solution pH produced a significant effect on the freeze dried CH-HA scaffold either at a macroscopic level either from the microstructure point of view. Following the same tendency exhibited by CH scaffolds (discussed in the previous section) the preparation from pH 5 solutions originated larger shrinkage. The calculated geometrical densities values presented in Table 5-3 reflect this pH shrinkage tendency.

Figure 5-12 illustrates the microstructure of the freeze-dried chitosan scaffolds loaded with different types of CaP particles (CH-HA scaffolds). Pictures of the used CaP particles for scaffolds loading are also presented in the same figure: (i) HA fibers produced by the method (4h-80ºC+72h-90ºC), and (ii) incipient monetite (30min-80°C reflux).

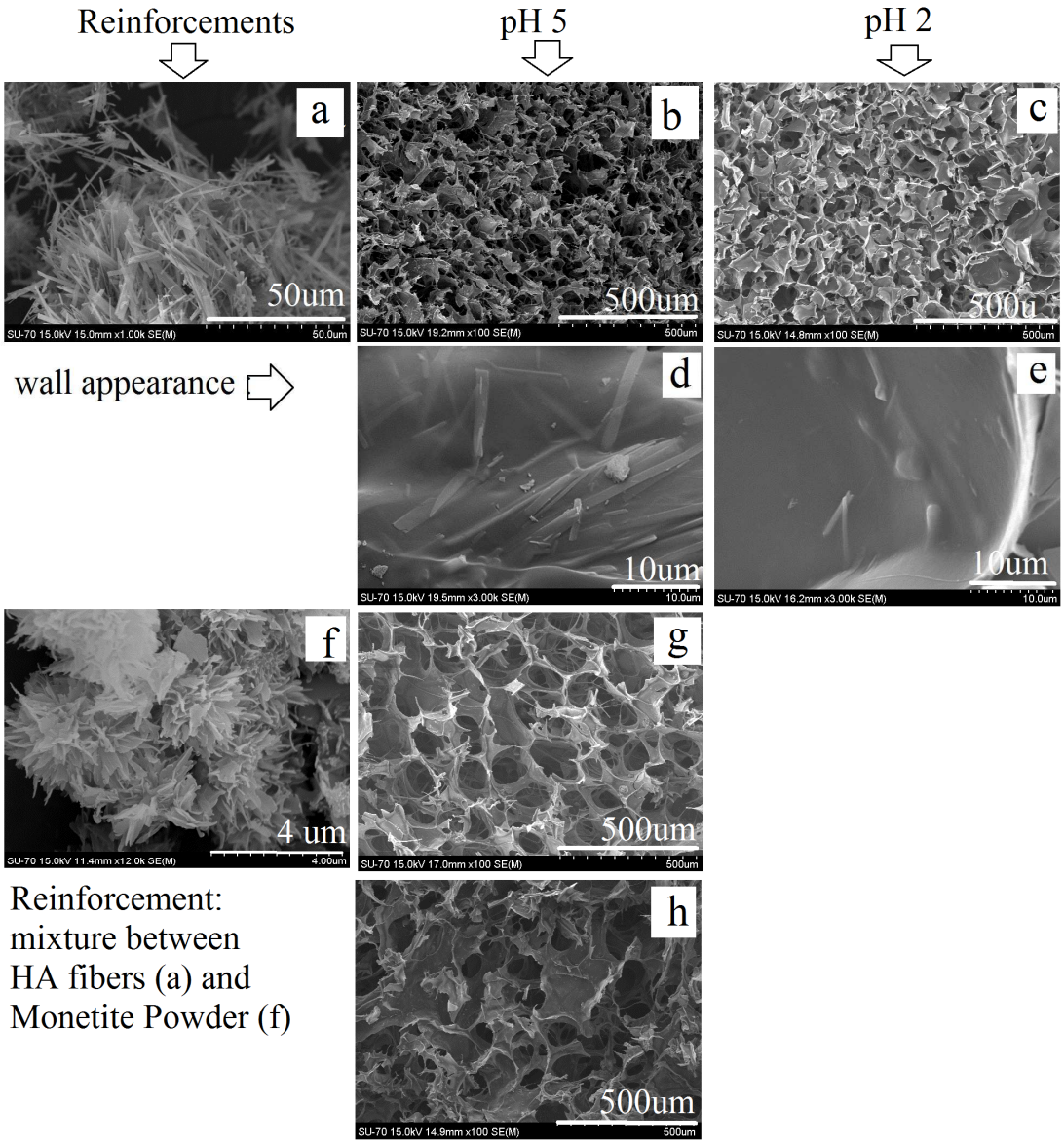

Figure 5-12 SEM images of reinforcement particles: (a) HA fibers and (f) incipient monetite powder and its produced scaffolds: CH-fibers at -15°C/pH 5 (b, d) and -15°C/pH 2 (c, e); incipient monetite at ~0°C/pH 5(g) and mixture of incipient monetite and HA fibers at -15°C/pH 5 (h)

In general, the scaffolds microstructures evidence porous bodies with differently sized open pores uniformly distributed with an apparent high degree of interconnectivity. Higher magnification views of the pore walls also allows us to detect the presence of the fibers embedded in the polymeric walls (Figure 5-12 d and e): in the case of the scaffolds prepared at pH 5 where fibers are clearly revealed (Figure 5-12 d) whereas for pH 2 fibers

are less abundant and shorter (Figure 5-12 e). In line with CH scaffolds behavior reported in the previous section, the CH-HA fibers scaffolds produced at pH 2 show smaller pore size as compared to those prepared at pH 5.

Concerning freezing temperature effects (Figure 5-13 a,b and d), the pore sizes of the samples prepared at -196°C (liq N_2) (Figure 5-13) appear to be larger than those obtained at -15°C (Figure 5-13 b) or 0°C (Figure 5-13 c).

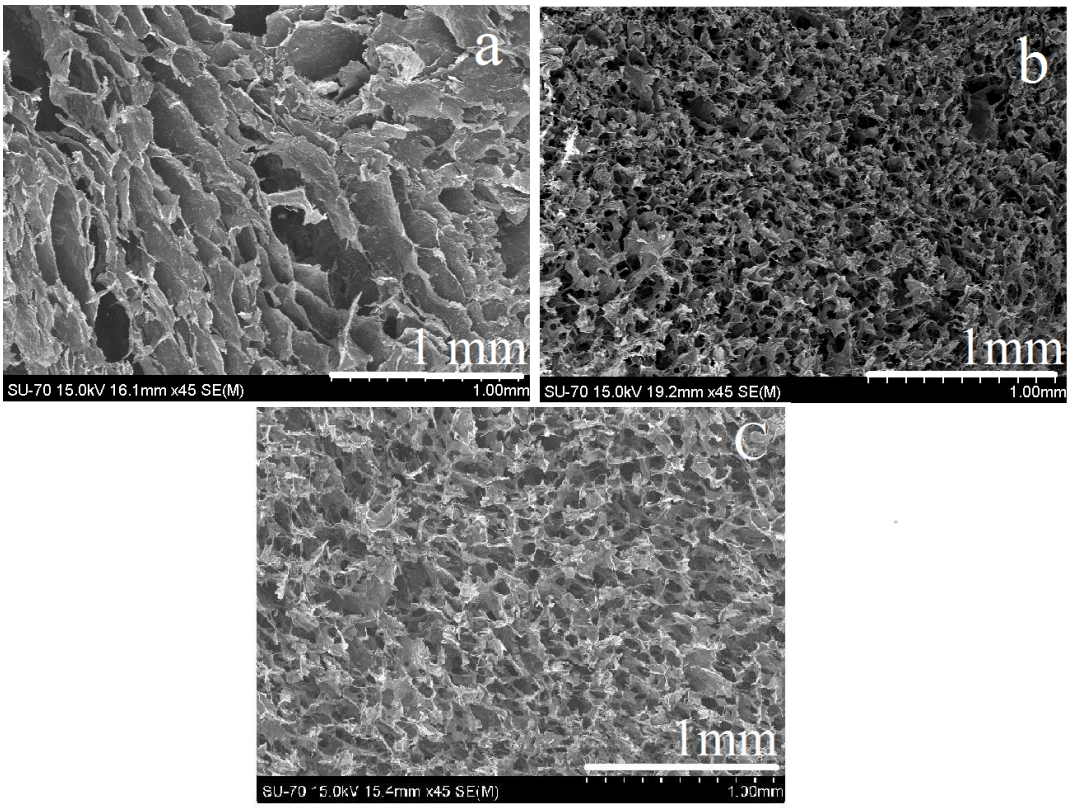

Figure 5-13 SEM images showing different pore sizes of CH/Fibers scaffold prepared at pH 5 with different temperature: (a) -196°C, (b) -15°C, and (c) 0°C

The 3D reconstruction obtained by µ-CT is shown in Figure 5-14 for selected scaffolds. The resulting porosity, pore size, and interconnectivity data are presented in Table 5-4. Total porosity and interconnectivity are seen to decrease as the freezing temperature decreases too. Using lower pH is also seen to decrease the pore size.

Table 5-4 Data obtained from *µ-CT* analysis

Sample	Porosity[a] (%)	Pore size (µm)	Interconnectivity[b] (%)
CH-HA fiber/pH5/LiqN2	80,6	190	91,6
CH-HA fiber/pH5/-15°C	90,7	152	98,5
CH-HA fiber/pH2/-15°C	90,7	136	98,0

[a] volume of pores divided by sum of volume of pores and scaffold x100%

[b]volume of interconnected pores divided by sum of interconnected pores and closed pore x 100% (in this calculation, pores smaller than 5µm are neglected)

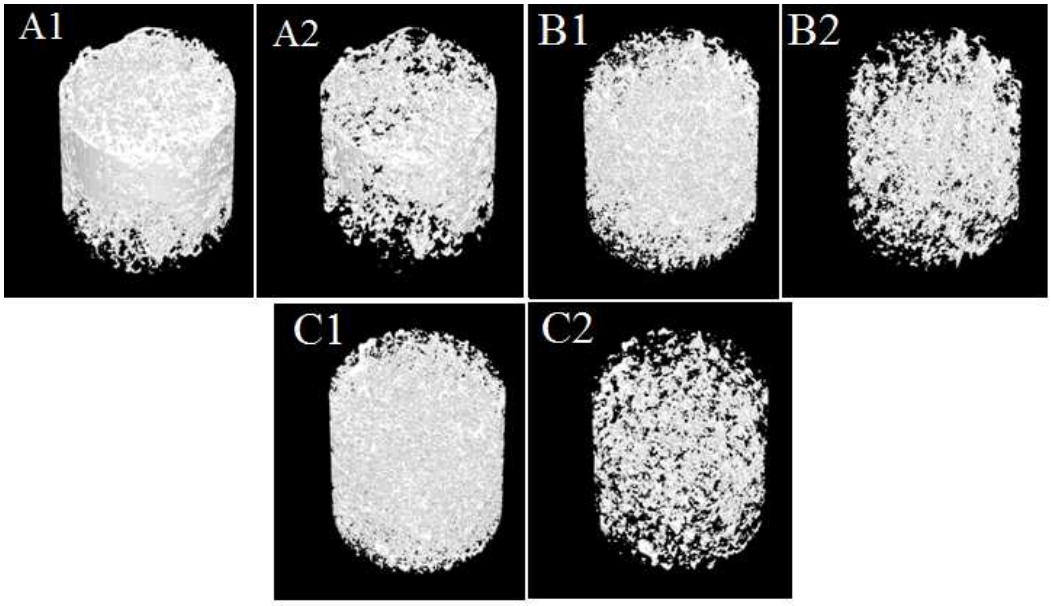

Figure 5-14 3D reconstruction made by µ-CT, A: CH-fiber/pH 5/LiqN2; B: CH-fiber/pH5/-15°C; C: CH-fiber/pH2/-15°C; where 1 refers to total reconstruction and 2 refers to reconstruction of the mineral part only

Figure 5-14 also shows that for the scaffolds prepared at -15ºC pH 2, the 3D reconstruction both in total and mineral reconstructions presents a more homogeneous structure than for scaffolds prepared at -196ºC; in this last case the interconnectivity is also lower than in the previous ones.

Chitosan scaffolds prepared with addition of CaP particles viewed as composite materials in which a continuous polymeric matrix hosts a discontinuous CaP phase aimed at reinforcing the scaffold structure. Composite properties are strongly influenced by the properties of the constituent materials, their distribution, and the interaction between them[61, 62]. Besides the properties of constituent materials, it is also necessary to address the geometry of the reinforcement (including shape, size and distribution size). The geometry of the reinforcement plays an important role in the strengthening mechanism.

The values of solution pH and freezing temperature influence the pore sizes of CH composite scaffolds in a way similar to that observed for pure CH scaffold. pH variation showed that smaller pore are obtained at pH 2 as compared to pH 5. Hence the pH role discussed for CH solutions seems to be maintained in CaP loaded CH solutions. The influence of temperature at pH 5 (Figure 5-13) revealed that freezing at (-15°C) resulted in smaller pore size than 0°C and Liq N_2. It is thus suggested that the incorporation of CaP particles in CH solution did not alter significantly the ice crystal nucleation and growth rates as compared to pure chitosan solution. Furthermore the shrinkage behavior of the scaffolds was also consistent with that observed with CH scaffolds: the size reduction was also larger for scaffold prepared at pH 5. Accordingly the density values of the CaP loaded

scaffolds showed to increase with pH, being obviously higher than those of their CH scaffolds counterparts (in Table 5-3).

SEM images have revealed the samples pores size while porosity and interconnectivity could be accessed by *μ-CT*. CH composite scaffolds prepared by quenching in liquid N_2 showed to display the lowest interconnectivity and porosity which confirmed the indication of SEM images (Figure 5-13) that this scaffold seems to be less interconnected than the remaining ones. Composite scaffolds prepared at -15°C under two different pH values showed similar porosity values, nearly similar interconnectivity and the same tendency of pore size variation evidenced by SEM pictures.

The obtained values of porosity and interconnectivity for the scaffolds CH-fiber/pH5/-15°C and CH-fiber/pH2/-15°C are quite satisfactory. The porosity value which is 90.7% is within in the range of the porosity typically required for promoting proper new bone growth (90%)[21]. The interconnectivity degrees, i.e. 98.5 and 98 respectively, are extremely valuable for perfusion and cell migration[63].

Quenching composite solution in liquid nitrogen resulted in lower porosity and interconnectivity degree. The value of porosity which is 80.6% is relatively low for bone regeneration. Regarding to interconnectivity degree, a clear reference to a minimum value could not be found in the literature, so far. For comparison, Darling and Sun[63] obtained PCL scaffold with interconnectivity degree in the range of 98.16-99.59% and Ho and Hutmacher[64] gained 100% interconnectivity by preparing scaffolds from copolymer of PEG, PCL and PLA with rapid prototyping. As compared to these data, 91.6% of interconnectivity seems to be apparently low.

5.2.2.2. Phase Composition

Figure 5-15 shows the XRD spectra of CH-HA fibers composite scaffolds prepared at different pH, i.e. pH=2 and pH=5. It is observed that the scaffold obtained from pH 5 chitosan solution reflects the peaks of HA superimposed on a baseline showing the chitosan hump at 2θ=20º. However for the scaffold prepared at pH=2, both HA peaks and brushite peaks are detected.

The presence of brushite in the CH-Fibers prepared at pH 2 indicates that part of HA transformed to brushite during the scaffold preparation. Such phase transformation probably occurred via partial dissolution of HA fibers in the acidic conditions (pH=2) of chitosan solution followed by brushite. This partial dissolution/recrystalization of HA fibers may also explain why less and smaller fibers are detected on the pore walls of the scaffolds prepared at pH 2 as compared to pH 5 (Figure 5-12 d and e)). A phase transformation was also observed on CH-incipient monetite scaffolds prepared at pH=5.Monetite was seen to transform into HA as shown in Figure 5-15 E. CaP dissolution and recrystallization as a crystalline phase different from the initial one has been seldom reported, depending on the pH conditions[72, 65].

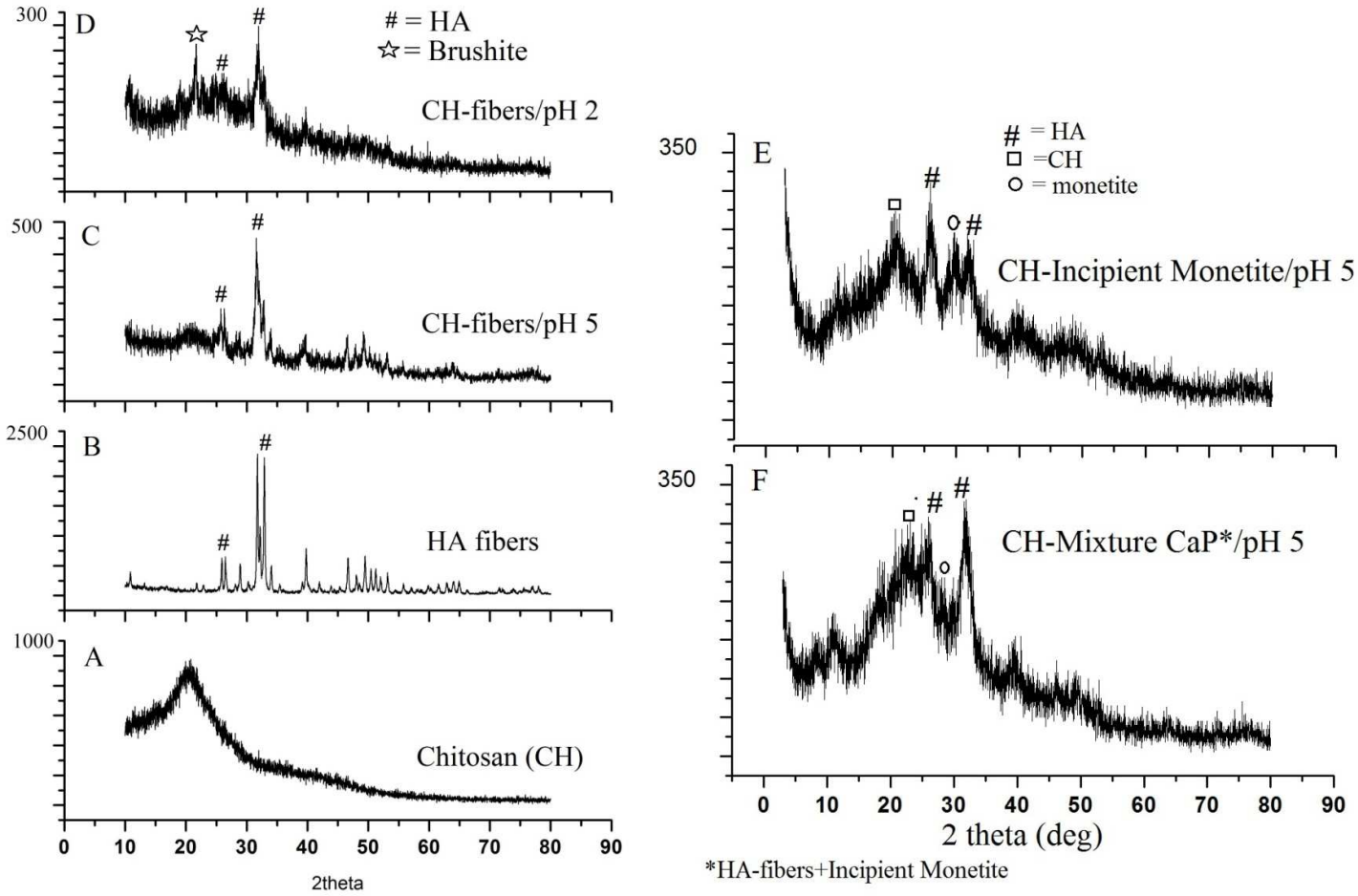

Figure 5-15 XRD Spectra of (A) pure CH, (B) HA fibers, and (C) CH-HA fibers/pH 5, (D) CH-HA fibers/pH 5, (E) CH-Incipient monetite/pH 5, all frozen at (-15^{o}C), and (F) CH-mixture CaP/pH 5 frozen at 0^{o}C

5.2.2.3. Mechanical Properties

In the case of composite scaffolds to be used as support for bone regeneration, the improvement of mechanical properties while ensuring an adequate microstructure with sufficient large pores for vascularization and tissue ingrowth is a critical issue. It is known that the type of reinforcement together with the processing variables may influence the pore structure and porosity and hence the mechanical response of the scaffold. Concerning the particles used as reinforcement, depending on their geometry, they may also affect differently the porosity[66] and pore orientation[67] and thus the mechanical properties. To exploit the simultaneous effects of these experimental variables, different processing conditions (pH and freezing temperature) and different CaP loading were selected for the present study.

Figure 5-16 shows the stress-strain curves of various scaffolds, including CH and CaP loaded CH scaffolds. The stress-strain curves evidence two main regions: (1) initial linear loading regime denoting an elastic behavior and (2) a plateau region which refers to the collapse or cell wall buckle[10]. Two main properties may be calculated from these curves: the compressive modulus – from the initial linear behavior and the compressive-strength – as the highest point which is taken from the intersection between linear behavior and plateau region. It is generally shown that (1) loading the chitosan matrix with calcium phosphate particles resulted in higher mechanical property; (2) the type of reinforcement also affected the scaffolds mechanical properties and (3) the CH-fibers composite scaffolds prepared at pH 2 (-15ºC) exhibited the highest compressive modulus and strength.

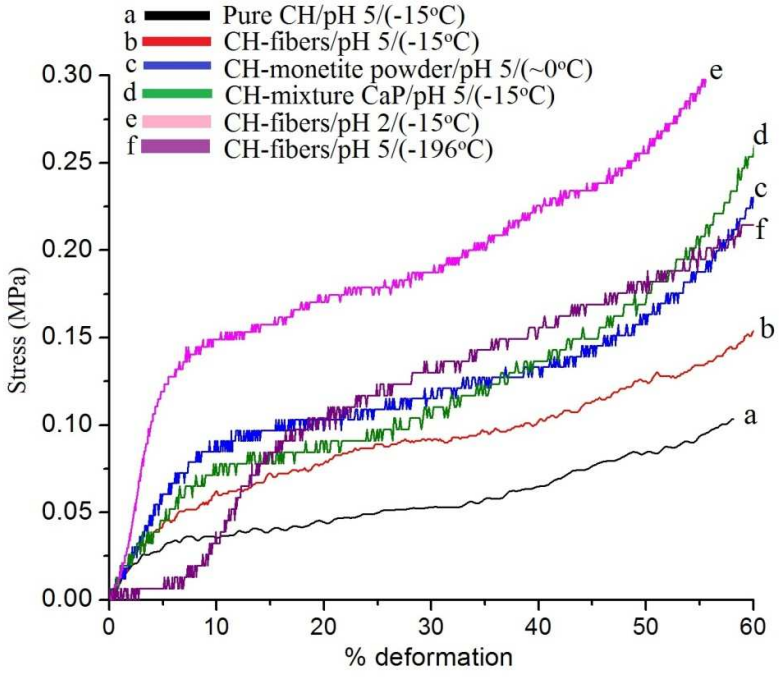

Figure 5-16 Mechanical Properties of CH and CH composite scaffold

Table 5-5 List of Scaffold Mechanical Properties (M: modulus; S: strength; both in MPa)

	pH 2	pH 2 loaded	pH 5	pH 5 loaded		
		HA Fibers		HA Fibers	Monetite Powder	Mixture (HA fibers + monetite powder)
-196°C	-	-	-	M= 0.616±0.10 S= 0.112±0.028	-	-
-15°C	M=0.2 S=0.02	M= 2.58±0.34 S= 0.158±0.022	M=0.65 S=0.025	M=0.79±0.4 S=0.048±0.007	-	M=0.64±0.16 S=0.079±0.007
0C	-	-		-	M=1.1±0.35 S=0.09±0.01	-

Table 5-5 summarizes the mechanical properties, i.e. the compressive modulus and the strength of the various CH and CH composite scaffolds prepared at different conditions. The rule of mixture[68] may explain the improvement of mechanical properties by loading CH scaffold with CaP particles: CaP phase is a ceramic more brittle and stronger than chitosan polymer[21].

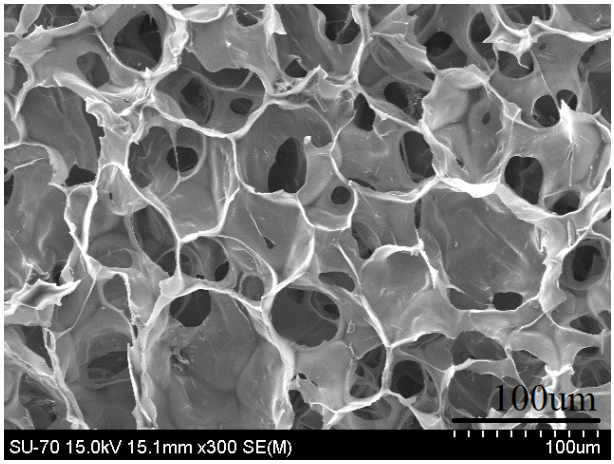

Figure 5-17 SEM image of CH-HA fibers prepared at pH 2 (-15°C) which has the best mechanical properties among the prepared scaffolds

Regarding the pH effect, scaffolds prepared at pH 2 showed better mechanical properties than scaffolds prepared at pH 5. Their modulus and compressive strength values (M: ~2,58 MPa; S: ~0,18 MPa) are comparable to the values reported by Zhang and Zhang[10]. It is worthy mentioning that in spite of having smaller pore size as compared to the scaffolds prepared at pH5, their microstructure seems to be rather uniform with well interconnected pores as illustrated in Figure 5-17. These conditions enhance the mechanical properties as reported by Yu et al.[69] who investigated the influence of pore size and porosity of PCL on scaffold mechanical properties. Their results showed that mechanical properties are influenced by pore size, porosity and interconnectivity. Smaller pore size, lower porosity, and lower interconnectivity lead to higher modulus. Among the

prepared scaffolds and in terms of biomedical applications, the scaffold illustrated in Figure 5-17 seems to be one offering a good combination of mechanical properties and microstructure for tissue regeneration purposes.

Furthermore, it was also shown that a partial dissolution and recrystallization of calcium phosphate fibers did occur. It is also thought that this fact may have favored a stronger bonding between the recrystallized particles and the polymer matrix thus contributing for mechanical properties enhancement too. It has been reported that the interaction between the reinforcement particles and the matrix is crucial for load transfer between the two phases as a lack of adhesion between them results in early failure/low mechanical properties[16]. Reinforcing chitosan polymer with HA particles under two different pH conditions may affect differently the chemical bonding between the matrix and the CaP particles as chitosan cationic groups may effectively condition the bonding strength between the two phases.

The results of Figure 5-16 also evidence that the freezing temperature during TIPS also affected the scaffolds mechanical properties. Comparing the HA fiber loaded scaffolds (pH5) frozen at different temperatures, i.e. -15ºC and 196ºC, an improvement of compression strength accompanied by a decrease of compression modulus is observed for the scaffold quenched in liquid nitrogen temperature. The reasons underlying this behavior are not completely clear. Probably, taking into account the results from SEM and µ-CT analysis (Figure 5-13 and Figure 5-12), it can be considered that close pores and thicker wall of pores (Figure 5-11) might be important reasons accounting for this phenomenon, in line with the findings of Yu et al.[70] .

Two types of reinforcements were used aiming to improve mechanical properties. A pH 5 CH solution was used in order to avoid CaP dissolution. Different values of mechanical properties were measured for scaffolds loaded with HA fibre, incipient monetite and mixture of HA fibers and incipient monetite (HA: monetite = 3 : 2).The results show that the incipient monetite powder and its mixture with HA fibers loading enabled higher compressive strength compared to CH-fibers. As pointed out before, properties of a composite depend on several variables such as reinforcement size, size distribution and shape. It has been reported that irregular shape is preferred to spherical shape since it can form better interfacial bonding with the polymer[62]. Figure 5-12 (a and f) shows the two type of reinforcements which were used: HA fibers and incipient monetite powder. It is here suggested that the better mechanical properties achieved with the mixture of HA fibers and incipient monetite powder compared to the reinforcement provided by HA fibers alone may be due to the irregular and non-smooth surfaces of incipient monetite powders which may favor a better connection between these particles and the polymer itself. The fibers flat surfaces are thought to ensure a lower mechanical interlock with the polymer as compared with monetite particles.

5.2.3. Bioactivity Test

In the beginning of the SBF soaking process the samples underwent a fast swelling. Hydrated scaffolds thus present a larger volume as compared to non-hydrated ones. Figure 5-18 shows how CH composite scaffold swelled due to hydration process during SBF immersion during the *in vitro* biomineralization test.

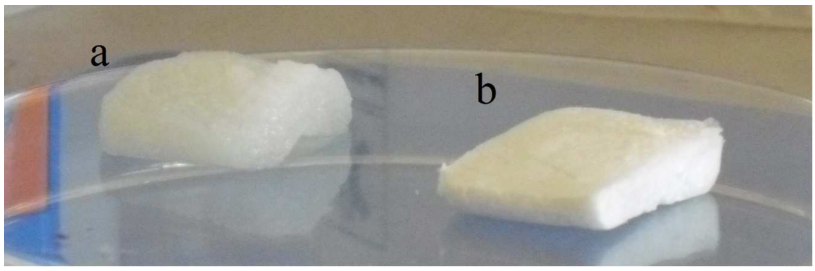

Figure 5-18 CH Composite scaffold: (a) fully hydrated and (b) as prepared/after ethanol treatment

Figure 5-21, 5-22, and 5-23 show the pore structure evolution of the scaffolds during bioactivity tests. It is shown that the pore structure didn't change significantly for the majority of the samples during SBF immersion except for CH-fibers/pH 5 after 21 days (Figure 5-21 d) which exhibited enhanced degradation behavior.

Higher magnification of a pore wall surface region allows observing the NaCl precipitates which were observed in all the scaffolds. The existence of NaCl was also detected in XRD (Figure 5-22) and EDS analysis (Figure 5-20). In spite of the repeated wash procedures, some NaCl crystals still persisted.

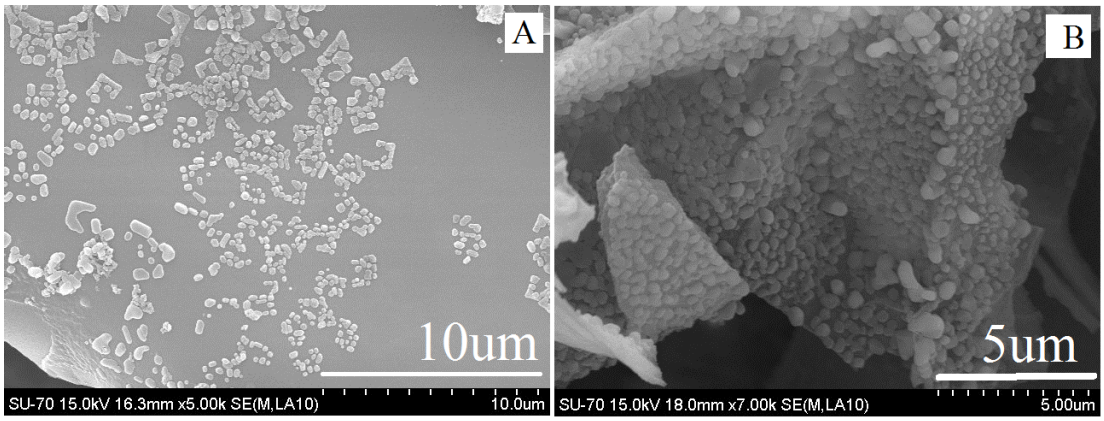

Figure 5-19 NaCl fomation on the wall of pure CH after 7 days (A) and CH-fibers/pH after 14 days (B) of SBF immersion

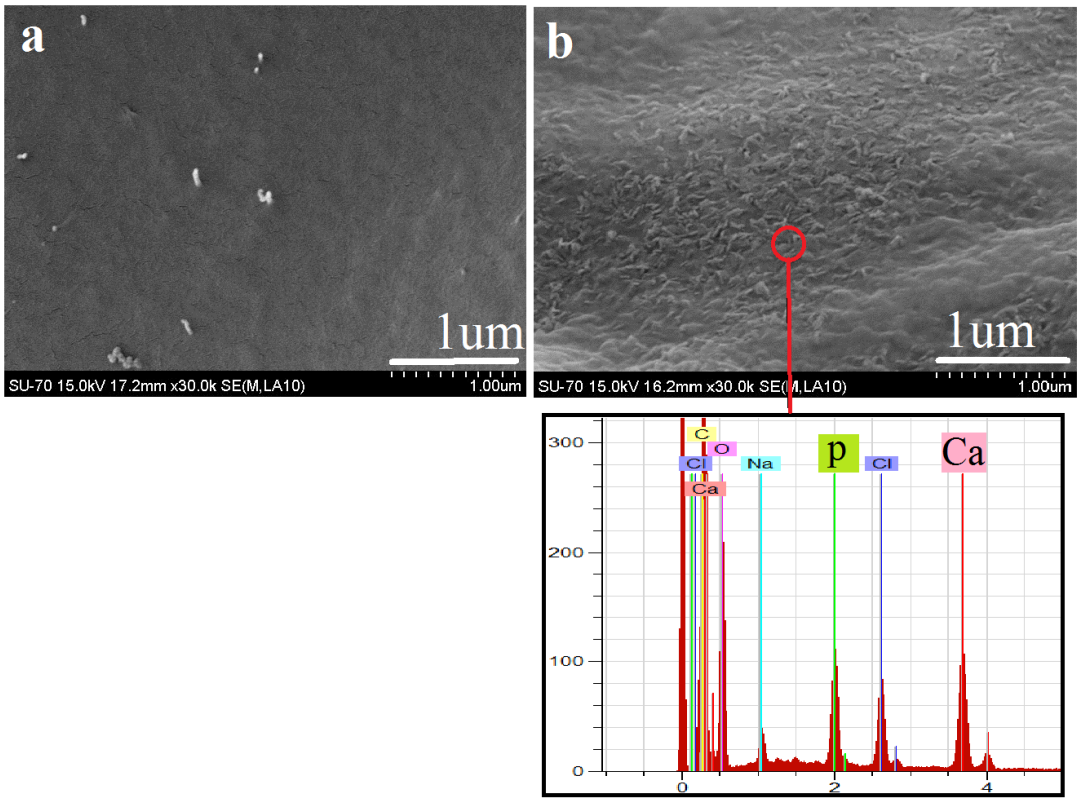

Figure 5-20 SEM images of scaffold after 21days of SBF immersion (a) pure chitosan; (b) CH-fibers/pH 2 showing rough wall in which the EDX spectrum showing Ca and P peaks (Ca/P = 1.65)

Besides NaCl precipitation, other type of surface morphology modifications occurred for the composite scaffolds during SBF immersion, but not detected in pure CH scaffold (as shown in Figure 5-20 a). Rougher walls are shown for the composite scaffolds (Figure 5-20 b). EDX analysis on CH-Fibers/pH 2 scaffolds after 21 days of immersion detected that CaP phase with a Ca/P of 1.65 is present. This value reflects the surface and underneath adjacent region compositions is close to that of stoichiometric HA (1.64). However EDX analysis of pure CH scaffolds after 21 days immersion did not evidence any presence of Ca or P.

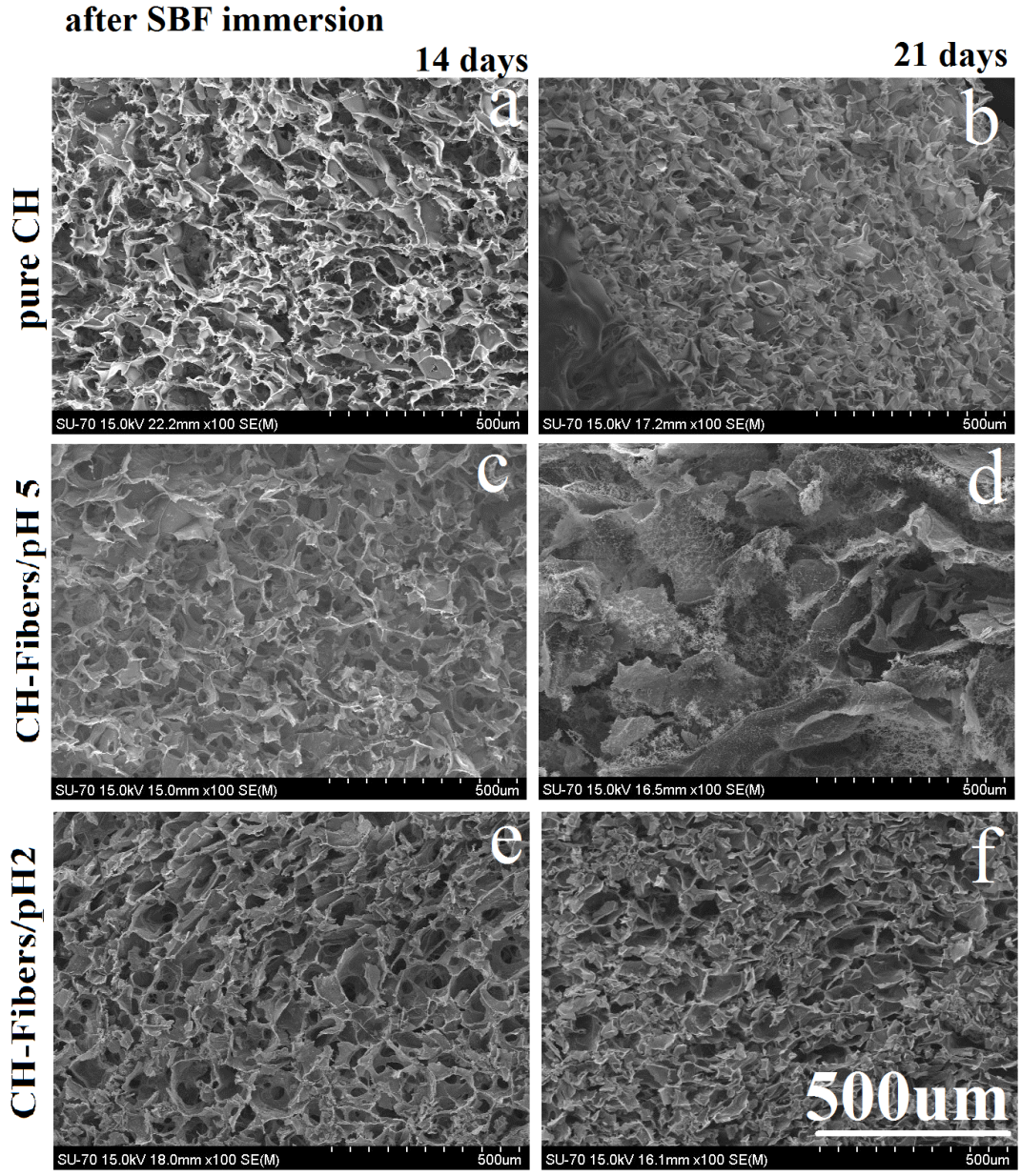

Figure 5-21 SEM images showing porous structures of different type of scaffolds after 14 and 21 days of SBF immersion. Structure damage can be seen clearly in Figure d.

FTIR-ATR and XRD spectra of the scaffolds after 21days of SBF immersion are shown in Figure 5-22 and Figure 5-23. XRD spectra indicated the existence of HA on both composite scaffolds. However, HA peaks were found to be better defined in CH-fibers/pH 2 as compared to CH-fibers/pH 5. In the pure CH scaffold, only NaCl peaks were observed.

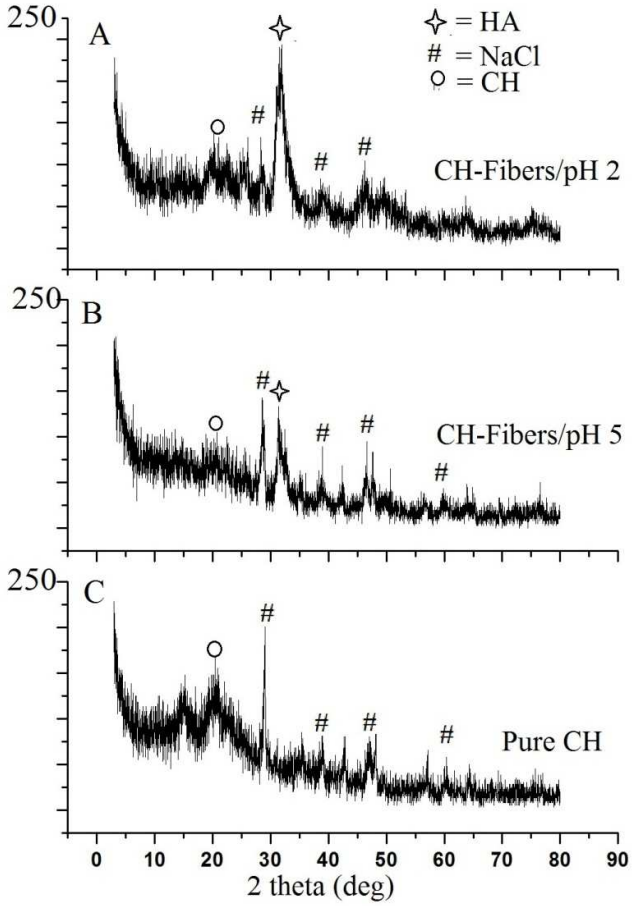

Figure 5-22 XRD pattern of scaffolds (A) CH-fibers/pH 2, (B) CH-fibers/pH5, and (C) pure CH frozen at (-15°C) after immersion in SBF for 21 days, showing HA peaks (*) on composite scaffold; and NaCl peaks (#) on pure CH scaffold.

Figure 5-23 and Table 5-6 shows the FTIR spectra and the list of the most important absorption bands. The spectra evidence stronger peaks at 635 cm^{-1} and at 1024-1095 attributed to the bending vibration of O-H in HA and to stretching vibration bands of phosphate group[71], respectively, on composite scaffolds as compared to pure CH. These bands are particularly intense in the scaffolds prepared at pH 2.

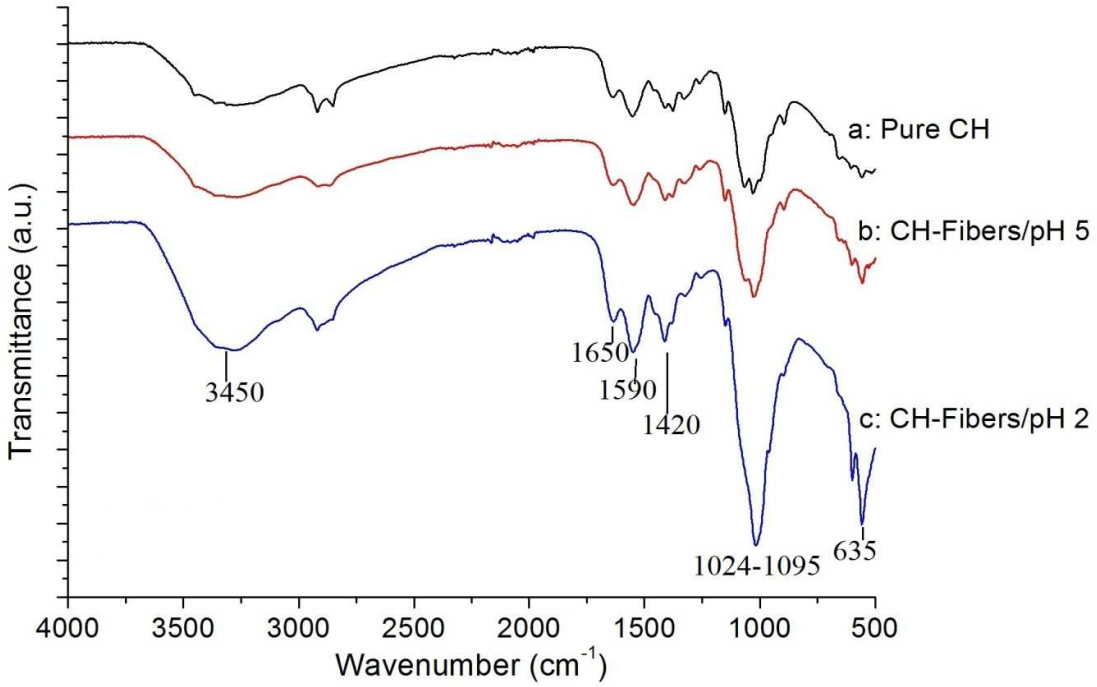

Figure 5-23 FTIR spectra scaffolds (A) CH-fibers/pH 2, (B) CH-fibers/pH5, and (C) pure CH frozen at (-15°C) after immersion in SBF for 21 days.

Table 5-6 Assignment of FTIR spectra[42] presented in Figure 5-23

IR absorption bands (cm^{-1})	Description	
~3450	Stretching vibration (N-H)	Chitosan
~1650	Stretching vibration (-C=O-) Amide I	Chitosan
~1590	Amine	Chitosan
~1420	Bending vibration (C-H)	Chitosan
~1153, 1070, 1031	Strecthing (C-O-C)	Chitosan
~1024-1095	Stretching vibration (P-O)	PO_4^{3-} (HA)
~956	Stretching vibration (P-O)	PO_4^{3-} (HA)
~635	Bending vibration (O-H)	(HA)

The Ca and P concentration variations in the immersion media (SBF) during the soaking period are expressed in Figure 5-24 as depletion amounts. It is observed that for CH-fibers composite scaffolds, the SBF solutions depletions increase with the immersion time whereas they are not significant in the case of pure CH scaffolds. In the case of the composite scaffolds, the CH-fibers/pH 2 scaffold showed to promote a larger depletion of SBF P ions as compared to CH-fibers/pH 5.

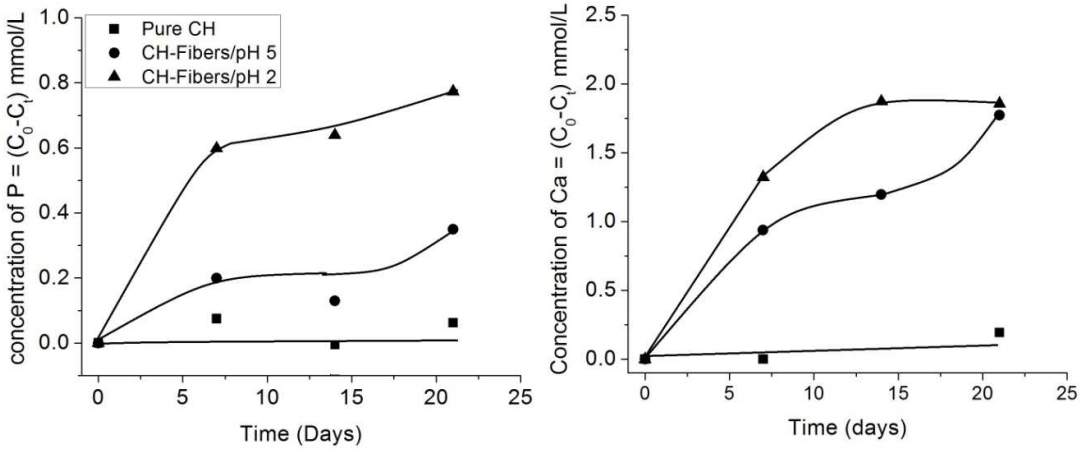

Figure 5-24 Variations on Ca and P concentrations decrease (C_0-C_t) of the immersion media after 0, 7, 14, and 21 days

The decrease of SBF Ca and P concentrations indicate that these ions were withdrawn from SBF solutions in the case of the composite scaffolds and precipitate on the scaffold pore walls as a CaP phase. For pure CH scaffolds the concentration of both Ca and P are relatively stable with negligible variations. Comparing the values of both ΔCa and ΔP of composite scaffolds (CH-fibers/pH 2 and CH-fibers/pH 5) and pure CH, the bioactivities of the scaffolds under analysis may be ordered as CH-fibers/pH 2> CH-fibers/pH 5> pure CH. This result is in line with XRD and FTIR spectra, in which HA peaks and phosphate stretching bands are sharper in CH-fibers/pH 2, followed by CH-fibers/pH 5, and then by pure CH.

Bioactivity qualifies the tendency of a material to form a chemical bond with the host bone[16] and is experimentally denounced by the formation of an apatite layer. The precipitation of such CaP layer requires nucleation sites for apatite nuclei to be formed and later start growing. CH composite scaffold/pH 2 present a smaller sized porous structure as compared to the one prepared at pH 5. Moreover it was shown that the crystalinity and crystal phase compositions of the CaP reinforcement (Figure 5-22) is different from that of the composite scaffold/pH5.

The studies on apatite nucleation in biomaterials have revealed that there are a number of different mechanisms depending on the materials[22]. For bioglass and glass ceramics which are based on the $Na_2O–SiO_2$ or $CaO–SiO_2$ binary system, the SiOH functional group favors the apatite nucleation. In the case of HA, Kokubo et al.[22] studied the mechanism of apatite formation by monitoring the zeta potential prior to immersion in SBF. It was shown that in the early time, HA became negatively charged due to its OH^- and PO_4^{3-} groups. Because of this negative charge, Ca^{2+} from SBF were combined with HA thus formed Ca-rich calcium phosphate which accumulated and allowed a final

positive charge. Further process was combination of PO_4^{3-} to the existing Ca-rich calcium phosphate to lower the Ca/P ratio until reaching the stoichiometric ratio of HA.

The above mechanism may explain a different stabilization tendency of Ca concentration as compared to P concentration. This tendency is clearly shown in CH-fibers/pH 2 scaffolds (Figure 5-24) as the Ca depletion curve started to stabilize after 14 days while the P depletion curve still showed an increasing trend until 21 days. Smaller or slower depletions of both Ca and P were observed for CH-fibers/pH 5 during the first two weeks. However after that initial period certain acceleration is noticed in both ions depletion. It is here suggested that the pore walls collapse illustrated in Figure 5-21(d) might have contributed for an enhancement of Ca and P removal from SBF solution. These results also indicate that CH-fibers/pH 2 promote faster Ca and P SBF ions consumption. However this tendency may be altered by polymer degradation which seems to start earlier for scaffolds prepared from CH solutions pH5.

Besides their different stabilization tendencies of Ca and P SBF concentration, it is also evident that depending on the CH solution pH, pH 2 and pH 5, different ΔCa/ΔP are observed. In CH-fibers/pH 2, the ΔCa/ΔP value after 21 days is close to 1.85 (Δwt /Δwt) or 1.4 (Δmol/Δmol) while in CH-fibers/pH 5 is close to 3.90(Δwt/Δwt) or to 2.9 (Δmol/Δmol). These values also qualify the bioactivity difference between the scaffolds prepared at different pH, as already confirmed by XRD and FTIR (Figure 5-22 and Figure 5-23). In CH-fibers/pH 2, the value of ΔCa/ΔP (1.4) is below the ratio of stoichiometric HAs (Ca/P= 1.6-1.7) while in CH-fibers/pH 5, the value of ΔCa/ΔP (2.90) indicates a different bioactivity in which the process of P absorption is delayed. The obtained curves anticipate that longer times will be required for CH-fibers/pH 5 if a value ΔCa/ΔP approaching that of stoichiometric HA is desired.

In the case of CH-fibers/pH 2, the as prepared scaffold contains brushite (XRD in Figure 5-15 A). After 21 days of SBF immersion (XRD in Figure 5-22 A), the peak of brushite has disappeared thus indicating that its dissolution and possible recrystallization as a different CaP type. It is known that acidic CaP, like brushite, is not stable at pH values above 6. This reason explains why in SBF (pH ~7), brushite transforms into a more stable CaP[72]. Zhang and Zhang[10] studied the bioactivity of β-TCP and glass reinforced chitosan composite scaffold and monitored the variations of Ca and P concentration during the first day prior to immersion. The results revealed that Ca and P concentrations increased due to dissolution of glass and β-TCP occurred during the first 20hours. Further observation showed the Ca and P concentrations decreased which indicated the formation of apatitic layer in the scaffold.

As explained before, preparing the scaffolds at pH 2 turned out to dissolve some amount of HA fibers giving place to brushite precipitation during the later freezing step. (section 5.2.2.). The existing brushite in the scaffold CH-fibers/pH 2 underwent dissolution and precipitation during SBF immersion. The CaP re-precipitation will originate smaller

particles as compared to the original HA fibers. Compared to CH-fibers/pH 5, in which only HA fibers (in the size of 50-200μm) are present in the scaffold, the existence of other smaller sized precipitates in CH-fibers/pH 2 is though to offer more nucleation sites for apatite formation. As mentioned by Alves et al.[73], smaller sized bioactive particles which reinforce in the composite enhance osteoblast proliferation and differentiation and thus further enhance biomineralization process.

5.3.Drug-Loaded Composite Scaffold

A study of the chitosan based scaffolds prepared in this work for the application of drug delivery system was carried out. HA granules either loaded or unloaded with dexamethasone were prepared in the laboratory and futher mixed with chitosan solution. Dexamethasone used as a model drug in this present study is one kind of anti inflammatory drug[6]. It is widely used in bone engineering application; in osteogenic media to direct the differentiation of stem cells towards the osteogenic lineage[74, 80]. Drug delivery study on this system was aimed to design locally the controlled release of DEX in order to effectively support the bone ingrowth.

5.3.1. Physicochemical Characterization

Figure 5-25 shows the hydroxyapatite-dexamethasone (HA-DEX) and HA granules prepared by spray drying. Both microspheres have similar appearance, with no clear details information related to dexamethasone location or appearance in the microsphere. Both types of microspheres were used for the preparation of chitosan based composites loaded with DEX as a model drug. The as prepared scaffolds by freeze-drying chitosan solutions with HA and HA-DEX granules, were subsequently immersed without any rehydration process (ethanol treatment) in PBS solution for assessing the DEX release behavior.

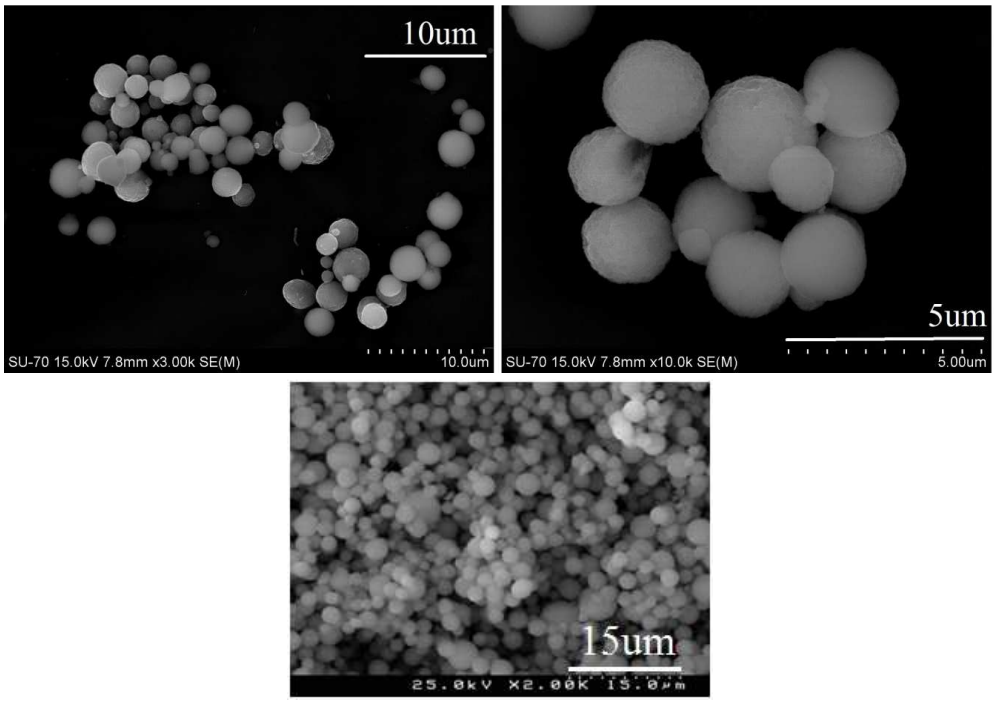

Figure 5-25 HA-DEX granules (top); pure HA granules (bottom) prepared by spray drying

The macroscopic observation of the scaffolds allowed verifying that they swelled and suffered dissolution for the drug delivery test. Such behavior is in agreement with the results of other authors[80]

The morphologies of drug-loaded chitosan based scaffolds (CH-HA-DEX) before and after 7 days of immersion in PBS solution are shown in Figure 5-26. From the micrographs it can be observed the dissolution of chitosan on the wall structure of the scaffold as prepared (prior to 7 days immersion).

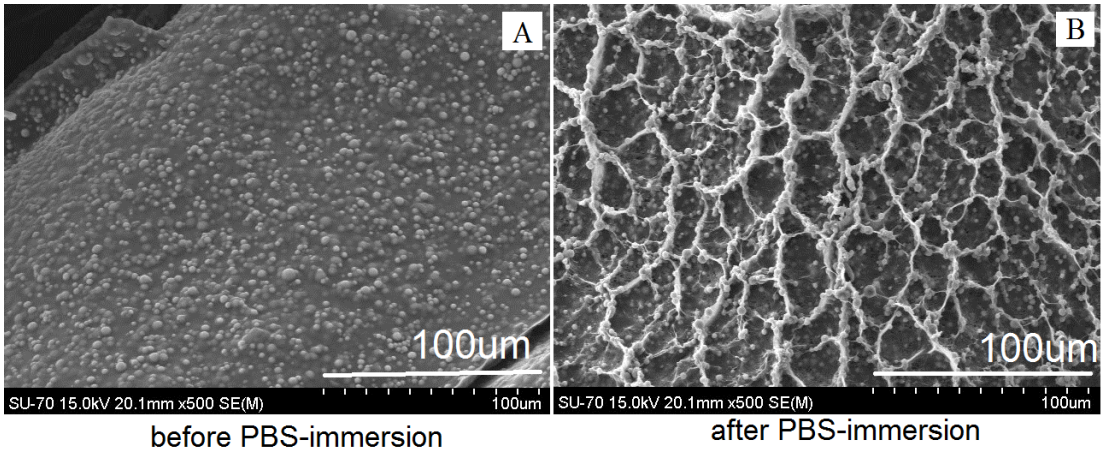

Figure 5-26 Wall appearance of drug-loaded chitosan based scaffold (prepared by procedure 2) before (A) and after 8 days of PBS immersion (B); indicating polymer dissolution in the wall structure

5.3.2. Drug Release Test

As mentioned in literature review (section 2.1.5), different materials and morphologies can be used as drug carriers for the sustained release of a therapeutic agent. There are different possibilities of loading the drug in a composite scaffold: (1) by direct mixing all the components, (2) by loading the drug in one of the components and mixing it with the other components or (3) by impregnating or coating a preformed structure with the drug[75].

In the present study, three routes were followed to prepare DEX loaded scaffolds: (1) pure HA granules and DEX were added to CH solution; (2) DEX-loaded HA granules were added to CH solution without any additional DEX; and (3) procedure 2 with additional DEX added to CH solution. A schematic illustration of these 3 methods is shown in Figure 5-27. In terms of DEX loaded amounts, procedure 3 uses the double of the drug amount corresponding either to procedure 1 or to procedure 2. The HA granules (Figure 5-25) used in the experiments were obtained in the laboratory[76] by spray drying HA or HA-DEX suspensions.

The in vitro DEX release profiles in PBS solution from the differently loaded composite scaffolds were followed during 30 days and are presented in Figure 5-28. In this figure, two types of curves are presented: (1) cumulative release percentage (A) and (2)

absolute amount of released drug (B). The results clearly show that the release pattern is dependent on the drug loading procedure.

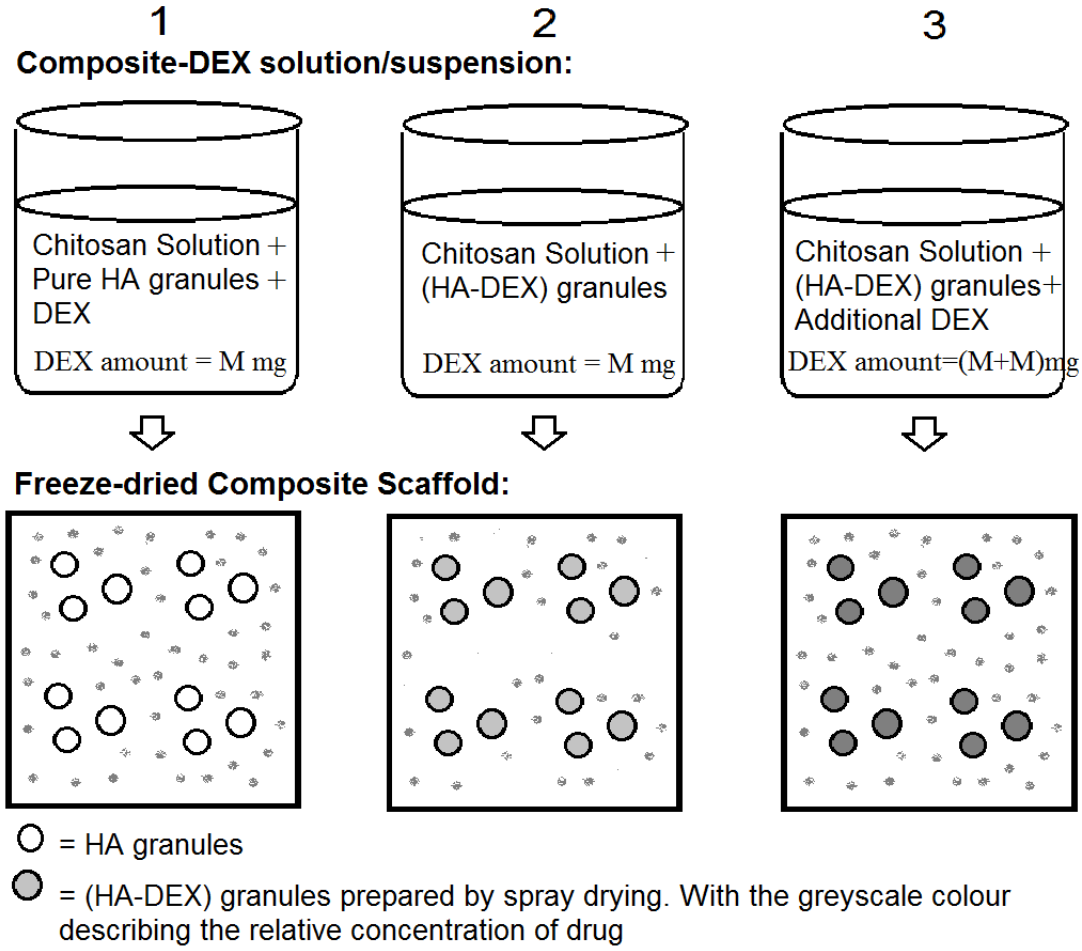

Figure 5-27 Illustration of composite-DEX solution preparation and the as prepared scaffold

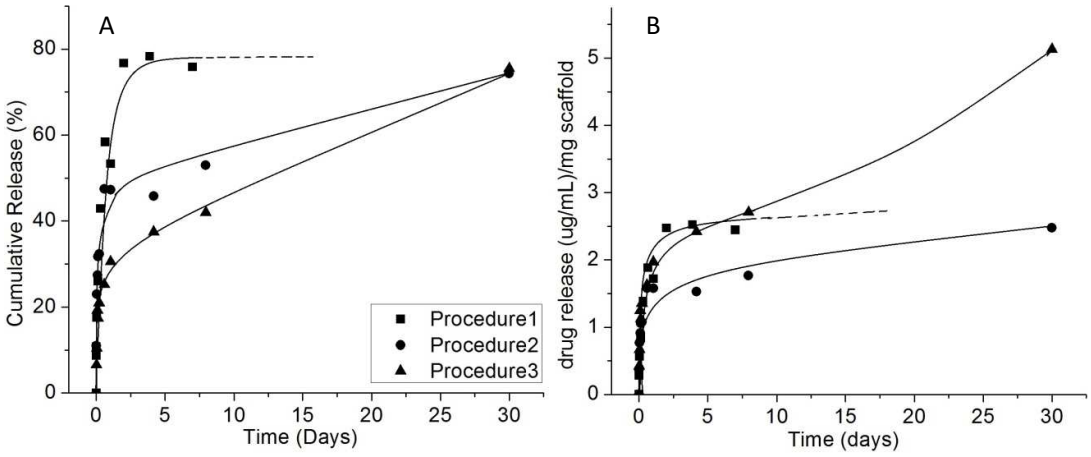

Figure 5-28 Drug release profile of chitosan based scaffold based on the percentage cumulative release (A), and absolute amount of released drug (B)

It can be observed for all the types of drug loaded scaffolds that an initial burst release occurred during the first 12 hours (Figure 5-28 and Figure 5-29). However, for longer release time, the scaffold prepared by *procedure 1* showed the faster release in which after 2 days, the release curve started to stabilize. For *procedures 2* and *3*, the drug release seems to be rather delayed , being the release pattern of procedure 3 a more retarded one (Figure 5-28 A).

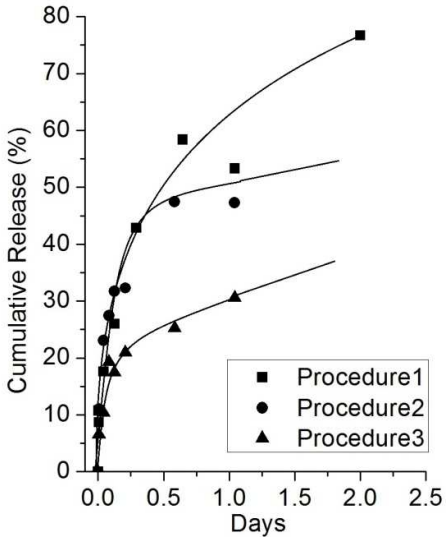

Figure 5-29 Higher amplification for shorter release time from Figure 5-28 A

The drug delivery profile from any delivery system depends on several factors: (1) the microstructure of the system, (2) the drug solubility, (3) the type of bond between the drug and the matrix, and (4) the mechanism of degradability of the matrix (if existing)[77]. From the point of view of polymer carriers, three main possible mechanisms are available for drug deliver: diffusion controlled, solvent-activation (swelling-osmotically controlled) and controlled by biodegradability (chemically-controlled)[78]. In the present study, the scaffolds were seen to degrade superficially (Figure 5-26 (b)). This indicates that besides diffusion, the biodegradability of the chitosan scaffold will be also contributing to the drug delivery.

In the *procedure* 1, the initial burst release accounts for almost all the released drug. As the drug was dissolved directly in the composite suspension (CH + HA microspheres), most of the drug remained probably located in polymer matrix sites with easy access to the release medium. Conversely, using DEX-HA loaded granules (*procedure 2* or *3*) resulted in a less accessible location of the drug to the release medium. The drug loaded into the granules has now to diffuse through the granules and then through the polymer matrix before reaching the release medium. It can thus be considered that the closer to polymer matrix surface, the faster is the release. This is supposed to be the case of *procedure 1* which showed the fastest drug release, with approximately ~80% of the DEX being released in less than 2days.

Furthermore the initial burst release during the first few hours exhibited by all the scaffolds indicates that all scaffolds possess a certain amount of drug located in the near surface region, including the scaffold prepared by *procedure 2*. For this one, even though the drug was loaded only into the HA granules, there is a probability that a certain amount of DEX diffused to the chitosan solution before freeze drying and then precipitated within the polymer matrix during freezing. Such behavior indeed decreased the effectiveness of drug loading into HA granules. Regarding the procedure 3, the addition of a certain amount of DEX to the chitosan solution decreases DEX concentration gradients throughout the whole system and thus minimizes the DEX diffusion out from the HA granules into the chitosan solution. By applying this method, the DEX concentration inside the HA granules is likely maintained and the diffusion from granules to chitosan solution minimized. This is confirmed by the curves in figure 5-27 (B) which show that the initial burst release in procedure 1 and 3 are essentially the same. This initial burst reflects the delivery of equivalent amounts of DEX existing within the polymer matrix which correspond to the same M mg of DEX dissolved in the CH solutions of both cases.

Compared to *procedure 1,* both *procedures 2* and *3* show the ability to retard the drug release. The scaffold prepared using *procedure 2* showed an initial burst drug release of about ~45% of the total loaded drug during the first 12 hours (Figure 5-29), followed by a slower release until 80% during the remaining 30days (Figure 5-28 (A)). The results also show that preparing the composite scaffolds by *procedure 3*,i.e. by adding an extra amount of DEX to the CH solution, allowed to reduce the initial burst release to ~30%, thus enabling a larger amount of DEX to be released slower during the remaining period. This fact demonstrates that the drug initially added to the chitosan solution succeeded to keep the drug confined to the granules during the initial period of drug release thus slowing down the overall release rate.

Fitting the initial burst release to Fickian diffusional release equation of the type:

$$\frac{M_t}{M_\infty} = kt^n \qquad (5.3)$$

where M_t is the amount of DEX released at t time, $M_\infty$is the total released amount at infinite time, t is the release time, k is a constant, and n is the diffusional exponent, it was observed that the initial burst release data corresponding to the release time ~10hours fit well the equation. The value obtained for n was close to ~0.42. This value of n is close to n = 0.5, which indicates a diffusion controlled release[74, 79]. It is thus suggested that diffusion controlled drug release occurs in all the prepared scaffolds during the initial release periods. Further studies are required to explain the mechanism applying to longer release times.

The drug loading methods of chitosan scaffolds used in the present work improved the DEX sustained release ability. Duarte et al.[80] prepared chitosan scaffold loaded with dexamethasone using supercritical impregnation, and the result showed that almost 90% of

the loaded drug was released after 2 hours. Chitosan composite scaffold with β-TCP and glass which were loaded by gentamicin sulphate via 48h of soaking showed initial burst releasing ~80% of the drug during 2 days and followed by slower release until ~20days[7]. Comparing with these two methods, it is worthy to mention the advantages of loading the drug into HA microspheres and further inserted them into the chitosan solution before freeze-drying (both *procedure 2* and 3). The results pointed out that those scaffolds were able to retard the drug release evidencing a sustained release profile of DEX, thus suggesting their potential to be used as controlled drug release system.

Chapter 6
Conclusions & Recommendations

A comprehensive study on chitosan based scaffolds for bone regeneration has been carried out in the present work. Different types of chitosan based scaffolds were prepared with different composition and under different conditions. HA fibers and monetite thin platelets were obtained by a precipitation method. These two types of CaP particles as well as a mixture of them were used as reinforcing elements of chitosan scaffolds. HA granules (loaded or unloaded with DEX) prepared by spray-drying were also used to load the scaffolds with DEX. Microstructure characteristics (pore size, porosity and interconnectivity), crystal phase composition, mechanical properties, bioactivity, and drug delivery performance of the produced scaffolds were studied.

CaP particles precipitation

HA fibers with a size in the range of 50-150µm were successfully produced by a precipitation method reported by Aizawa et al.[38] and Zhang et al.[39], in moderately acidic solution. Three main stages were identified in the precipitation (1) formation of platelet shaped monetite, (2) formation of fibers-like OCP, and (3) transformation of fibers-like OCP crystal into HA. The fiber morphology was defined in the first 24 hours of refluxing at 80ºC while increasing refluxing temperature to 90ºC ensured the transformation of OCP into HA. It was also demonstrated that modifying Zhang method by anticipating the 90ºC refluxing does enable to reduce the time required for obtaining HA fibers.

Chitosan based Scaffolds

Highly interconnected macroporous scaffolds with pore sizes in the range of 50-300µm, interconnectivity around 91-98.5%, and porosity higher than 80% were produced by freeze-drying. Three dimensional chitosan based scaffold loaded either with HA fibers, or with monetite platelets or a mixture of both were characterized in terms of microstructure, crystal phase composition, mechanical and bioactive behaviors and compared to pure chitosan scaffold. The pH of chitosan solution, the freezing temperature during TIPS and the type of loaded calcium phosphate particle were confirmed to have a significant influence in the properties of the obtained scaffolds. These variables showed to play an important role in defining the scaffold microstructure. Larger pores were normally obtained when using higher freezing temperature, higher pH CH solutions and by HA fibers loading (pH 5).

The mechanical properties of the scaffolds were seen to be highly dependent on pore size and on the type of reinforcement. Low pH values and freezing temperatures resulted in scaffolds of smaller pore and hence with better mechanical properties. Conversely, high pH value and freezing temperature resulted in larger pore but lower mechanical properties. The morphology of the reinforcing-particles was also a critical variable. Monetite thin platelets displayed a better reinforcing ability as compared to HA fibers, being this effect attributed to

the irregular and smaller sized platelet shape which allowed a better bonding with polymer matrix. From the point of view of bioactivity, chitosan composite scaffold loaded with HA fibers exhibited enhanced bioactive response as compared to pure chitosan. Continuous variation of Ca and P concentrations in SBF solution during scaffolds soaking indicated deposition of apatite layer in the materials. This behavior was not observed in pure chitosan scaffold.

Some experimental conditions combinations were found appropriated for obtaining scaffolds which porosity, pore size, interconnectivity and mechanical properties point out a potential applicability in bone tissue engineering, CH-fibers/pH 2 frozen at -15^{o}C demonstrated the best bioactivity and mechanical properties (compressive modulus: 2.58Mpa, compressive strength: 0.18Mpa) while displaying an average pore size of ~136µm. Other produced scaffolds were found to have larger pore sizes such as CH-fibers/pH 5 frozen at -15^{o}C (~152µm) and CH-fibers/pH 5 frozen at -196^{o}C (~190µm) but lower mechanical properties. CH-monetite/pH 5 frozen at 0^{o}C showing the second best mechanical properties (compressive modulus: 0.7-0.87Mpa, compressive strength: 0.07-0.11Mpa) with an average pore size (~170µm) is also worthy mentioning. These pore size values are already close to the size required (200-400µm) for good cell proliferation. However, from the point of view of mechanical properties, the obtained scaffolds still need to be improved.

Chitosan based Scaffolds DDS

Loading dexamethasone as a drug model into HA granules and inserted them further in chitosan scaffold was proved to be a good strategy to retard the drug release. Three different methodologies of drug loading into to the scaffolds were confirmed to affect significantly the drug release rate. Immobilizing the drug in HA granules by spray drying before combining with the chitosan solution demonstrated slower release as compared to mixing directly the drug with the CH solution. An even slower release rate could be obtained by adding DEX to the chitosan solution in order to minimize DEX concentration gradients: 25% of DEX was released during the first 14hours being followed by a slow release of DEX until 80% during the remaining 30days. This method showed to provide a slower release rate as compared to other reports

This study underscores the chitosan based scaffold as a potential scaffold for bone regeneration and drug delivery system.

Recommendations for Future Work

The results obtained in the present work revealed some needs of further studies aiming to clarify the following issues:

1. Freezing temperature during TIPS was shown to be a critical variable for determining the pore structure which in turns determines the mechanical properties. However freezing at -196ºC is though to have a potential for pore orientation which was not exploited in the

present work. It is thus suggested to test sufficiently low freezing temperatures combined with different freezing methologies for exploiting the method potentialities for pore alignment.

2. The effects of increasing loads of CaP particles in CH scaffolds need to be investigated for assessing its effect on both the scaffold pore size and mechanical properties.
3. Drug release studies with various drug concentrations should be undertaken for assessing the active mechanisms during drug release for longer times, It is expected that such studies might contribute to identify the scaffold parameters that rule DEX release.
4. Biocompatibility test (cell culture tests) should be carried out in order to study the cell response (attachment and or proliferation).dependence on the scaffolds characteristics.

REFERENCES

[1] Kim, I.-Y. et al. Chitosan and its derivatives for tissue engineering applications. *Biotechnol. Adv* **26**, 1-21 (2008).

[2] Leong, K.-F., Du, Z., Chua, C.-K. & Yang, S. The design of scaffolds for use in tissue engineering. Part 1. Traditional factors. *Tissue Engineering* **7**, 679-89 (2004).

[3] Mistry, A.S. & Mikos, A.G. Tissue engineering strategies for bone regeneration. *Adv. Biochem. Eng. Biotechnol* **94**, 1-22 (2005).

[4] Burg, K.J.L., Porter, S. & Kellam, J.F. Biomaterial developments for bone tissue engineering. *Biomaterials* **21**, 2347-2359 (2000).

[5] Place, E.S., George, J.H., Williams, C.K. & Stevens, M.M. Synthetic polymer scaffolds for tissue engineering. *Chem Soc Rev* **38**, 1139-1151 (2009).

[6] Mouriño, V. & Boccaccini, A.R. Bone tissue engineering therapeutics: controlled drug delivery in three-dimensional scaffolds. *Journal of The Royal Society Interface* **7**, 209 - 227 (2010).

[7] Zhang, Y. & Zhang, M. Calcium phosphate/chitosan composite scaffolds for controlled in vitro antibiotic drug release. *Journal of Biomedical Materials Research* **62**, 378-386 (2002)

[8] Kong, L. et al. Preparation and characterization of nano-hydroxyapatite/chitosan composite scaffolds. *J Biomed Mater Res A* **75**, 275-282 (2005).

[9] Zhang, Y. & Zhang, M. Microstructural and mechanical characterization of chitosan scaffolds reinforced by CaPs. *Journal of Non-Crystalline Solids* **282**, 159-164 (2001).

[10] Zhang, Y. & Zhang, M. Synthesis and characterization of macroporous chitosan/CaP composite scaffolds for tissue engineering. *J. Biomed. Mater. Res* **55**, 304-312 (2001).

[11] Zhang, Y., Ni, M., Zhang, M. & Ratner, B. CaP-chitosan composite scaffolds for bone tissue engineering. *Tissue Eng* **9**, 337-345 (2003).

[12] Chu, P.K. & Liu, X. *Biomaterials fabrication and processing handbook*. (CRC Press/Taylor & Francis: 2008).

[13] Uskoković, V. & Uskoković, D.P. Nanosized hydroxyapatite and other calcium phosphates: chemistry of formation and application as drug and gene delivery agents. *J. Biomed. Mater. Res. Part B Appl. Biomater* **96**, 152-191 (2011).

[14] Salgado, A.J., Coutinho, O.P. & Reis, R.L. Bone Tissue Engineering: State of the Art and Future Trends. *Macromolecular Bioscience* **4**, 743-765 (2004).

[15] Dorozhkin, S.V. Calcium Orthophosphates in Nature, Biology and Medicine. *Materials* **2**, 399-498 (2009).

[16] Wagoner Johnson, A.J. & Herschler, B.A. A review of the mechanical behavior of CaP and CaP/polymer composites for applications in bone replacement and repair. *Acta Biomater* **7**, 16-30 (2011).

[17] Boccaccini, A.R. & Maquet, V. Bioresorbable and bioactive polymer/Bioglass® composites with tailored pore structure for tissue engineering applications. *Composites Science and Technology* **63**, 2417-2429 (2003).

[18] Madihally, S.V. & Matthew, H.W.T. Porous chitosan scaffolds for tissue engineering. *Biomaterials* **20**, 1133-1142 (1999).

[19] Karageorgiou, V. & Kaplan, D. Porosity of 3D biomaterial scaffolds and osteogenesis. *Biomaterials* **26**, 5474-5491 (2005).

[20] Whang, K. et al. Engineering bone regeneration with bioabsorbable scaffolds with novel microarchitecture. *Tissue Eng* **5**, 35-51 (1999).

[21] Rezwan, K., Chen, Q.Z., Blaker, J.J. & Boccaccini, A.R. Biodegradable and bioactive

porous polymer/inorganic composite scaffolds for bone tissue engineering. *Biomaterials* **27**, 3413-3431 (2006).

[22] Kokubo, T., Kim, H.-M. & Kawashita, M. Novel bioactive materials with different mechanical properties. *Biomaterials* **24**, 2161-2175 (2003).

[23] Di Martino, A., Sittinger, M. & Risbud, M.V. Chitosan: A versatile biopolymer for orthopaedic tissue-engineering. *Biomaterials* **26**, 5983-5990 (2005).

[24] Kokubo, T. & Takadama, H. How useful is SBF in predicting in vivo bone bioactivity? *Biomaterials* **27**, 2907-2915 (2006).

[25] Hutmacher, D.W. & Martina, M. Biodegradable polymers applied in tissue engineering research: a review. *Polymer International* **56**, 145-157

[26] Malafaya, P.B., Silva, G.A., Baran, E.T. & Reis, R.L. Drug delivery therapies I: General trends and its importance on bone tissue engineering applications. *Current Opinion in Solid State and Materials Science* **6**, 283-295 (2002).

[27] Biondi, M., Ungaro, F., Quaglia, F. & Netti, P.A. Controlled drug delivery in tissue engineering. *Advanced Drug Delivery Reviews* **60**, 229-242 (2008).

[28] Lee, S.-H. & Shin, H. Matrices and scaffolds for delivery of bioactive molecules in bone and cartilage tissue engineering. *Advanced Drug Delivery Reviews* **59**, 339-359 (2007).

[29] Denkbas, E.B. & Ottenbrite, R.M. Perspectives on: Chitosan Drug Delivery Systems Based on their Geometries. *Journal of Bioactive and Compatible Polymers* **21**, 351 - 368 (2006).

[30] Malafaya, P.B., Silva, G.A. & Reis, R.L. Natural-origin polymers as carriers and scaffolds for biomolecules and cell delivery in tissue engineering applications. *Advanced Drug Delivery Reviews* **59**, 207-233 (2007).

[31] Jayakumar, R., Menon, D., Manzoor, K., Nair, S.V. & Tamura, H. Biomedical applications of chitin and chitosan based nanomaterials--A short review. *Carbohydrate Polymers* **82**, 227-232 (2010).

[32] Alves, N.M. & Mano, J.F. Chitosan derivatives obtained by chemical modifications for biomedical and environmental applications. *International Journal of Biological Macromolecules* **43**, 401-414 (2008).

[33] Habraken, W.J.E.M., Wolke, J.G.C. & Jansen, J.A. Ceramic composites as matrices and scaffolds for drug delivery in tissue engineering. *Adv. Drug Deliv. Rev* **59**, 234-248 (2007).

[34] Wang, L. & Nancollas, G.H. Calcium Orthophosphates: Crystallization and Dissolution. *Chemical Reviews* **108**, 4628-4669 (2008).

[35] Dorozhkin, S.V. Calcium Orthophosphates in Nature, Biology and Medicine. *Materials* **2**, 399-498 (2009).

[36] Yuan, H. et al. A comparison of the osteoinductive potential of two CaP ceramics implanted intramuscularly in goats. *J Mater Sci Mater Med* **13**, 1271-1275 (2002).

[37] Shi, D. *Introduction to biomaterials*. (清华大学出版社: 2006).

[38] Aizawa, M. Preparation of spherical apatite particles by the homogeneous precipitation method in the presence of magnesium ions and their ion-exchange properties. *MATER RES B* **34**, 1215-1225 (1999).

[39] Zhang, H., Wang, Y., Yan, Y. & Li Precipitation of biocompatible hydroxyapatite whiskers from moderately acid solution. *Ceramics International* **29**, 413-418 (2003).

[40] van Kemenade, M.J.J.M. & de Bruyn, P.L. A kinetic study of precipitation from supersaturated calcium phosphate solutions. *Journal of Colloid and Interface Science* **118**, 564-585 (1987).

[41] Nancollas, G. H., The involvement of calcium phosphate in biological mineralization and demineralization processes. Pure & Appl. Chem. **64**, No. 11, 1673-1678 (1992)

[42] Thein-Han, W.W. & Misra, R.D.K. Biomimetic chitosan-nanohydroxyapatite composite scaffolds for bone tissue engineering. *Acta Biomater* **5**, 1182-1197 (2009).

[43] Kong, L. et al. A study on the bioactivity of chitosan/nano-hydroxyapatite composite scaffolds for bone tissue engineering. *European Polymer Journal* **42**, 3171-3179 (2006).

[44] Zhao, F., Grayson, W.L., Ma, T., Bunnell, B. & Lu, W.W. Effects of hydroxyapatite in 3-D chitosan-gelatin polymer network on human mesenchymal stem cell construct development. *Biomaterials* **27**, 1859-1867 (2006).

[45] Peter, M. et al. Preparation and characterization of chitosan-gelatin/nanohydroxyapatite composite scaffolds for tissue engineering applications. *Carbohydrate Polymers* **80**, 687-694 (2010).

[46] Han, J., Zhou, Z., Yin, R., Yang, D. & Nie, J. Alginate-chitosan/hydroxyapatite polyelectrolyte complex porous scaffolds: Preparation and characterization. *International Journal of Biological Macromolecules* **46**, 199-205 (2010).

[47] Ang, T.H. et al. Fabrication of 3D chitosan-hydroxyapatite scaffolds using a robotic dispensing system. *Materials Science and Engineering: C* **20**, 35-42 (2002).

[48] Zhang, Y. & Zhang, M. Cell growth and function on calcium phosphate reinforced chitosan scaffolds. *Journal of Materials Science: Materials in Medicine* **15**, 255-260 (2004).

[49] Ma, P.X. Scaffolds for tissue fabrication. *Materials Today* **7**, 30-40 (2004).

[50] Chung, H.J. & Park, T.G. Surface engineered and drug releasing pre-fabricated scaffolds for tissue engineering. *Advanced Drug Delivery Reviews* **59**, 249-262 (2007).

[51] Leong, K.F., Cheah, C.M. & Chua, C.K. Solid freeform fabrication of three-dimensional scaffolds for engineering replacement tissues and organs. *Biomaterials* **24**, 2363-2378 (2003).

[52] Nam, Y.S. & Park, T.G. Biodegradable polymeric microcellular foams by modified thermally induced phase separation method. *Biomaterials* **20**, 1783-1790 (1999).

[53] Lim, J.I. et al. A Novel Method for Porous Chitosan Scaffold. *KEM* **342-343**, 65-68 (2007).

[54] Maquet, V. & Jerome, R. Design of Macroporous Biodegradable Polymer Scaffolds for Cell Transplantation. *MSF* **250**, 15-42 (1997).

[55] http://astronomy.swin.edu.au/cms/astro/cosmos/s/Sublimation (retrieved on 06/06/2011)

[56] Aizawa, M., Porter, A.E., Best, S.M. & Bonfield, W. Ultrastructural observation of single-crystal apatite fibres. *Biomaterials* **26**, 3427-3433 (2005).

[57] www.nhn.ou.edu/~bumm/NanoLab/ppt/X-ray_Diffraction.ppt (Retrieved on 06/06/2011)

[58] Zmora, S., Glicklis, R. & Cohen, S. Tailoring the pore architecture in 3-D alginate scaffolds by controlling the freezing regime during fabrication. *Biomaterials* **23**, 4087-4094 (2002).

[59] Rinaudo, M. Chitin and chitosan: Properties and applications. *Progress in Polymer Science* **31**, 603-632 (2006).

[60] Lu, S., Song, X., Cao, D., Chen, Y. & Yao, K. Preparation of water-soluble chitosan. *Journal of Applied Polymer Science* **91**, 3497-3503 (2004).

[61] Agarwal, B.D. & Broutman, L.J. *Analysis and performance of fiber composites.* (Wiley: 1990).

[62] Šupová, M. Problem of hydroxyapatite dispersion in polymer matrices: a review. *J Mater Sci: Mater Med* **20**, 1201-1213 (2009).

[63] Darling, A.L. & Sun, W. 3D microtomographic characterization of precision extruded poly-epsilon-caprolactone scaffolds. *J. Biomed. Mater. Res. Part B Appl. Biomater* **70**, 311-317 (2004).

[64] Ho, S.T. & Hutmacher, D.W. A comparison of micro CT with other techniques used in the characterization of scaffolds. *Biomaterials* **27**, 1362-1376 (2006).

[65] Araujo Junior, J. V., Compositos polimero/fosfato de calico para aplicacoes biomedicas, PhD Thesis, Ceramics Department, Universidade de Aveiro (2005)

[66] Li, X., Feng, Q., Jiao, Y. & Cui, F. Collagen-based scaffolds reinforced by chitosan fibres for bone tissue engineering. *Polymer International* **54**, 1034-1040 (2005).

[67] Jell, G. et al. Carbon nanotube-enhanced polyurethane scaffolds fabricated by thermally induced phase separation. *J. Mater. Chem.* **18**, 1865 (2008).

[68] Mittal, V. *Optimization of Polymer Nanocomposite Properties*. (Wiley-VCH: 2010).

[69] Yu, H., Matthew, H.W., Wooley, P.H. & Yang, S. Effect of porosity and pore size on microstructures and mechanical properties of poly-ε-caprolactone- hydroxyapatite composites. *Journal of Biomedical Materials Research Part B: Applied Biomaterials* **86B**, 541-547 (2008).

[70] Yu, H., Matthew, H.W., Wooley, P.H. & Yang, S. Effect of porosity and pore size on microstructures and mechanical properties of poly-ε-caprolactone- hydroxyapatite composites. *Journal of Biomedical Materials Research Part B: Applied Biomaterials* **86B**, 541-547 (2008).

[71] Peter, M. et al. Novel biodegradable chitosan-gelatin/nano-bioactive glass ceramic composite scaffolds for alveolar bone tissue engineering. *Chemical Engineering Journal* **158**, 353-361 (2010).

[72] Prado Da Silva, M.H. et al. Transformation of monetite to hydroxyapatite in bioactive coatings on titanium. *Surface and Coatings Technology* **137**, 270-276 (2001).

[73] Alves, N.M., Leonor, I.B., Azevedo, H.S., Reis, R.L. & Mano, J.F. Designing biomaterials based on biomineralization of bone. *J. Mater. Chem.* **20**, 2911 (2010).

[74] Duarte, A.R.C., Mano, J.F. & Reis, R.L. Dexamethasone-loaded scaffolds prepared by supercritical-assisted phase inversion. *Acta Biomaterialia* **5**, 2054-2062 (2009).

[75] Soundrapandian, C., Sa, B. & Datta, S. Organic–Inorganic Composites for Bone Drug Delivery. *AAPS PharmSciTech* **10**, 1158-1171 (2009).

[76] Puga, J. B., Spray dried hydroxyapatite-dexamethasone granules for drug delivery system, Project Report, Ceramics Departement, Universidade de Aveiro, Portugal (2011)

[77] Ginebra, M.P., Traykova, T. & Planell, J.A. Calcium phosphate cements as bone drug delivery systems: A review. *Journal of Controlled Release* **113**, 102-110 (2006).

[78] Liechty, W.B., Kryscio, D.R., Slaughter, B.V. & Peppas, N.A. Polymers for Drug Delivery Systems. *Annu. Rev. Chem. Biomol. Eng.* **1**, 149-173 (2010).

[79] Ritger, P.L. & Peppas, N.A. A simple equation for description of solute release II. Fickian and anomalous release from swellable devices. *Journal of Controlled Release* **5**, 37-42 (1987).

[80] Duarte, A.R.C., Mano, J.F. & Reis, R.L. Preparation of chitosan scaffolds loaded with dexamethasone for tissue engineering applications using supercritical fluid technology. *European Polymer Journal* **45**, 141-148 (2009).

APPENDICES

Table A-1 Average pore size (µm) from SEM and µCT, interconnectivity, porosity of the prepared scaffolds

	pH 2	pH 2 loaded	pH 5	pH 5 loaded		
		HA Fibers		HA Fibers	Monetite Powder	Mixture (HA fibers + monetite powder)
-196°C	Pore Size SEM: 57.9±10	-	Pore Size SEM: 222±91	Pore size µCT: 190 porosity: 80.6% intercn: 91.6%	-	-
-15°C	Pore Size SEM: 127±16	Pore Size SEM: 99.5±21 µCT: 136 porosity: 90.7% intercn: 98%	Pore Size SEM: 130±35	Pore Size SEM: 136.5±23 µCT: 152 porosity: 90.7% intercn: 98.5%	-	Pore Size SEM: 129.24±24
0C	Pore Size SEM: 154±37	-	Pore Size SEM: 166±26		Pore Size SEM: 157±31	-

Table A-2 Mechanical properties of the prepared scaffolds (M: Compressive Modulus; S: Compressive Strength in MPa)

	pH 2	pH 2 loaded	pH 5	pH 5 loaded		
		HA Fibers		HA Fibers	Monetite Powder	Mixture (HA fibers + monetite powder)
-196°C	-	-	-	M= 0.616±0.10 S= 0.112±0.028	-	-
-15°C	M=0.2 S=0.02	M= 2.58±0.34 S= 0.158±0.022	M=0.65 S=0.025	M=0.79±0.4 S=0.048±0.007	-	M=0.64±0.16 S=0.079±0.007
0C	-	-		-	M=1.1±0.35 S=0.09±0.01	-

Table A-3 Geometrical density (g/cm^3) of the prepared scaffolds

	pH 2	pH 2 loaded	pH 5	pH 5 loaded		
		HA Fibers		HA Fibers	Monetite Powder	Mixture (HA fibers + monetite powder)
-196°C	-	-	0.0524	0.0714	-	-
-15°C	0.03686	0.05074	0.0541	0.0628	-	0.0689
0C	-	-	-	-	0.06167	-

Drug Release Test

Standard Curve of DEX

Standard curve was made by preparing DEX solution in several concentrations; such as 5, 10, 20, and 30 µg/mL in PBS solution. The absorbance was observed with UV-Vis spectroscopy and noted as follows:

Table A-4 Absorbance of DEX solution in PBS

[C] µg/ml	Absorbance
0	0
5	0.195
10	0.372
20	0.73
30	1.078

From the absorbance data written above, curve was built and line equation was made, as shown in the figure below:

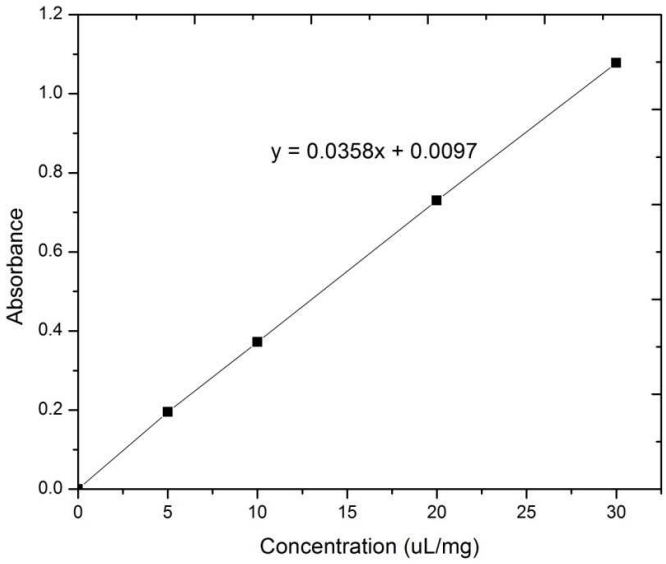

Figure A-1 Standard Calibration Curve for DEX solution in PBS

With: y is the absorbance; x is the concentration in (µg/mL).
Based on the linear equation above, for one known absorbance (from UV Vis spectroscopy), the concentration can be calculated as follows:

$$x = \frac{y - 0.0097}{0.0358} \left({}^{\mu g}/_{mL}\right)$$

Drug Release Test

Table A-5 CH/HA Composite Solution/Suspension for DDS

	Procedure 1	Procedure 2	Procedure 3
2%wt CH solution	10 g	10 g	10 g
HA granules	100 mg pure HA granules	100 mg spray dried HA-DEX granules	100 mg spray dried HA-DEX granules
Additional DEX	-	-	10 mg

Procedure 1

Amount of DEX in freeze-dried scaffold:
Mass of freeze-dried scaffold is assumed to be chitosan & HA granules
10g CH composite solution contains 2%wt chitosan (0.2g) and 1%wt pure HA granules (0.1g).
Amount of added drug = 10mg/10 g CH composite solution
Amount of DEX in freeze-dried scaffold = 10mg/(0.2g CH + 0.1g HA + 10mg DEX)
= 10mg DEX/0.31g freeze-dried scaffold.

Percentage of drug release:
Drug release = Ct/Co x 100%
Ct = concentration of DEX at certain time (µg/mL)
Ct (µg/mL) = (abs-0.0097)/0.0358
Abs = aborbance obtained from UV-Vis analysis
# Co = concentration of DEX if 100% drug release (µg/mL)
Co (µg/mL) = (10mg/0.31g) x mass of scaffold x1000 / 10mL (PBS)

Table A-6 DDS Release Test – Procedure 1

No	Mass Scaffold (g)	Time	Absorbance	Drug Release	
				(%)	(µg/mL)/mg of scaffold
1	0.0106	5 min	0.141	10.72	0.346
2	0.0153	10 min	0.163	8.67	0.279
3	0.0144	60 min	0.300	17.57	0.567
4	0.0158	3h	0.484	25.99	0.838
5	0.0165	7h	0.827	42.89	1.383
6	0.0108	15h 30min	0.738	58.39	1.883
7	0.0178	25h	1.106	53.33	1.720
8	0.0145	2days	1.294	76.69	2.474
9	0.0177	4days	1.610	78.290	2.525
10	0.0163	7days	1.437	75.823	2.445

Procedure 2

Amount of DEX in freeze-dried scaffold:
Mass of freeze-dried scaffold is assumed to be chitosan & HA granules
10g CH composite solution contains 2%wt chitosan (0.2g) and 1%wt pure HA granules (0.1g).
Amount of drug = in HA granules (10%wt) = (10% . 0.1g) = 10mg

Amount of DEX in freeze-dried scaffold = 10mg/(0.2g CH + 0.1g HA)
= 10mg DEX/0.30g freeze-dried scaffold.

Percentage of drug release:
Drug release = Ct/Co x 100%

Ct = concentration of DEX at certain time (µg/mL)
Ct (µg/mL) = (abs-0.0097)/0.0358

Abs = aborbance obtained from UV-Vis analysis
# Co = concentration of DEX if 100% drug release (µg/mL)
Co (µg/mL) = (10mg/0.30g) x mass of scaffold x1000 / 10mL (PBS)

Table A-7 DDS Release Test – Procedure 2

No	Mass Scaffold (g)	Time	Absorbance	Drug Release	
				(%)	(µg/mL)/mg of scaffold
1	0.0147	10min	0.202	10.96	0.365
2	0.0114	60min	0.323	23.02	0.767
3	0.0149	2hours	0.498	27.46	0.915
4	0.0136	3hours	0.525	31.75	1.058
5	0.0168	5hours	0.657	32.28	1.076
6	0.0108	14hours	0.621	47.43	1.581
7	0.0104	1day	0.597	47.32	1.577
8	0.0142	4days	0.786	45.81	1.527
9	0.0099	8days	0.635	52.92	1.764
10	0.0108	30days	0.968	74.35	2.478

Procedure 3

Amount of DEX in freeze-dried scaffold:
Mass of freeze-dried scaffold is assumed to be chitosan & HA granules
10g CH composite solution contains 2%wt chitosan (0.2g) and 1%wt pure HA granules (0.1g).
Amount of drug
= in HA granules (10%wt) + additional DEX 10mg/10 g CH composite solution
= (10% . 0.1g) + (10mg) = 20mg
Amount of DEX in freeze-dried scaffold = 20mg/(0.2g CH + 0.1g HA + 10mg DEX)

= 20mg DEX/0.31g freeze-dried scaffold.

Percentage of drug release:
Drug release = Ct/Co x 100%
Ct = concentration of DEX at certain time (µg/mL)
Ct (µg/mL) = (abs-0.0097)/0.0358
Abs = aborbance obtained from UV-Vis analysis
# Co = concentration of DEX if 100% drug release (µg/mL)
Co (µg/mL) = (20mg/0.31g) x mass of scaffold x1000 / 10mL (PBS)

Table A-8 DDS Release Test – Procedure 3

No	Mass Scaffold (g)	Time	Absorbance	Drug Release	
				(%)	(µg/mL)/mg of scaffold
1	0.0148	10min	0.234	6.56	0.423
2	0.0133	60min	0.329	10.39	0.670
3	0.0118	2hours	0.536	19.31	1.245
4	0.0145	3hours	0.594	17.44	1.125
5	0.014	5hours	0.688	20.97	1.353
6	0.0128	14hours	0.756	25.24	1.628
7	0.012	1day	0.857	30.57	1.972
8	0.0145	4days	1.266	37.51	2.420
9	0.0139	8days	1.358	41.99	2.709
10	0.0117	30days	2.16	79.57	5.133